UNIVERSITÀ DEGLI STUDI DI UDINE

Facoltà di Ingegneria
Dipartimento di Ingegneria Elettrica, Gestionale e Meccanica – DIEGM

Corso di Dottorato di Ricerca in Ingegneria Industriale e dell'Informazione
Ciclo XXVI

Tesi di Dottorato di Ricerca

POWER LINE COMMUNICATIONS FOR SMART HOME NETWORKS: MODELING, SIMULATION AND OPTIMIZATION

Dottorando:
Ing. LUCA DI BERT

Tutor:
Prof. ANDREA TONELLO

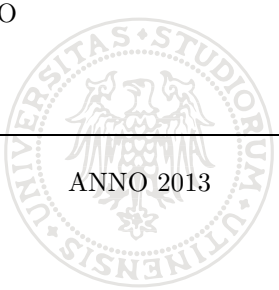

ANNO 2013

Acknowledgements

The PhD course has been an amazing experience and I feel I can recommend it to all of you.

During these years, I devoted myself to the academic research, trying to actively contribute to the scientific community as best I could. I also had the opportunity to work with great persons that made me grow both professionally and culturally.

First of all, I want to acknowledge my tutor, Prof. Andrea Tonello, for giving me the possibility to start this journey, for wisely guiding me through the obstacles, and for teaching me how to do academic research in the best way.

Afterwards, I want to a acknowledge my WiPLi Lab colleagues. Collaborating with them was stimulating and enhanced my research interest. In particular, a special thank goes to my friend Marco for the vitality he brought every day inside the Lab.

Finally, I want to thank my family because I could not have done it without their love and support. I especially care about my mother Carla, for the soothing words that cheered me up during hard times.

Luca Di Bert

San Giorgio di Nogaro
February 3, 2014

Contents

List of Tables

List of Figures

List of Acronyms

ACK acknowledge

ADP adaptation

AGC automatic gain control

AM area manager

AMM automatic meter management

AMR automatic meter reading

AODV ad-hoc on-demand distance vector

AP access point

ARIB Association of Radio Industries and Businesses

AWGN additive white Gaussian noise

BB baseband

BB-PLC broadband PLC

BER bit error rate

BFSK binary FSK

BPSK binary PSK

CAP contention access period

CB circuit breaker

CCDF complementary CDF

CDF cumulative distribution function

CENELEC European Committee for Electrotechnical Standardization

CFP contention-free period

CP cyclic prefix

CRC cyclic redundancy check

CSMA carrier sense multiple access

CSMA/CA CSMA with collision avoidance

CSMA/CD CSMA with collision detection

DA destination address

DAP distribution access point

DES discrete event-based simulation

DBPSK differential BPSK

DCSK differential code shift keying

DHCP dynamic host configuration protocol

DLL data link layer

DPSK differential PSK

DQPSK differential QPSK

DRESs distributed renewable energy sources

DSAP destination service access point

DSSS direct-sequence spread spectrum

EHS European Home Systems

EN end node

ESP energy service provider

FCC Federal Communications Commission

FCH frame control header

FCS frame check sequence

FEC forward error correction

FER frame error rate

FHSS frequency-hopping spread spectrum

FFT fast Fourier transform

FSK frequency shift keying

GFSK gaussian FSK

GTS guaranteed time slot

HAN home area network

HD-PLC high definition PLC

HPCC HomePlug Command & Control

HPGP HomePlug GreenPHY

HPAV HomePlug AV

HVAC heating, ventilation and air conditioning

KKT Karush Kuhn Tucker

ICT information and communication technology

IETL Internet Engineering Task Force

INI initialization

IP Internet protocol

ISM industrial, scientific and medical

ITU International Telecommunication Union

ITU-T International Telecommunication Union - Telecommunication Standardization Sector

LAN local area network

LLC logical link control

LP linear programming

LV low voltage

L2CAP logical link control and adaptation protocol

MAC medium access control

MIMO multiple input multiple output

MP main panel

MV medium voltage

NB-PLC narrow band PLC

NED network description

NL network layer

OFDM orthogonal frequency division multiplexing

PAN personal area network

PB passband

PHY physical

PLC power line communication

PPM pulse-position modulation

PRIME power line intelligent metering evolution

PS-OFDM pulse shaped OFDM

PSD power spectral density

PSDU PHY service data unit

PSK phase shift keying

QoS quality of service

QPSK quadrature PSK

RS Reed-Solomon

SA source address

SFD starting frame delimiter

SG smart grid

SH smart home

SHG smart home gateway

SNR signal to noise ratio

SOHO small office home office

SSAP source service access point

TDMA time division multiple access

THR aggregate network throughput

TP twisted pair

UPB Universal Powerline Bus

UTP unshielded twisted pair

UWB ultra wide band

WLAN wireless LAN

WPAN wireless personal area network

W-OFDM wavelet-OFDM

6LoWPAN IPv6 over low power wireless personal area networks

Abstract

In recent years, research and development efforts are devoted to the deployment of information and communication technology (ICT) within residential buildings and houses, in order to provide services that will increase the quality of life. Although this trend is originated in the late 60's as a result of the application of industrial automation to residential buildings and houses, i.e., home automation, nowadays, further services are offered to the final users, i.e., home networking and energy management. In fact, a lot of effort is put on the joint delivery of these services in order to make the home, namely the smart home (SH), an integral part of the future smart grid (SG). The concept of SH can be described as a house equipped with electronic systems and appliances, namely, "smart" appliances, which are able to exchange information by means of a communication network. However, these systems are characterized by a broad variety of communication technologies, standards and protocols, so that they often cannot interconnect, and/or interoperate and in some cases even coexist.

In our opinion, coexistence, interconnection and interoperability problems represents the bottleneck to a pervasive deployment of smart appliances and systems within residential buildings and houses. To this respect, the first topic that we consider in this thesis is the definition of the SH network architecture and devices, which allows to obtain convergence among smart appliances. To this aim, a survey of the communication technologies, standards, protocols

and also media, which can be used for SH applications, is necessary in order to define a network topology that is able to be scalable, extensible, and rather reliable. Moreover, in order to achieve interconnectivity among "smart" appliances, we define a shared common layer that is able to manage heterogeneous lower layers allowing network convergence.

Once defined the SH network architecture and its network devices, we focus on power line communication (PLC) technologies and we implement a network testbed in order to evaluate some of the functionalities of the SH network within real environments. From the analysis of field trial data, we are able to highlight performances and disadvantages of two representative narrow band PLC (NB-PLC) solutions. Furthermore, exploiting the network testbed where broadband PLC (BB-PLC) technology is used to provide an Ethernet backbone for NB-PLC devices, we achieve interconnectivity between heterogeneous devices and we observe a significant improvement of the performances.

Although NB-PLC technologies have been conceived for the development of low data rate applications and, in particular, for automatic meter reading (AMR), we focus our attention on the G3-PLC technology, for which we propose enhancements at the medium access control (MAC) sub-layer to allow the implementation of SH applications that could potentially require higher data rate than AMR. The G3-PLC technology has been taken into account since (i) it has been used as baseline technology for the development of popular communication standards for SG applications, and (ii) we have found, from the field trials, that the performance of NB-PLC may be poor in large houses where the signal is strongly attenuated because it spans large distances and crosses different circuit breakers (CBs), e.g., in multi-floor houses.

Furthermore, an innovative cross-platform simulator that allows to realistically simulate the G3-PLC technology up to the network layer is presented. The proposed cross-platform consists of two different simulators jointly connected: one for the physical (PHY) layer and one for the data link layer (DLL)/ network layer (NL). The PHY layer simulator is implemented in MATLAB, while the DLL/network simulator in OMNeT++. A convergent network architecture that permits the integration of the G3-PLC technology within a

switched Ethernet network is also presented with the aim of improving the G3-PLC performance in large scale houses/buildings. The performance of the considered communication technology are presented through extensive numerical results for the in-home application scenario.

Finally, the cross-platform simulator is used to evaluate G3-PLC systems for SG applications in the access network scenario. This is fundamental since the interaction of the outside world, i.e., the access network, with the SH is mandatory in order to achieve and exploit the SG concept. Moreover, to improve the performance and coverage of G3-PLC, a simple adaptive tone mapping algorithm together with a routing algorithm are also presented.

Chapter 1

Introduction

In this thesis, we focus on the smart home (SH) networks. In particular, we define a general SH network architecture together with its main network devices, protocols and procedures in order to address challenging issues (i.e., the coexistence, the interconnectivity and the interoperability) as well as to improve the network performances. Moreover, focusing on a representative power line communication (PLC) technology, we model its physical (PHY) and medium access control (MAC) behavior in order to better characterize its performances within a home scenario. We also propose an innovative contention-free MAC scheme to provide performance improvements. Finally, we present a cross-platform simulator which allows to realistically simulate the PLC technology within in-home scenarios. For sake of completeness, we use the cross-platform simulator to evaluate the PLC technology in an outdoor, i.e., access network, scenario.

In this chapter, we set the background of the thesis, and we give an overview of its organization. More precisely, in Section 1.1, we introduce the road to smart home (SH) and we describe the SH concept. Then, in Section 1.2, we set the objectives of the thesis and we give a brief outline. Finally, in Section 1.3, we list the papers where part of the work of this thesis has been published.

1.1 From Home Automation to the Smart Home

Home automation concept is often confused with SH concept. Nevertheless, the home automation concept (also known as *domotics*), is originated in the late 60's as a result of the application of industrial automation to residential buildings and houses. It refers to the use of computer and information technology to control home appliances and features. Some examples of home automation are: remote doors/gates lock, and centralized control of lighting and heating, ventilation and air conditioning (HVAC). In order to satisfy the growing of **home automation services**, industrials started to develop home automation systems and technologies in the early 70s thus, nowadays, systems and technologies are widely available.

Besides home automation services, in recent years, new concepts such as ubiquitous and pervasive computing have been largely developed with the aim of moving people and machines closer. In fact, research and development efforts are put on the deployment of information and communication technology (ICT) within houses and buildings to provide services that will improve quality of life. In this perspective a relevant role is played by the delivery of broadband Internet access that enables a huge development of **home networking services**.

On the other hand, due to sustainable development issues, the housing has become an attractive focus for industrials and academia. In order to achieve power saving targets, the smart energy management is identified as fundamental objective. Moreover, the efficiency increase of the power distribution grid, which includes houses and buildings, is a worldwide priority and. This is going to shift the vision of the power grid to a distributed large scale system that needs to smartly manage flows of electricity produced by big or small plants, i.e., a smart grid (SG). Therefore, since the house is considered as a part of the power distribution grid, it is necessary to develop and offer **energy management services**.

From the previous discussion, it is now clear that the joint delivery of home automation, home networking and energy management services is mandatory

to realize the the smart home (SH) concept, as depicted in Figure 1.1. The main difference with home automation is the transversal layer covered by this solution. In fact, the SH needs an overall architecture, including home automation systems (usually autonomous) as well as external services, such as high speed Internet access, home entertainment, and management of local energy production (e.g., solar panels).

Figure 1.1: The Smart Home services.

In a schematic way, the SH can be described as a house equipped with electronic appliances, namely, "smart" appliances, which are able to exchange information by means of a communication network. These appliances are connected to a home network (i.e., the SH network) in order to send information about their states and/or receive instructions. The home network allows to transport information between smart appliances and a residential gateway, which is responsible of the management of smart appliances and allows for connecting the SH to the outside world, i.e., the Internet and/or the the energy service provider (ESP) network. In this perspective, the SH is fully connected, controlled externally as well as internally. This statement is fundamental since the interaction of the outside world with the home is mandatory

in order to achieve and exploit the SG concept.

1.2 Thesis Objectives and Outline

As described in the previous section, the SH concept deals with the seamless offer of different services. Since, each service can be delivered through heterogeneous communication technologies, standards and protocols, the SH needs a accurate network design in order to avoid problems related to coexistence, interconnectivity and interoperability. In this context, in Chapter 2 we firstly survey the state-of-the-art of communication technologies for in-home networks. Then, the we provide detailed specifications for the SH network architecture and executive procedures for the networking devices, which is the first objective of the thesis.

Once defined the specifications, another interesting topic discussed in Chapter 3 is the realization of a network testbed in order to evaluate the SH network previously presented. By means of a trial campaign performed in real environments, some of the functionalities of the SH network have been evaluated. Moreover, since the network testbed is mainly focused on NB-PLC technologies for SG applications, we evaluate their performances taking into account to the in-home scenario. Eventually, exploiting the BB-PLC technology, we have improved NB-PLC performances and we have extended the network coverage.

Nevertheless, the analysis of performances obtained through field test trials are influenced by hardware platforms and are limited to few network nodes. Therefore, we think that an exhaustive performance analysis needs the development of a network simulator. To this respect, in Chapter 4, we face with the implementation of the main communication technologies and network devices in order to build a realistic simulation environment. Focusing on G3-PLC and Ethernet technologies, the simulator allows to inspect the network performances in peculiar and boundary conditions. From this exhaustive analysis, we point out another interesting objective, i.e., the enhancement of G3-PLC MAC by the introduction of a contention-free access scheme. We notice that the choice of considering the G3-PLC solution is motivated by the two following reasons: (i) it has been used as baseline technology for the nowadays standard,

and (ii) it has been used for field trials and has exhibited poor performances in large houses.

In order to improve the network simulator built in Chapter 4, we propose an innovative approach to realistically simulate the G3-PLC technology in Chapter 5. In fact, another interesting objective of the thesis, is the simulation methodology proposed, which consist of two different simulators, one for the physical (PHY) layer and one for the data link layer (DLL)/network layer (NL), jointly connected. This approach is due to the implementation issues related to physical (PHY) layer modeling within today's network simulators, which have not been thought for these purposes. It is worth noting that, the cross-platform simulator can be used to verify whether a communication technology, e.g., G3-PLC, satisfies a given set of requirements for a certain application scenario.

In this perspective, the cross-platform simulator is used to evaluate G3-PLC systems for SG applications in the access network scenario. Although its is partially out of the scope of this thesis, it is interesting to present G3-PLC performances in outdoor environment since the SH network has to be connected to the access network in order to enable the SG concept. Moreover, to improve the performance and coverage of G3-PLC, we propose a simple adaptive tone mapping algorithm together with a routing algorithm.

Finally, the conclusions follow in Chapter 7. Figure 1.2 summarize the structure of the thesis.

1.3 Related Publications

The main results of the work presented in this thesis have been the subject of publications.

Journal Papers

[J-1] L. Di Bert, S. D'Alessandro and A. M. Tonello, "Enhancements of G3-PLC Technology for Smart-Home/Building Applications," *Journal of Electrical and Computer Engineering*, vol. 2013, Article ID 746763, p.

11, 2013.

[J-2] L. Di Bert, S. D'Alessandro and A. M. Tonello, "Cross-Platform Simulator for G3-PLC Evaluation," under submission.

Conference Papers

[C-1] L. Di Bert, P. Caldera, D. Schwingshackl and A. M. Tonello, "On Noise Modeling for Power Line Communications," in *Proc. of IEEE Int. Symp. on Power Line Commun. and its App.* (ISPLC 2011), Udine, Italy, 2011.

[C-2] L. Di Bert, S. D'Alessandro and A. M. Tonello, "An Interconnection Approach and Performance Tests for In-home PLC Networks," in *Proc. of IEEE Int. Symp. on Power Line Commun. and its App.* (ISPLC 2012), Beijing, China, 2012.

[C-3] L. Di Bert, S. D'Alessandro and A. M. Tonello, "MAC Enhancements for G3-PLC Home Networks," in *Proc. of IEEE Int. Symp. on Power Line Commun. and its App.* (ISPLC 2013), Johannesburg, South Africa, 2013.

[C-4] L. Di Bert, S. D'Alessandro and A. M. Tonello, "A G3-PLC Simulator for Access Networks," submitted to *IEEE Int. Symp. on Power Line Commun. and its App.* (ISPLC 2014), Glasgow, Scotland, 2014.

Other Contributions

[O-1] "Brief Tutorial on the Statistical Top-Down PLC Channel Generator," [Online], Dec., 2010. Available: `http://www.diegm.uniud.it/~/tonello/PAPERS/WHITE/TUTORIAL_CHAN_2010.pdf`.

[O-2] POR FESR 2007-2013, Project Living for All Kitchen (LAK), Deliverable RA1, "Specifiche di dettaglio della rete domotica del progetto LAK," Mar., 2011.

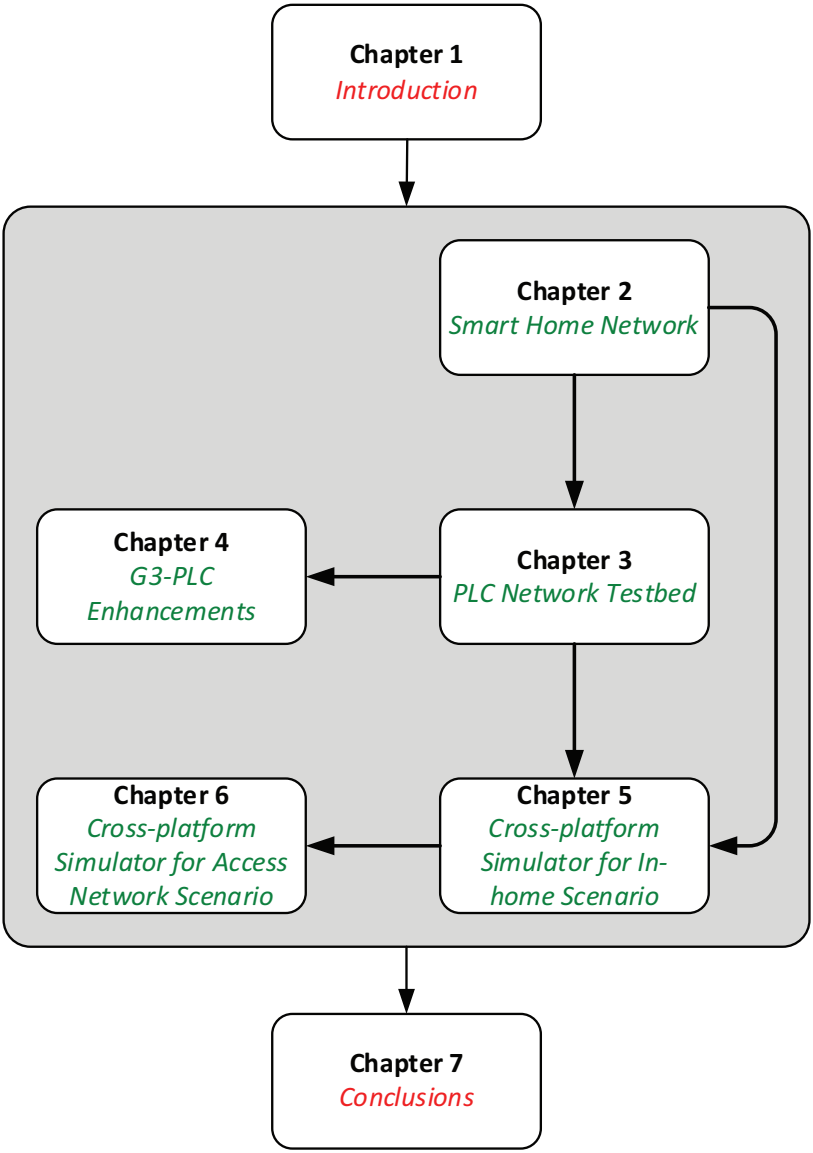

Figure 1.2: Thesis structure.

Chapter 2

The Smart Home Network

Several communication technologies, which are suitable for in-home applications, are nowadays available on the market. However, they make use of different media and protocols to communicate, and consequently, they may not be able to provide interconnectivity, interoperability and in some cases even coexistence. This is one of the major obstacles for the realization of the smart home, i.e., an environment where heterogeneous services like home networking, home automation and energy management (making it an integral part of the future SG), are offered transparently to the final users. This chapter firstly surveys existing wireline, wireless and PLC technologies, then presents a network architecture, which enables scalability and provides convergence for communication technologies. Interconnectivity is reached through the definition of a shared common network layer while interoperability can be obtained via middleware solutions.

2.1 Introduction

Research and development efforts are currently devoted to the deployment of information and communication technology (ICT) within houses and buildings to provide services that will improve quality of life. Among these services, three classes can be identified: home networking, home automation, and smart energy management. Home networking services, e.g., triple play (high speed

Internet access, television, telephone), infotainment, and resource sharing in local area network (LAN), are those that usually require high speed communication systems. On the other hand, home automation services are those that usually require low speed communication systems, e.g., for the automation of windows and doors, for the control of HVAC, for lighting and audio/video distribution. While home networking and home automation are well-established applications, smart energy management has only recently attracted significant interest. This is because the efficiency increase is a worldwide priority of the power distribution grid which includes houses and buildings. Energy efficiency and power savings were identified in 2010 as fundamental objectives to contribute to the Sustainable Growth specified in the "Europe 2020" strategy [1]. In the near future, the power grid will become a distributed large scale system that needs to smartly manage flows of electricity produced by big or small plants, i.e., a SG [2, 3]. An important role is played by communication technologies that enable, in the home/building context, the smart management of household appliances, power metering, the control of local renewable energy plants (e.g., photovoltaic generators) the monitoring of electric vehicles charge, etc.. These technologies will allow the implementation of demand side and demand response mechanisms so that prosumers will actively collaborate in the use and delivery of energy.

From the previous discussion, it is evident that the realization of the smart home (SH) requires the joint delivery of *home networking*, *home automation* and *energy management* services. Despite the existence on the market of a broad variety of communication technologies, the bottleneck to their pervasive deployment is that they often cannot interconnect, and/or interoperate and in some cases even coexist.

In the rest of the chapter, coexistence and interconnectivity are discussed in Section 2.2 while interoperability is discussed in Section 2.3 together with current key middleware solutions. A survey of the communication technologies, which can be used for SH applications, is presented in Section 2.4. As explained, in general, these technologies operate over different media and/or use different standard/protocols. Therefore, they may lack for interconnectivity.

To solve this problem, in Section 2.5, a SH network architecture is described. It potentially enables for connectivity, scalability, flexibility, distributed control, reliability, and easy integration of different communication technologies, thanks to the use of a shared common network layer that is able to manage heterogeneous lower layers. Finally, main findings follow in Section 2.6.

2.2 Coexistence and Interconnectivity

The coexistence is a very rich and complex topic. However, a standing definition for coexistence in given in [4]: the ability of one system to perform a task in a given shared environment where other systems may or may not be using the same set of rules. The coexistence is a well-known concept that arise when dealing with physical broadcast medium, e.g., wireless and PLC, and related to the ability of sharing the same physical medium by two or more devices. Usually, the coexistence is obtained regulating different frequency bands at the PHY layer, or through the use of MAC protocols.

The interconnectivity is another challenging topic. It is the capability of systems to exchange information regardless of their own environment and/or set of rules. In telecommunications, it is the ability of systems to exchange data regardless of the heterogeneity of their own communication technology, standard and protocol. Clearly, interconnectivity requires coexistence and and can be achieved with a convergent layer either above the PHY or above the DLL, e.g., the network layer.

Industrial and standardization organizations are facing with these challenging topics. Representative examples are: as regards wireless communications, the IEEE 802.19 working group [5] develops standards for coexistence between wireless standards of unlicensed devices and reviews coexistence assurance (CA) documents produced by working groups developing new wireless standards for unlicensed devices; as regard PLC, the IEEE P1901 working group [6] with its Technical Subgroup 4 (TSG4, dedicated to coexistence) presented a draft annex describing the Inter-System Protocol (ISP) that enables various BB-PLC devices and systems to share communication resources (frequency/time) when installed in a network with common electrical wiring.

Furthermore, the G.hn standard [7], ratified by International Telecommunication Union - Telecommunication Standardization Sector (ITU-T) [8], has been conceived with the aim of offering interconnectivity among in-home high speed communication devices that work over telephone wires, power lines, and coax (G.hn specifies the PHY and the MAC layers and addresses the coexistence between protocols that operate on different media); the solution developed within the EU-FP7 OMEGA project [9], according to which devices belonging to the OMEGA network share the same inter-MAC layer and consequently they can coexist and they are interconnected.

To this aim, in the Section 2.4, we survey the communication technologies that can be used for SH applications

2.3 Interoperability and Middleware Solutions

In general, interoperability is referred to the capability to communicate, execute programs, or transfer data among various functional units in a manner that requires the end user to have little or no knowledge of the unique characteristics of those units [10]. Focusing on network domain, it is the ability to send and receive data between interconnected devices or networks providing the level of quality expected by the end user without any negative impact to the sending/receiving devices or networks. Clearly, from the previous definition, interoperability requires interconnection which, in turn, requires coexistence. Therefore, the interoperability concept is related to network up to application layer. In fact, data exchanged between two systems (devices or networks) has to be meaningfully and accurately interpreted in order to produce useful results as defined by the end users of both systems. Therefore, since interoperability handles the semantic of data, it requires a common reference model where information exchanged are unambiguously defined.

In this perspective, in order to realize the presented SH network, we deem to reconsider the SH network according to the distributed systems theory, where devices communicate and coordinate their actions exchanging messages by means of a communication network [11]. In such a system, the interoperability among network devices can be achieved through the introduction of a

higher level of abstraction: the *middleware* layer. Then, the management of services – which can be centralized or distributed, e.g., home networking, home automation, and energy management, – will rely on the application software.

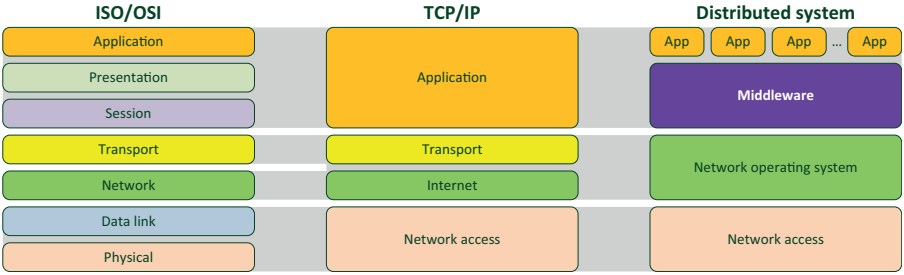

Figure 2.1: ISO/OSI, TCP/IP and distributed system protocol stack.

The middleware is a software layer placed between the network operating system and the applications as depicted in Figurefig:middleware. Its aim is to simplify access to heterogeneous and distributed resources. It provides a higher degree of abstraction in distributed system programming by decoupling applications from the lower layers consisting of heterogeneous operating systems, hardware platforms and communication protocols. In this perspective, the most relevant middleware solutions are the *Universal Plug and Play* [12], the *Open Service Gateway initiative* [13] and the *Java intelligent network infrastructure* [14].

2.3.1 Universal Plug and Play

UPnP is an emerging standard based on a peer-to-peer software architecture for network connectivity of, possibly, any kind of electronic device. The framework is designed to be independent of any particular operating system, programming language and physical medium. It is also open and based on the TCP/IP protocol stack. Devices belonging to an UPnP network can be classified into controlled devices (or simply devices) and control points. A controlled device acts as a server, responding to client requests from control points. Note that, a device and a control point can operate simultaneously on the same

physical node.

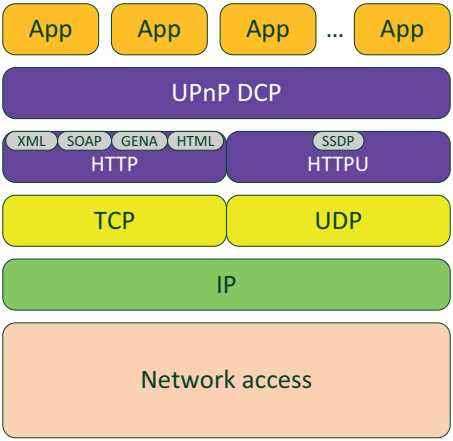

Figure 2.2: UPnP protocol stack.

As shown in Figure 2.2, the engine of this framework is given by the Device Control Protocol (DCP). It defines the communication between devices and control points exploiting well known protocols and languages, e.g., addressing (DHCP or AutoIP), discovery (SSDP), description (XML), control (SOAP), eventing (GENA) and presentation (HTML). Therefore, the UPnP network does not require any configuration from the user. In fact, once a device (or a control point) is connected to the network, it is automatically detected and configured. Furthermore, it exchanges information with the network about services provided and capabilities offered. However, since UPnP is based on the TCP/IP protocol stack, the connectivity among heterogeneous network devices, which are non IP-based, is not always ensured.

Currently, UPnP has been applied for multimedia applications such as audio or video streaming by the digital living network alliance [15]. Unfortunately, its application for home automation and energy management services may be limited due to the complexity of running the protocol stack inside devices with low computational capability, e.g., sensors and actuators.

2.3.2 Open System Gateway Initiative

OSGi provides open specifications for service delivery into networked environments. Since it is based on Java, it is operating system independent. OSGi basically consists of a network framework and a set of standard service definitions. The main role is played by the service gateway that coordinates the interaction between the client and the service provider. The latter can be either located within the same network (e.g., for home monitoring and automation) or spread over the Internet (e.g., for a remote alarm system, for web multimedia streaming).

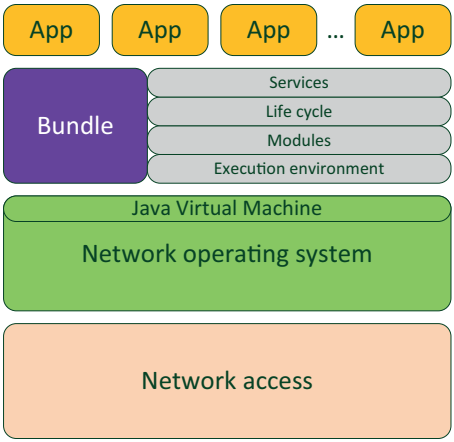

Figure 2.3: OSGi protocol stack.

Figure 2.3 shows the system protocol details: applications or components are packed into bundles and delivered throughout the network. Each bundle carries information about service interfaces, service implementation and required resources. Therefore, the service provider copes with the packaging and advertisement of bundles, while the client downloads and executes the required bundles through the service gateway. Although OSGi was originally designed for service gateways, now it is considered for application in a broad variety of devices, e.g., set-top boxes, Cable/DSL modems, PCs as well as mobile phones.

The main strength of OSGi is the idea of centralizing the network management in the service gateway. However, this can also be a weakness since it limits the system scalability and represents a single point of failure problem.

2.3.3 Java Intelligent Network Infrastructure

Jini defines a set of network architecture specifications for the implementation of a distributed system. It allows for federating clients, services and the resources required by those services. Jini is operating system independent but Java-based since it is an evolution of the Java Remote Method Invocation (RMI). It is also open and based on the TCP/IP protocol stack.

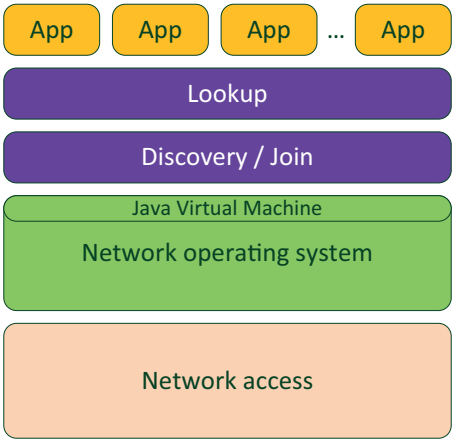

Figure 2.4: Jini protocol stack.

According to Figure 2.4, the core of Jini is represented by the discovery, join and lookup protocols. Furthermore, three main components can be defined, i.e., the service, the client and the lookup service. A given service, originated by a service provider, has to be registered in the lookup service before being acquired and used by the client. The service provider stores a set of service attributes into the lookup service using the discovery and join protocols. When the client requests for a service, the lookup protocol moves the service attributes from the lookup service to the client. Eventually, the

client is able to exploit these service attributes to obtain the required service directly from the service provider. In this perspective, the lookup service acts both as a repository of service providers and as service trader for clients.

The flexibility of the discovery mechanism and the scalability offered by the number of lookup services, which may increase according to the network load, are the main strengths of Jini systems. Nevertheless, the transfer of service attributes (i.e., Java bytecode) requires an amount of memory that is not always available in small devices.

2.4 Survey of In-home Network Communication Technologies

Within the home, we can find several electronic devices that make use of different media and protocols to communicate. In this perspective, we survey the communication technologies that can be used for in-home networking. In particular, we focus on wireline, wireless and PLC technologies.

2.4.1 Wireline

Wireline networking is typically represented by communication technologies that exploit twisted pair (TP) cables and coax cables.

The communication over TP is used for the deployment of IP based LAN. Cables are categorized by their cut-off frequency that determines the transmission data rate. With reference to this classification, we highlight cables Cat 5, Cat 5e with a 100 MHz cut-off frequency. These cables support the IEEE 802.3 standard family [16], also known as Ethernet. In particular, Fast Ethernet with data rate up to 100 $Mbps$ over Cat 5 cables is termed 100BASE-TX (standardized by IEEE 802.3u), while Gigabit Ethernet with data rate up to 1 $Gbps$ over Cat 5e is termed 1000BASE-T (standardized by IEEE 802.3ab). For this reason, TP cables are also known as Ethernet cables. The Ethernet coverage is up to 100 m both for Fast and Gigabit Ethernet using Cat 5/5e unshielded twisted pair (UTP).

Besides LAN application, coax has been also proposed for delivering entertainment and multimedia services within the home and in the access network.

In 2007, the Multimedia over Coax Alliance [17] ratified the v1.0 and v2.0 specifications for communication over coax with data rate up to 250 $Mbps$ and 1.4 $Gbps$, respectively. Recently, ITU-T has ratified the Gigabit Home Network standard (G.hn [18, Chapter 7]) that specifies the PHY and MAC layers for interconnection of devices using coax, TP, and power line communications. Its PHY layer is based on orthogonal frequency division multiplexing (OFDM) and offers data rate up to 1 $Gbps$, while the MAC layer is based on hybrid time division multiple access (TDMA)/carrier sense multiple access (CSMA). Eventually, the HomePNA technology provides specifications for home networking over existing coax cables and phone wires offering data rate up to 320 $Mbps$ [19].

2.4.2 Wireless

There are several wireless technologies that can be used for in-home applications. Essentially, they can be grouped according to the offered data rate and the coverage. Roughly speaking, devices that offer high data rate and large coverage are developed for LAN applications, e.g., Wi-Fi. Whereas, devices that offer high data rate and short coverage range are developed for personal area network (PAN) applications, e.g., WiMedia Alliance compliant devices [20]. Finally, devices that offer low data rate and a relatively large coverage are developed for command and control applications, e.g., ZigBee [21]. All these wireless devices work in the frequency bands known as industrial, scientific and medical (ISM).

In the following, we provide some more details about the wireless technologies.

High data rate wireless technologies ($> 10\ Mbit/s$)

This category is defined by the standard family IEEE 802.11 [22] and are known with the term Wi-Fi. They work in the frequency bands 2.4 GHz (802.11b/g/n) or 5 GHz (802.11a/n). Their data rate equals 11 $Mbps$ for 802.11b, 54 $Mbps$ for 802.11a/g, and 600 $Mbps$ for the 802.11n using multiple

input multiple output (MIMO) techniques. Moreover, the indoor coverage is up to 70 m [9].

All these technologies have the physical layer based on direct-sequence spread spectrum (DSSS) or OFDM, while the MAC protocol based on CSMA with collision avoidance (CSMA/CA) (see Table 2.1) that allows for coexistence. Although WiFi and Ethernet have different PHY/MAC layers, they converge towards the same logical link control (LLC) layer (defined in IEEE 802). Therefore, they exhibit the same interface towards the network layer and thus they are interconnected.

Other high data rate wireless technologies are the ones based on ultra wide band (UWB) modulations. Two examples are the WiMedia and the WirelessHD [23] standard compliant devices. Both standards are based on multi-band OFDM and are designed for short range communications (< 10 m). WiMedia compliant devices work in the frequency band 3–10 GHz and reach data rate up to 1 $Gbps$, whereas WirelessHD devices work in the frequency band 57–66 GHz and reach data rate up to several $Gbps$.

Low data rate wireless technologies (< 3 $Mbit/s$)

Now we consider the most used low data rate wireless technologies, i.e., Z-Wave, ZigBee, Wavenis [24] and Bluetooth [25]. These technologies have been conceived with the scope of being embedded in small chips and require low power consumption. In this perspective, Table 2.2 highlights that simple modulation techniques are used, e.g., binary FSK (BFSK) and binary PSK (BPSK), whereas OFDM is disregarded since the computational cost that negatively affects battery duration. On the other hand, in many cases, spread spectrum techniques are taken into account, e.g., DSSS and frequency-hopping spread spectrum (FHSS).

It is interesting to note that some of the listed technologies work in the same frequency band and can coexist due to the medium access technique usually based on CSMA/CA. However, they cannot exchange data due to the lack of a defined convergent higher layer.

Table 2.1: High data rate wireless technologies.

	802.11a	**802.11b**	**802.11g**	**802.11n**	**WiMedia**	**WirelessHD**
Spectrum $[GHz]$	5	2.4	2.4	2.4/5	3.1–10.6	57–66
Modulation	OFDM	DSSS	OFDM, DSSS	OFDM	OFDM	OFDM
Data rate $[Mbit/s]$	54	11	54	150/600	1024	7 *Gbps*
Coverage $[m]$	35–120	35–140	38–140	70–250	-	up to 10
Medium access	CSMA/CA	CSMA/CA	CSMA/CA	CSMA/CA	CSMA/CA, TDMA	TDMA

Table 2.2: Low data rate wireless technologies.

	Z-Wave	**Bluetooth**	**ZigBee**	**Wavenis**
Spectrum $[GHz]$	0.868/0.968/2.4	2.4	0.868/0.968/2.4	0.433/0.868/0.968/2.4
Modulation	BFSK	GFSK/DPSK, FHSS	BPSK/QPSK, DSSS	GFSK, FHSS
Data rate $[kbit/s]$	9.6–200	1–3 $Mbit/s$	20–250	4.8–0.100
Coverage $[m]$	30–100	10–100	10–100	200–1000
Medium access	CSMA/CA	L2CAP	CSMA/CA, TDMA	CSMA/CA

2.4.3 Power Line Communication

Power line communication (PLC) makes use of the existing power line grid to transmit data signals. There is a broad range of applications for which PLCs have been or being used, e.g., remote metering, command and control of domotic systems, small office home office (SOHO), and recently, SG applications.

Essentially, the PLC devices can be grouped into two categories, i.e., BB-PLC and NB-PLC devices, according to the data rate that they can achieve.

Broadband PLC Technologies

They have been developed with the aim of offering SOHO and multimedia services. Essentially, BB-PLC devices work on the frequency band 2–30 MHz, and make use of advanced modulation techniques such as OFDM and bit-loading to offer data rates in the order hundreds of $Mbps$. The most relevant examples of commercial devices are the ones compliant with the HomePlug AV (HPAV) [26] and the high definition PLC (HD-PLC) [18, Chapter 7] industry standard. Their MAC layer is based on TDMA for high quality of service traffic, and to CSMA/CA for best effort traffic. Furthermore, they exhibit convergence towards Ethernet. In Table 2.3, we summarize the characteristics of BB-PLC devices. It is interesting to note that both solutions, i.e., HPAV and HD-PLC, have been used as baseline for the PHY layer specification of the IEEE P1901 standard [6], released in December 2010. Moreover, HomePlug GreenPHY (HPGP) version 1.1 has been recently ratified for SG applications within the customer premises maintaining interoperability with HPAV and P1901 [27].

Narrow Band PLC Technologies

They have been developed with the scope of offering indoor (home automation) and outdoor (SG) command and control services. These technologies are cheap and offer low data rates; some of them have been designed tens of years ago, e.g, Universal Powerline Bus (UPB) and X10, exploiting a basic modulation

technique (pulse-position modulation (PPM)) that facilitates high reliability but poor data rates. The frequency bands dedicated from standardization organizations to NB-PLC devices vary among the continents. In the EU, the European Committee for Electrotechnical Standardization (CENELEC) issued the standard EN 50065 that specifies four frequency bands for communications over power line networks [18]. The band A (3–95 kHz) is reserved exclusively to power utilities, the bands B (95–125 kHz) for any application, the band C (125-140 kHz) for in-home networking, and the band D (140148.5 kHz) for alarm and security systems. In US and Asia, the regulation is different: Federal Communications Commission (FCC) and Association of Radio Industries and Businesses (ARIB) allow PLC devices to work in the band from 3 kHz up to 490 kHz or 450 kHz, respectively.

In Table 2.4, we report the NB-PLC technologies developed for home automation applications. It is worth noting that most of NB-PLC technologies not open standard, e.g., LonWorks and HomePlug Command & Control (HPCC), thus the specifications are not detailed. For the interested reader, more details can be found in [18, Chapter 7]. It is noticeable that the listed technologies work in different frequency bands and adopt different PHY and MAC layers. Therefore, these technologies can coexist but they do not allow for interconnection. Furthermore, technologies with overlapping operating bands can coexist exploiting MAC specific protocols. To this aim, we highlight CENELEC band C, i.e., reserved for technologies that adopt the CSMA protocol.

In this scenario, a relevant role is played by G3-PLC [28] and power line intelligent metering evolution (PRIME) [29] solutions since they exhibit higher reliability and data rates. In fact, nowadays they are playing a relevant role for SG applications and therefore they have been ratified by ITU-T in [30] and [31], respectively.

Regarding the standardization aspect, we notice that recently two working groups, the IEEE P1901.2 [32] and the ITU-T G.hnem [33], have specified the PHY and the MAC layers of NB-PLC solutions for communication below 500 kHz.

Table 2.3: Broadband PLC technologies.

	HPAV	**HPGP**	**ITU-T G.hn**	**HD-PLC**	**IEEE P1901**
Spectrum [MHz]	2–35 (1) 2–70 (2)	2–30	2–100 (BB) 100–200 (PB)	4–30	2–28 2–60
Modulation	OFDM Bit loading	OFDM, QPSK	OFDM Bit loading	W-OFDM Bit loading	W-OFDM Bit loading
Data rate [$Mbit/s$]	200 (1)/500 (2)	10	1 $Gbit/s$	190	540
Medium access	CSMA/CA, TDMA	CSMA/CA	CSMA/CA, TDMA	CSMA/CA, TDMA	CSMA/CA, TDMA

Table 2.4: Narrow band PLC technologies.

	Insteon	**KNX**	**X10**	**CEBus**	**LonWorks**
Spectrum	CENELEC C	CENELEC B	CENELEC B	CENELEC C, FCC, ARIB	CENELEC A, C, FCC
Modulation	BFSK	Spread FSK	PPM	Spread spectrum	BPSK
Data rate [$kbit/s$]	2.4	1.2	0.05	8.5	5.4
MAC	-	CSMA	CSMA/CD	CSMA/CD	CSMA/CA, CSMA/CD
	UPB	**HPCC**	**G3-PLC**	**PRIME**	**ITU-T G.hnem**
Spectrum	50 Hz 60 Hz	CENELEC A, C, FCC, ARIB	CENELEC A–D, FCC	CENELEC A	CENELEC A–D, FCC
Modulation	PPM	DCSK	OFDM	OFDM	OFDM
Data rate [$kbit/s$]	0.48	7.5	240	122	1 $MBit/s$
MAC	-	CSMA/CA	CSMA/CA	CSMA/CA, TDMA	CSMA/CA

2.5 Smart Home Network Architecture

To obtain convergence of network technologies and enable the delivery of a broad set of in-home services, the general SH network architecture (depicted in Figure 2.5) is envisioned.

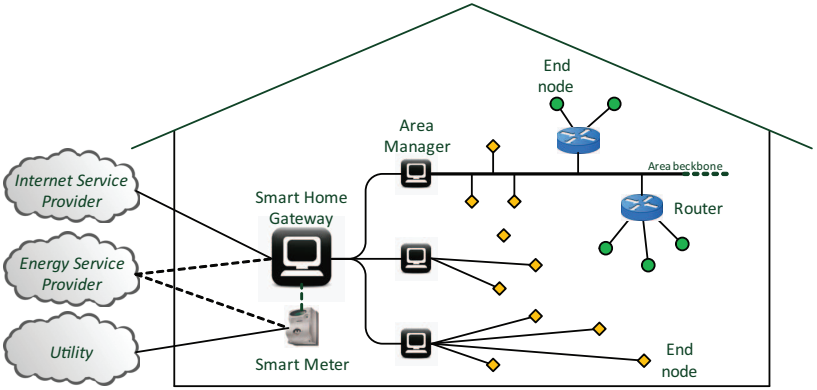

Figure 2.5: The Smart Home network architecture.

Nowadays, the most common technologies for home area network (HAN) and LAN applications are based on Ethernet and/or WiFi. Although the physical topology of Ethernet and WiFi is different, they exhibit the same logical topology, i.e., the star topology. In fact, each network node is connected to a central hub (a switch and an access point, respectively for Ethernet and WiFi, with a point-to-point connection. On the other hand, PLC systems exhibit both physical and logical bus topology.

Therefore, we adopt a tree topology – as a combination of bus and star topologies – for the SH network architecture. The major benefit deriving from the use of such a topology is its ability to be scalable, extensible, and rather reliable. From the top down, the hierarchy is characterized by a smart home gateway (SHG) (root), area manager (AM), router and, finally, end node (EN) (leaf).

Interconnection among different communication technologies can be reached through the definition of a shared common layer that is able to manage het-

erogeneous lower layers allowing network convergence. To this aim, we define 4 representative network devices, i.e., EN, router, AM and SHG. Since they play a relevant role in achieving convergence, their behavior is detailed in the following.

2.5.1 End Node

End nodes represent the leaves of the network and they directly interact with the surrounding environment. According to Figure 2.5, ENs can be classified according to Ethernet compliancy (diamond) or non-compliancy (green circle). It is worth noting that, in general, home automation devices (e.g., sensors, actuators and dimmers) use a proprietary communication protocol, usually non-compliant with Ethernet. In fact, these devices exhibit simple circuitry and poor computational capabilities in order to fulfill low power consumption requirements. Therefore, they need to be virtualized within the Ethernet network exploiting the router capabilities.

2.5.2 Router

Nodes compliant to a given standard, non Ethernet-based, are grouped in a subnetwork. Each subnetwork is reachable through a Router (see Figure 2.5). The main role of the Router is thus to virtualize each node of its subnetwork within the Ethernet network. This leads to interconnectivity among the network nodes. According to the architecture depicted in Figure 2.6, a router has to:

- Associate a virtual address (e.g., Internet protocol (IP) address) to each EN of the subnetwork.
- Get and store the information about each node, i.e., the kind of service provided (e.g., remote sensing), the physical link quality and the set of data that the node needs to exchange (e.g., the temperature or power consumption measured by a sensor).
- Generate a list that specifies the address and the information of each node of its subnetwork.

- Relay frames from Ethernet networks to networks characterized by different communication protocols, and vice versa.

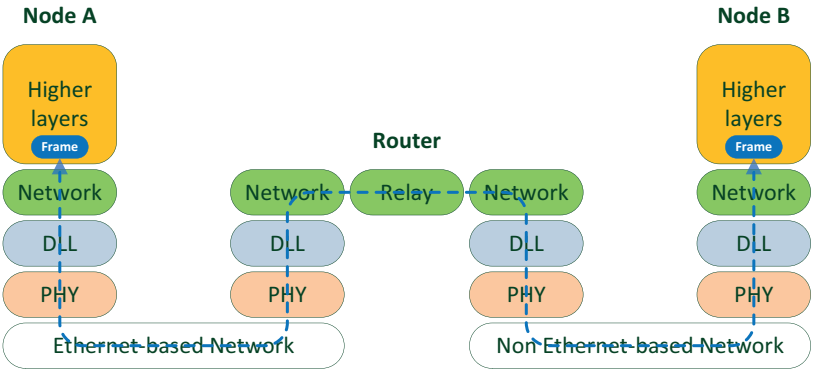

Figure 2.6: General router architecture and frame relaying.

It is important to highlight that the use of routers is beneficial for increasing the network coverage. In fact, a subnetwork can be split in more subnetworks in the case that some of its nodes are not in visibility. This concept will be stressed later in Chapter 3 where network a network testbed is developed and some performances are shown.

2.5.3 Area Manager

The SH network can be split into areas. Each area represents one or more rooms and it is managed by an AM. Different AMs can manage the same class of service, e.g., home networking, home automation, energy management, in different ways. This enables to offer, in a simple way, a specific set of services to a given area of the house. For instance, it is known that the kitchen is the area of the house that needs the highest safety level, therefore, a *Kitchen-AM* will offer ad-hoc services for the kitchen.

The AM retrieves the information regarding the ENs and their corresponding subnetworks, thus it contains a data base with all the information regarding its area. The AM is also envisioned to be responsible of the routing within

its area. In particular, each AM is able to forward frames taking into account the energy efficiency, i.e., the selected paths are the ones that need the lowest energy consumption to satisfy given quality of service (QoS) constraints (e.g., bit-rate, latency, delay). Finally, the AM, under request, can send its own database to the SHG. By doing this, the SHG has a complete vision of the network and can request the AMs to make actions as a consequence of an event or a user request coming from another area of the house. It is worth noting that the use of more AMs within the house also increases the fault tolerance and the network extensibility. Finally, it is noticeable that an AM can be a physical or a logical entity. For example, in the latter case, it could be a software that runs in a platform that has an Ethernet connection.

2.5.4 Smart Home Gateway

The SHG plays the role of central coordinator and offers Internet connectivity. This is to provide remote management/alert/monitoring of the network and the delivery of web information and entertainment services. Note that the Internet connectivity can be also exploited to connect the house to the ESP for exchanging data about energy usage and tariffs. Furthermore, since the network can integrate different communication technologies, it is also conceivable to have connectivity between the smart meter, which is typically own by the utility, and the SHG. It is worth noting that, although the integration of SG and conventional home networking applications violates an accepted paradigm, the isolation between the utility network, the energy and Internet service providers can be handled by higher layer, e.g., exploiting middleware functionalities.

On the other hand, the SHG communicates with the AMs connected to the same backbone. The main features of the SHG can be summarized as follows:

- Addressing (if necessary): assign the IP address to the AMs, e.g., dynamic host configuration protocol (DHCP) server.

- Service lookup and publication: get the information about nodes from the AMs, and consequently generate its own data base containing the

information regarding all network nodes.

- Service maintenance: update its own data base following a network event.
- Routing (if necessary): set up a routing table among the AMs taking into account the reliability or energy efficiency of the links.
- Home function control: ask the AMs to make an action as a consequence of an event or an user request.
- Fault detection: detect and report failures of devices.
- Remote access: users can access and/or manage the overall network from a remote position.

As discussed for the AMs, the routing path can be chosen according to a tradeoff between energy consumption and QoS constraints satisfaction. An example of such an approach is given by the IPv6 Routing Protocol for Low power and lossy networks [34], recently approved by the Internet Engineering Task Force (IETL).

2.6 Main Findings

Several communication technologies, suitable for in-home applications, are surveyed in this chapter, focusing on wireline, wireless and PLC. Nevertheless, they make use of different standards, protocols and even different media to communicate, and consequently, they are not interoperable/interconnected and/or can not even coexist. To this respect, in this chapter, we focus on coexistence, interconnectivity and iteroperability issues as the major obstacles to the realization of the SH where full penetration of heterogeneous services is required. Then, we present a convergent network architecture in order to achieve the interconnectivity. This is done through the definition of a of a shared common layer that is able to manage heterogeneous lower layers allowing network convergence. Furthermore, we discuss in detail the features of main network devices.

Chapter 3

PLC Network Testbed for In-home Performance Evaluation

The concept of the electrical grid conceived as an infrastructure that only delivers power to the end users is going to disappear. In the next years, the electrical grid will be viewed as a smart grid (SG), namely, a distributed complex large scale system that needs to smartly manage flows of electricity produced by big or small plants. To fully exploit the SG potentialities, we think that it is mandatory to extend the SG concept to the home. In our vision the smart home (SH) network has to be developed to offer a broad variety of heterogeneous services that will improve the quality of life, yet addressing energy consumption challenges, and in parallel providing the delivery of information and entertainment services.

In this chapter, some of the functionalities of the SH network are evaluated through an implementation of a network testbed. More precisely, we consider a real environment where appliances have been plugged and unplugged. In this scenario, we first show the performance – in terms of aggregate network throughput (THR) and frame error rate (FER) – of two representative NB-PLC solutions, i.e., one based on OFDM, and the other based on frequency shift keying (FSK). The test results show that the performance of the OFDM-based solution are very poor when working in the multi floor scenario. To solve this problem, we implement an IP-based network prototype

where BB-PLC devices are used to provide an Ethernet backbone that leads to a significant improvement of the performances of the OFDM-based solution, and further it offers connectivity between heterogeneous devices belonging to different subnetworks.

3.1 Introduction

In the last years, we have assisted to an increased interest of the utility companies towards the development of communication technologies that allow the remote automatic meter management (AMM).

Besides the need of AMM technologies, nowadays the utility companies are facing with new challenges such as [35]: the safe integration and the management of renewable energy sources; the management of plug-in electric vehicles that may cause a large load increase on sections of the grid; the management of demand side and demand response allowing the customers to collaborate in order to adapt the production and the delivery of electricity to achieve energy efficiency and saving.

In the next years, the electrical grid will be viewed as a smart grid (SG), namely, a distributed complex large scale system that needs to smartly manage flows of electricity produced by big or small plants. Therefore, the management of the SG will require a pervasive telecommunication infrastructure to allow the entire supply chain of electricity, to benefit from a bidirectional, reliable, short and long distance communication.

Industries and standardization organizations have proposed the use of NB-PLC to support the requirements of the outdoor (bulk generation, transmission and distribution domains) SG applications. On the other hand, BB-PLC solutions are spreading to the in-home network market. This happens because the PLC infrastructure is indeed pervasively deployed and its exploitation for communication purposes does not require any additional cost.

To fully exploit the SG potentialities, we think that it is mandatory to extend the SG concept to the home, namely, the customers domain. In our vision the SH network has to be developed to offer a broad variety of heterogeneous services that will improve the quality of life, yet addressing energy

consumption challenges, and in parallel providing the delivery of information and entertainment services. Nevertheless, the full deployment and exploitation of a broad variety of electronic appliances and devices, e.g., TVs, HVACs, PCs as well as sensors, detectors and actuators, is nowadays limited by coexistence and interconnection problems, hence, interoperability. In fact, a large number of vendors has put on the market devices for in-home applications that use different technology, standard, protocol, and even different media to communicate. In our opinion this is the main obstacle to the growth of the SH market.

In this chapter, we show some of the functionalities of the presented SH solution through an implementation of a network testbed. More precisely, we first show the performance - in terms of throughput and frame error rate - obtained testing in a real environment, represented by a single floor (see Figure 3.1a) and in a multi floor house (see Figure 3.1b), two representative NB-PLC solutions, i.e., one based on OFDM, and the other based on FSK. The test results show that the performance of the OFDM-based solution are very poor when working in the multi floor scenario where channels cover longer distances and exhibit higher attenuation than the single floor house. To solve this problem, we implement an IP-based network prototype where BB-PLC devices are used to provide an Ethernet backbone that leads to a significant improvement of the performances of the OFDM-based solution, and further it offers interconnectivity between heterogeneous devices belonging to different subnetworks.

The reminder of the chapter is as follows. In Section 3.2, we describe the testbed network architecture, together with the communication technologies and the performance metrics considered. The test campaign results are reported in Section 3.3 where NB-PLC technologies are compared. Interconnectivity and range extension are discussed in Section 3.4, and finally, the main findings follow in Section 3.5.

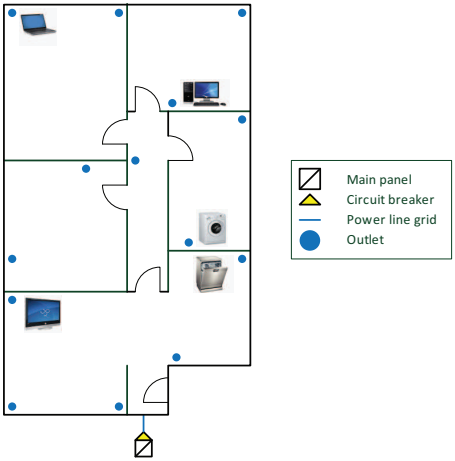

(a) Single floor house.

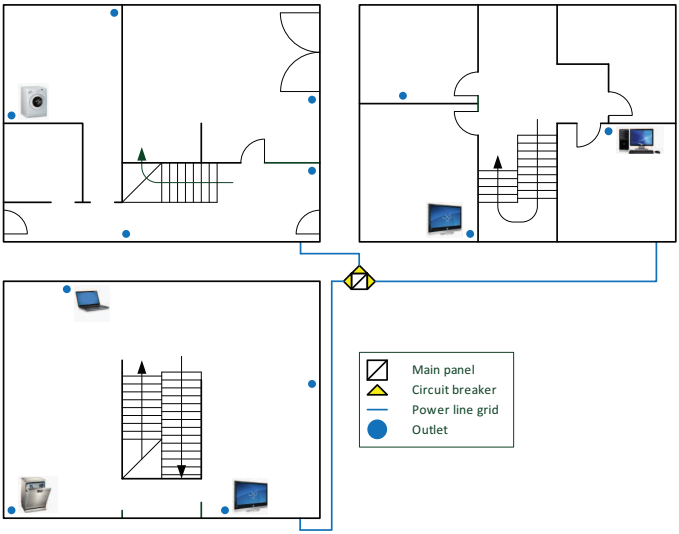

(b) Multi floor house.

Figure 3.1: Real environment for the network testbed.

3.2 Testebed Network Architecture

In order to test some of the functionalities of the network architecture – in particular, the interconnection between NB-PLC and BB-PLC devices and the range extension – we have developed a network testbed consisting of different areas connected through an Ethernet backbone based on HPAV technology. Each area represents a given floor of the house and comprises NB-PLC/Ethernet router and a NB-PLC end node (EN) (modem). The router functionalities have been implemented by means of a network software running on a PC with network adapters towards both Ethernet and NB-PLC. Note that, in the specific scenario, the absence of a AM is not restrictive at all. In fact, the presence of a SHG or AMs enable the interoperability, i.e., the management of SH services, which is related to application layer, and can be later implemented, e.g., exploiting middlewares (see Section 2.3). Whereas, in this case, we are facing with coexistence and interconnection problems that are required to develop interoperability and enable the SH concept.

3.2.1 Metrics Definition for Performance Evaluation

The first test that we will consider is meant to compare FSK and OFDM based NB-PLC solutions. To this end, we define two representative metrics, namely, the aggregate network throughput (THR) and the frame error rate (FER). Firstly, the THR is evaluated as

$$THR = \sum_{u=1}^{N} THR^{(u)} \quad [bps]\,, \tag{3.1}$$

where N is the number of network nodes and $THR^{(u)}$ is the average throughput achieved by the u-th node, which can be evaluated both for PHY and MAC layer as

$$THR^{(u)}_{\mathrm{PHY}} = 8m\hat{N}^{(u)}_{RX} \quad [bps]\,, \tag{3.2}$$

$$THR^{(u)}_{\mathrm{MAC}} = 8n\hat{N}^{(u)}_{RX} \quad [bps]\,, \tag{3.3}$$

where $\hat{N}_{RX}^{(u)}$ is the number of correct received frames per second by the u-th node, which are detected exploiting either the knowledge of the transmitted frame or the frame check sequence (FCS) field. Furthermore, m and n respectively represent the PHY payload length (data encapsulated at the PHY layer) and the MAC payload length (data from higher layer) expressed in bytes. Therefore, assuming that the number of nodes N goes to infinity, in Eq. 3.1 the THR goes to zero because all the nodes are simultaneously contending for the medium access so that, in the end, there is not any correct received frame. As it will be clarified in the following, we make use of a couple of NB-PLC modems, i.e., a transmitter and a receiver. Therefore, Equation 3.1 is calculated for $N = 2$, whereas the contribution of transmitter to the cumulative sum is equal to zero. In this perspective, the THR defined in Equation 3.1 corresponds to the average throughput of Equations 3.2 and 3.3.

Secondly, the FER can be obtained as

$$FER^{(u)} = \frac{N_{RXtot}^{(u)} - N_{RX}^{(u)}}{N_{RXtot}^{(u)}}, \tag{3.4}$$

where $N_{RXtot}^{(u)}$ and $N_{RX}^{(u)}$ are respectively the total number of frames and the number of correct frames received by the u-th node. We notice that the FER takes into account corrupted frames as well as missed frames. As it will be clarified in the following, for each modem under test, we can set the total number of transmitted frames ($N_{TX}^{(u)}$). Since we take into account a couple of modems ($u = 1, 2$), the number of transmitted frames set into transmitter corresponds to the total number of received frames by the receiver ($N_{TX}^{(1)} = N_{RXtot}^{(2)}$).

3.2.2 FSK-based System Details

To test a FSK NB-PLC solution, we use the hardware platform developed by ADD [36]. A general PHY frame encapsulation has the structure depicted in Figure 3.2 where the 6 bytes long preamble is used for synchronization, whereas the 2 bytes long header is used to define the type of frame. The following field

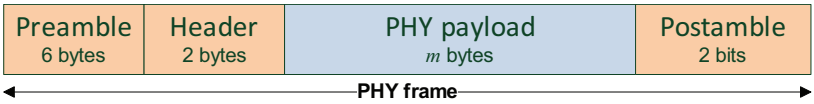

Figure 3.2: PHY frame format of a FSK-based system.

is represented by the payload. As shown in Figure 3.3, three different types of payload are available according to the error correction mechanism, namely, *low*, *medium* and *high* protection. Low protection (see Figure 3.3a) makes use of error detection FCS but drops any kind of error correction. Medium protection (see Figure 3.3b) introduces 6 bits of forward error correction (FEC) for every data byte making the system capable of correcting 3 bit error burst in a 14 bit block. High protection (see Figure 3.3c) exploits a convolutional encoder with bit interleaving. Finally, two bits of postamble terminate the frame. It is worth noting that each data byte in the payload is part of the

(a) Low protection: $m = 8\,(n+2)$ bits.

(b) Medium protection: $m = 14\,(n+2)$ bits.

(c) High protection: $m = 16\,(n+2)$ bits.

Figure 3.3: FSK-based payload structure for n data bytes.

higher layer frame, i.e., the MAC frame.

When showing numerical results, we set the hardware platform with the following parameters. The central frequency is set to 72 kHz with a working baud rate of 4800 *bps*. The two FSK tones are at frequency 69.6 kHz, and 74.4 kHz. Therefore, the system works in the CENELEC band A. Finally, we choose to transmit the maximum amount of data bytes, i.e., $n = 64$. Consequently, the payload length is set to $m = \{528, 924, 1056\}$ bits for low, medium

and high protection, respectively.

It is worth noting that FSK is also implemented in the KNX-PL132 standard [37] that is derived by the European Home Systems (EHS) protocol specifications [38].

3.2.3 OFDM-based System Details

To test an OFDM NB-PLC solution, we use a hardware platform developed by Maxim. According to [39], in Figure 3.4 we show a general PHY frame. The preamble is a multi symbol field used to perform carrier sense operations, to enable control functions and to synchronize the receiver and the transmitter. Then, the header field carries control information required to correctly demodulate the received signal. The combination of header, destination address (DA), source address (SA) and n data bytes is processed by a Reed-Solomon (RS) encoder which takes into account the transmission mode, i.e., *normal* or *robust*. In fact, the PHY payload length (m) is lengthen by 16 or 8 bytes of RS parity, respectively for normal or robust mode transmission. Moreover, in robust mode, besides RS encoder, there is a repetition code that repeats each bit following the preamble 4 times. Consequently, the PHY frame langth is the same for the two modalities since the repetition code. The PHY frame is terminated by 2 bytes of FCS for error detection purposes. The length of data is set to $n = 97$ bytes for the normal mode ($m = 113$ bytes), and $n = 8$ bytes for the robust one ($m = 16$ bytes).

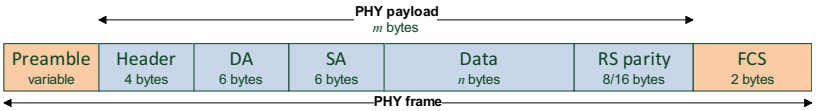

Figure 3.4: PHY frame format of an OFDM-based system.

The system works in the frequency band 32–95 kHz (CENELEC band A) and its specification are detailed in Table 3.1.

It is worth noting that the hardware platform tested implements part of the PHY and the MAC layer specifications taken from G3-PLC standard [28, 40].

Table 3.1: OFDM-based system specifications

Number of FFT points (N_{FFT})	256
Number of modulated carriers (N_c)	14
Number of overlapped samples (N_o)	8
Number of cyclic prefix samples (N_{CP})	60
Modulation	DBPSK, DQPSK
Sampling frequency (f_s)[MHz]	0.4
Number of preamble symbols (N_{pre})	9.5

3.3 FSK vs. OFDM

In order to compare the NB-PLC solutions above described, we performed two trial campaigns connecting, at each time, a couple of modems to two power sockets within a house.

The first campaign took place in a single floor house. Whereas, the second took place in a three-floor house, whose electricity is distributed from the main panel (MP) to each floor through a floor circuit breaker (CB) located at the MP. In the latter case, we considered either the transmission between outlets belonging to the same floor or between outlets belonging to different floors. Moreover, we considered a non-stationary scenario where appliances have been plugged and unplugged, e.g., television, washing machine, battery charger, fluorescent lamps, fridge, and so on.

During the test campaign, we considered different types of communication modes. More in details, for the FSK-based system we used low and high robust transmission, while for the OFDM-based system, we used normal and robust transmission modes.

Figure 3.5a and Figure 3.5b respectively show the complementary CDF (CCDF) of the throughput, and cumulative distribution function (CDF) of the FER for the FSK-based solution. Although not shown, we notice that no corrupted or lost frames have been observed using the FSK solution in the single floor house. Therefore, the throughput only depends on the modality by which the frames have been transmitted. The behavior changes when con-

sidering the multi floor house. As we can see, both the THR and the FER are much more degraded for channels belonging to the multi floor house. This is simply explainable observing that channels associated to multi floor houses cover in average larger distances than those in single floor houses, and they experience higher attenuation. We note the same behavior for OFDM (Figures 3.6a, and 3.6b).

Now, in Table 3.2, we report the average MAC throughput and FER values. From this table and Figures 3.5, and 3.6, we note that, in general, OFDM allows for higher peak or average throughput than FSK. However, it has also to be said that, FSK offers better robustness, where with robustness we mean the highest probable throughput value. For example, considering the multi floor case and FSK low/OFDM normal transmission modes, with probability equal to 0.9, FSK and OFDM respectively achieve a throughput of 2.079 $kbit/s$, and 0.055 $kbit/s$. Nevertheless, the choice between FSK and OFDM has to be done in conjunction with the required service.

Table 3.2: Average values for MAC throughput and FER.

	THR_{MAC} $[kbit/s]$		FER	
	Single Floor	Multi Floor	Single Floor	Multi Floor
FSK low	2.3098	2.2659	0	0.0190
FSK high	1.5208	1.5117	0	0.0060
OFDM normal	18.909	3.4345	0.0033	0.7856
OFDM robust	1.3198	0.3992	0.0010	0.6646

3.4 Interconnectivity and Range Extension

We now focus on the interconnection between NB-PLC and BB-PLC devices. Looking at Figures 3.6a and 3.6b, we see that OFDM shows very poor performance in terms of THR and FER. Analyzing the data, we notice that the highest performance degradation occurs during communication across different floors due to larger distances covered by PLC channels.

To cope with this problem, we introduce the testbed architecture, according to Figure 3.7. In details, the router is characterized by network adapters

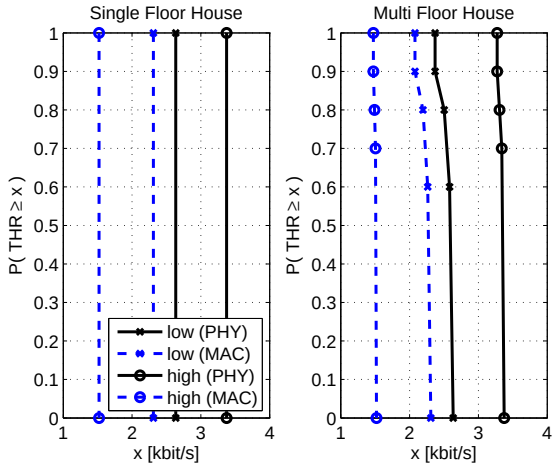

(a) PHY and MAC throughput for low and high robustness.

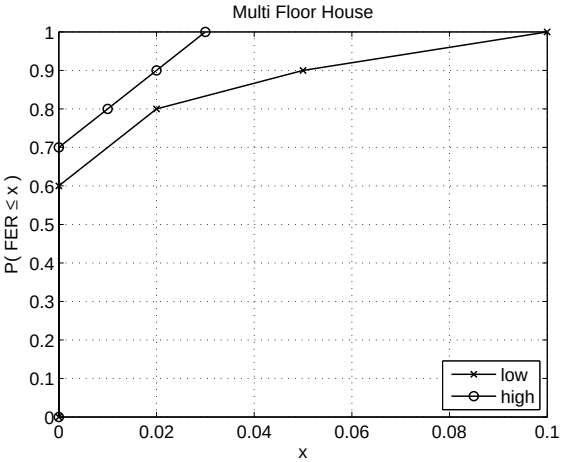

(b) FER for low and high robustness.

Figure 3.5: FSK-based system performances within single and multi floor houses.

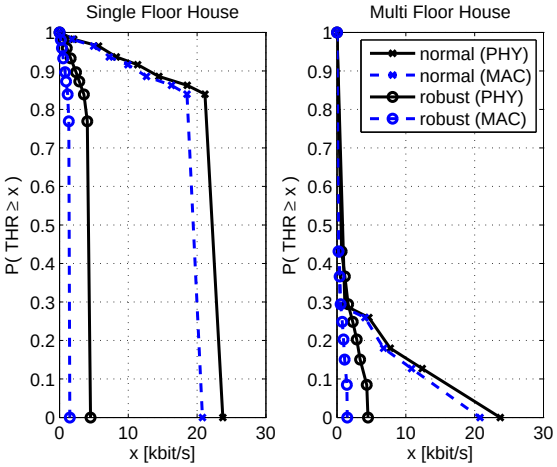

(a) PHY and MAC throughput for normal and robust mode transmission.

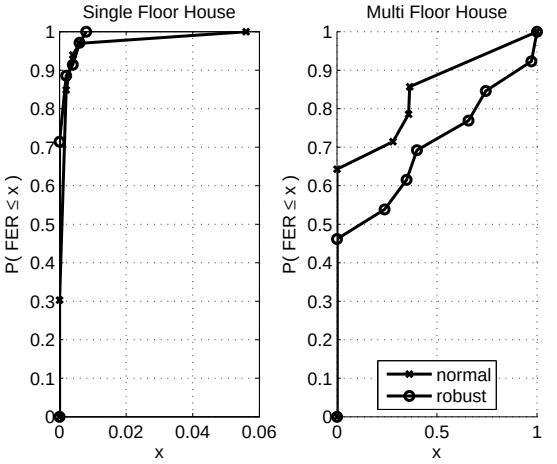

(b) FER for normal and robust mode transmission.

Figure 3.6: OFDM-based system performances within single and multi floor houses.

both towards NB-PLC, i.e., OFDM technology, and BB-PLC, i.e., HPAV technology, while the core unit is represented by a PC running ad-hoc network software. It is worth noting that the HPAV backbone can be considered as an Ethernet backbone since HPAV modems exhibit the Ethernet interface. Therefore, the use of the HPAV modems allows to extend the Ethernet backbone through different floors, while router functionalities provide the interconnection between OFDM and HPAV. In this perspective, the communications between OFDM modems (end node and router) takes place on the same floor (where PLC cables are shorter), while the communication across different floors (where PLC cables are longer) is handled by the Ethernet backbone. Hence, the frame goes from source to destination node throughout the logical path depicted in Figure 3.7 (red dotted line).

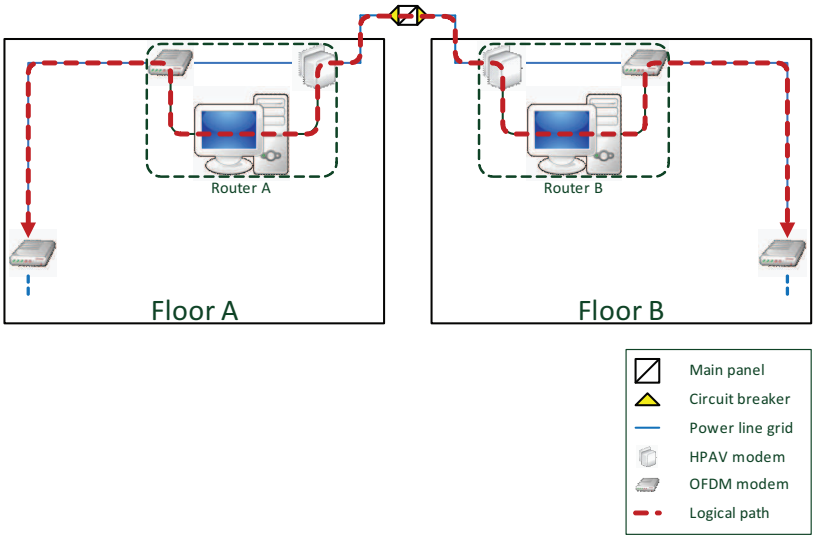

Figure 3.7: Testbed architecture for interconnectivity and range extension.

In Figures 3.8a and 3.8b are depicted the CCDF of the THR and the CDF of the FER (for the PHY layer), obtained using the HPAV extension. It is worth noting that there is a huge performance improvement.

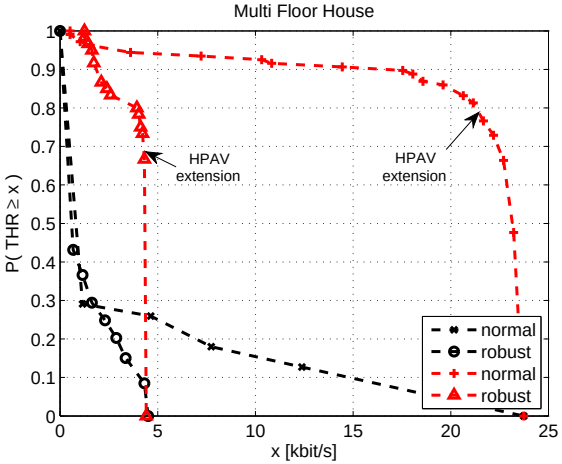

(a) THR for normal and robust mode transmission.

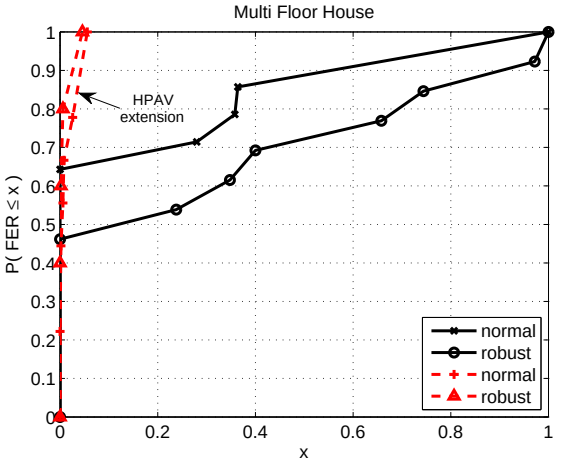

(b) FER for normal and robust mode transmission.

Figure 3.8: OFDM-based system performances within multi floor house with HPAV extension.

3.5 Main Findings

In this chapter, we have tested, in single and multi floor houses, two representative NB-PLC devices, i.e., one based on FSK and the other based on OFDM. Test results have shown that, although OFDM, in general, allows for higher peak throughput than FSK, it exhibits poor performance in terms of FER, thus throughput, when working in the multi-floor house. This issue has been solved developing a network testbed where BB-PLC devices are used to provide an Ethernet backbone that allows for (i) connectivity between NB-PLC and BB-PLC devices, and (ii) range extension.

Chapter 4

Enhancements of G3-PLC Technology for Smart Home Applications

To enable the smart grid (SG) concept, it is fundamental to consider the in-home/building context where, besides the conventional home networking services, home automation and smart energy management services have to be offered. Power line communication (PLC) is a key technology in this context since it exploits the power line grid that is pervasively deployed within houses/buildings. Thus, no new wire is needed, which reduces deployment costs.

In this chapter, we consider the in-home/building scenario, for which we apply a convergent network architecture to enhance the performance of the narrow band G3-PLC technology through its integration into an Ethernet network. To this end, we define the protocols characterizing the network modules, namely, switches and routers, which allow for integrating the G3-PLC with Ethernet devices. Since Ethernet represents a convergent standard for many communication devices, by adding this functionality to G3-PLC, interconnectivity with other heterogeneous nodes can be offered. Furthermore, since the G3-PLC medium access control layer is based on a carrier sense multiple access (CSMA) scheme, its performance decreases when the number of network nodes that contend for the channel increases. Therefore, we evaluate the network performance when a time division multiple access (TDMA) scheme is

adopted instead of CSMA. The proposed convergent network architecture has been implemented in the OMNeT++ network simulator.

4.1 Introduction

In the near future, the power grid needs to become a distributed large scale system that has to smartly manage flows of electricity produced by big or small plants, i.e., a SG. Demand side and demand response mechanisms have to be implemented, so that consumers and producers will actively collaborate in the use and delivery of energy [2, 3].

In this perspective, an important role is played by the communication technologies, which can enable, the smart home concept, i.e., the penetration of the SG within the home/building context, by means of smart management and monitoring of household appliances, control of local renewable energy plants (e.g., photovoltaic generators), monitoring of electric vehicles charge, etc..

Several NB-PLC solutions and standards have been developed with the SG concept in mind, e.g., the PRIME [29] and the G3-PLC [28] technologies for smart metering applications, the new IEEE P1901.2 and ITU-T Ghnem standard for SG applications [41]. However, we highlight that so far, only PRIME and G3-PLC solutions have been largely used, and in particular, for AMR.

In this chapter, we consider the G3-PLC solution, for which we propose enhancements at the medium access control (MAC) sub-layer to allow the implementation of SG applications that could potentially require higher data rate than AMR. The choice of considering the G3-PLC solution is motivated by the two following reasons. Firstly, it has been used as baseline technology for the development of the IEEE P1901.2 and ITU-T G.hnem standard [41]. Secondly, through field trial tests (see Chapeter 3), we found that the performance of NB-PLC may be poor in large houses where the signal is strongly attenuated because it spans large distances and crosses different circuit breakers (CBs), e.g., in multi-floor houses.

The first enhancement that we propose is a convergent network consisting

of different network devices, i.e., *end nodes*, *routers* and *switches*, to integrate G3-PLC with Ethernet devices. This, in turn, leads to an increased network coverage and improves the network throughput.

The second enhancement that we propose is the adoption of a contention-free MAC scheme based on time division multiple access (TDMA), instead of the CSMA with collision avoidance (CSMA/CA) scheme specified by G3-PLC. In particular, we implement an optimized version of the beacon-enabled mode of the IEEE 802.15.4 standard [42]. The reason behind the use of a TDMA scheme is that the performance of CSMA/CA decreases with an increasing number of network nodes.

The convergent network performance together with the TDMA scheme are evaluated through the implementation in the OMNeT++ network simulator [43]. Numerical results show considerable performance improvements in different network configurations.

The remainder of the chapter is as follows. In Section 4.2, we summarize the main characteristics of the OMNeT++ network simulator. Then, in Section 4.3 we discuss the G3-PLC and Ethernet characteristics. The convergent network implementation and its main devices are discussed in Section 4.4, while simulation setup and preliminary results are presented in Section 4.5. The TDMA optimization is presented in Section 4.6 together with extensive simulation results. Finally, in Section 4.7, we draw the main findings.

4.2 OMNeT++ Network Simulator

Network simulation is one of the most predominant evaluation methodologies in the field of computer networks. It allows to model a given computer network by specifying both the behavior of network nodes and the communication channel characteristics. Moreover, a simulation software platform allows for:

- Overcome problems related to hardware platforms.
- Integrate new communication technologies, architectures and protocols.
- Evaluate the network performance in peculiar conditions (e.g., varying the number of nodes).

- Analyze potentialities and boundary conditions of the network.

Most available network simulation toolkits are based on the paradigm of discrete event-based simulation (DES) [44]. The key concept of DES is represented by network nodes that trigger events. In particular, events are messages characterized by an execution time, and sent from nodes both to other nodes and to themselves. The simulator keeps trace of events maintaining a queue where events are sorted according to the scheduled execution time. The final simulation is performed by successively processing and executing the events in the queue.

OMNeT++ is an object-oriented modular DES framework. Differently from other network simulators, e.g., ns-2 [45], ns-3 [46], JiST [47], etc., OMNeT++ is not a real network simulator, but rather provides infrastructure and tools for writing simulations. However, according to [48], it is capable of carrying out large-scale network simulations in an efficient way, representing a smart choice for the SH implementation. Moreover, with its INET package [49], it provides a comprehensive collection of models for networking technologies, standards and protocols.

The basic idea of OMNeT++ is a component architecture for simulation models. Models are assembled from reusable components called *modules* which communicate with message passing. According to Figure 4.1, different module types are considered. The basic module is termed *simple module* (solid line) and its behavior is defined through C++ language exploiting the simulation class library of the same name. Simple modules can be grouped into *compound modules* (dotted line) and so forth. Finally, the top hierarchical level is represented by the *network*, which is special compound module without gates to the external world. It is worth noting that when a module type is used as a building block, there is no distinction whether it is a simple or a compound module. This allows the user to transparently split a module into several simple modules within a compound module, or, vice versa, concentrate the functionalities of a compound module in one simple module. Modules exchange messages typically through *gates* (blue box), but it is also allowed to send messages directly to the destination modules. Gates are the input and output interfaces

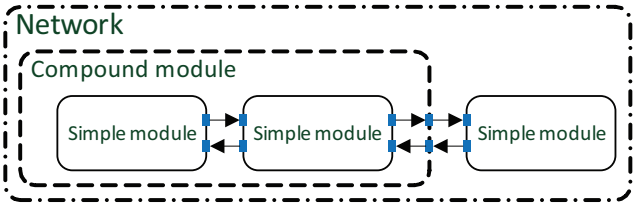

Figure 4.1: General model structure in OMNeT++.

of modules: messages are sent out through output gates and arrive through input gates. An input and an output gate can be linked with a connection (arrow). Connections are created within a single level of module hierarchy, i.e., within a compound module, corresponding gates of two submodules, or a gate of one submodule and a gate of the compound module can be connected. Connections spanning across hierarchy levels are not permitted since it would hinder reusability of modules. Modules can have *parameters* that are used to pass configuration data and to define model topology. Furthermore, connection can be characterized by properties such as propagation *delay*, *data rate* and *bit error rate*.

The structure of the model is defined by the user in network description (NED) language. NED allows simple module declarations, compound module definitions and network definitions. Simple module declaration describes the interface (gates) of the simple module and its parameters. Compound module definition consists of the definition of inner simple modules and their interconnection, in addition to the declaration of the external interface (gates) and parameters. Eventually, network definition is represented by the declaration of compound and simple modules that qualify the overall network, and the definition of parameters that have to be passed to modules. Hence, NED files also define the model topology.

Since the separation of different aspects of a simulation has to be achieved, model behavior is captured in C++ files, while model topology and parameters are defined by the NED files. However, in order to evaluate the simulation behavior with different inputs, the values assigned to network parameters may

differ according to different simulation runs. Therefore, these values may neither be assigned to the behavior (C++ code) nor the topology (NED files). To this aim, initialization (INI) files are used to store values of network parameters and specify a set of different values run by run.

4.3 Communication Technologies

In this section, we describe the communication technologies that have been take into account to realize the SH network simulation. In particular we focus on G3-PLC technology, i.e., the standardized version of with the OFDM-based system described in Section 3.2.3, and on Ethernet technology. Further details are discussed in the following.

4.3.1 G3-PLC

G3-PLC is thought to facilitate high-speed, highly-reliable, long-range communication over the existing power line grid for grid asset management, meter management, in-home energy display/management, electric vehicle charging, lighting automation, factory automation. It has been used as the basis and it is part of the IEEE P1901.2 [32] standard and the ITU-T G.hnem [33] standard for SG applications.

Its PHY and MAC layers specifications were completed in 2009 and are briefly discussed in the following.

According to [50], the G3-PLC technology has been designed to support CENELEC bands in the frequency range 3–148.5 kHz and FCC band in the frequencies range 9–490 kHz. In detail, CENELEC specifies four frequency bands: the band A (3–95 kHz) that is reserved exclusively to power utilities, the band B (95–125 kHz) can be used for any application, the band C (125–140 kHz) is dedicated to in-home networking systems, the band D (140–148.5 kHz) is reserved to alarm and security systems. Besides this classification, G3-PLC is able to work in a combination of two or more CENELEC bands, i.e., BC, BCD and BD.

The block diagram of the G3-PLC transceiver, depicted in Figure 4.2,

highlights the use of pulse shaped OFDM (PS-OFDM) technique combined

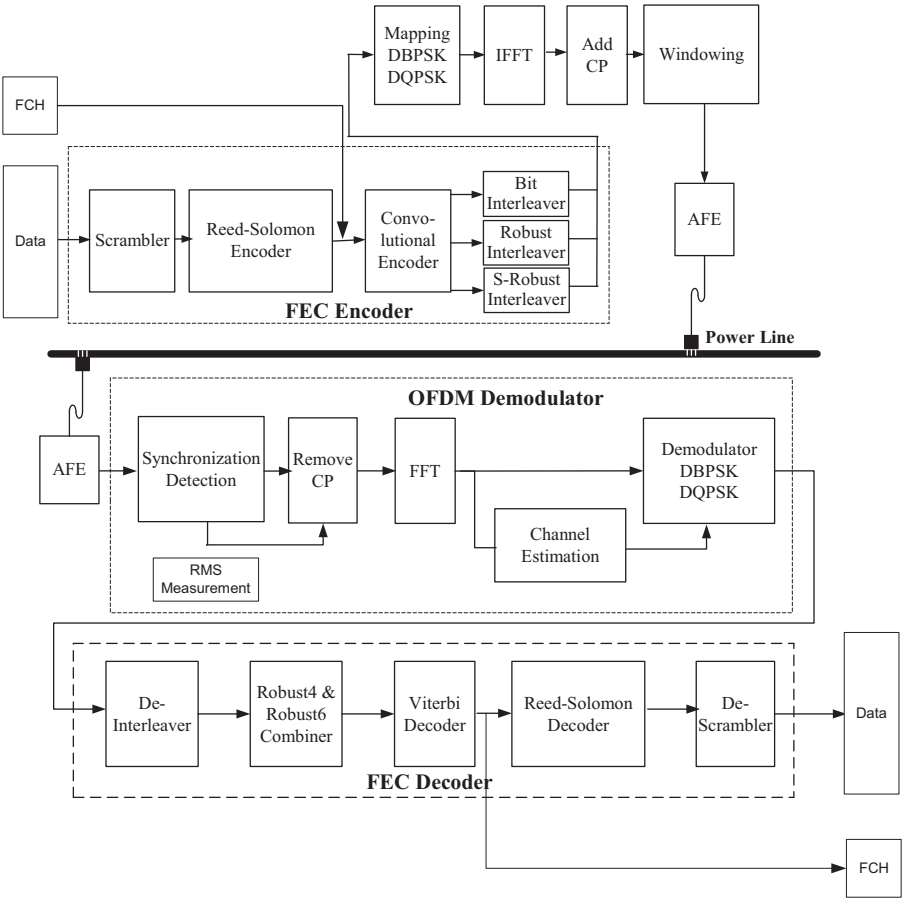

Figure 4.2: Block diagram of G3-PLC transceiver [28].

with a differential BPSK (DBPSK) or differential QPSK (DQPSK) modulation scheme where the phases of carriers in the adjacent symbol are taken as reference for detecting the phases of the carriers in the current symbol. Two different transmission modes are allowed, namely, *normal* and *robust*. In normal mode, FEC encoding (thus decoding) is composed of a RS and a convolutional encoder, while, in robust mode, beside RS and convolutional

encoding, there is a repetition code (RC) that repeats each bit following the preamble 4 times, making the system more robust to channel impairments. It is worth noting that normal and robust transmission mode are related to DBPSK modulation, while DQPSK always performs in normal mode.

The PHY frame format, depicted in Figure 4.3 (bottom), is characterized by (i) the preamble, which is a multi symbol field used to perform carrier sense operations, to enable control functions and to synchronize the receiver and the transmitter, (ii) the frame control header (FCH), which carries control information required to correctly demodulate the received signal, and (iii) the PHY payload, namely, the PHY service data unit (PSDU). It is worth noting that the PHY payload length (n) depends on the transmission mode, i.e., normal and robust.

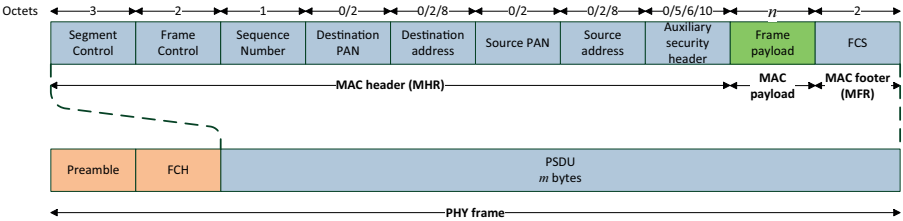

Figure 4.3: General PHY and MAC frame format for G3-PLC technology.

When showing simulation results, we consider G3-PLC working in the CENELEC band A[1]. In this case, it uses PS-OFDM with a raised cosine window, and 36 out of 256 sub-channels are used in the 35.9–90.6 kHz frequency band. Furthermore, we assume that each PHY frame is composed of 40 PS-OFDM symbols, each carrying data modulated with DQPSK. This assumption respectively leads to 163 bytes of data and 16 RS parity check bytes. Consequently, the maximum achievable bit-rates is 30.4 $kbps$. Table 4.1 reports other reference PHY layer parameters for the CENELEC band A.

According to [40], the MAC sub-layer is based on the IEEE 802.15.4–2006 specifications for low-rate wireless personal area network (WPAN) [42].

[1]Despite the fact that CENELEC-A is generally not used for home networking, performance is not significantly affected by the operating band.

Basically, the channel access method is based on CSMA/CA mechanism and a random backoff time. The general MAC frame format, depicted in Figure 4.3 (top), is substantially based on the 802.15.4–2006 specifications, except for the *segment control* field, which is defined in [40] and is used for tone mapping, contention handling and segmentation purposes.

When showing simulation results, we assume a minimum MAC overhead of 8 bytes. Therefore, according to the amount of data bytes defined in the PHY, the maximum MAC payload is 155 bytes in normal mode. For the sake of implementation simplicity, we assume that the transmission does not wait for any acknowledge (ACK) frame reception. Table 4.1 reports other MAC layer reference parameters.

Table 4.1: G3-PLC reference parameters.

Number of IFFT/FFT points (M)	256
Number of modulated carriers (N_c)	36
First modulated carrier frequency (f_1) $[kHz]$	35.938
Last modulated carrier frequency (f_2) $[kHz]$	90.625
Available bandwidth ($f_2 - f_1$) $[kHz]$	54.688
Sampling frequency (f_s) $[MHz]$	0.4
Frequency spacing(f_s/M) $[kHz]$	1.5625
Number of overlapped samples (N_o)	8
Number of cyclic prefix samples (N_{CP})	30
Number of FCH symbols (N_{FCH})	13
Number of preamble symbols (N_{pre})	9.5
Preamble duration $[ms]$	6.08
PS-OFDM symbol duration $[\mu s]$	695
Number of PS-OFDM symbols per PHY frame (N_s)	40
PHY frame duration $[ms]$	42.9
PSDU dimension (m) $[bytes]$	179
MAC overhead $[bytes]$	8
MAC payload dimension (n) $[bytes]$	155
Maximum PHY data rate $[kbps]$	30.4

4.3.2 Ethernet

Nowadays, Ethernet, namely IEEE 802.3, is the most widely deployed technology for HAN and LAN. As mentioned in Section 2.4, IEEE 802.3 specifications offer a convergent LLC sub-layer (defined in IEEE 802) for many different PHY layers and MAC sub-layers, e.g., coax, twisted pair as well as optical fiber and wireless. The Ethernet frame format is depicted in Figure 4.4. The preamble,

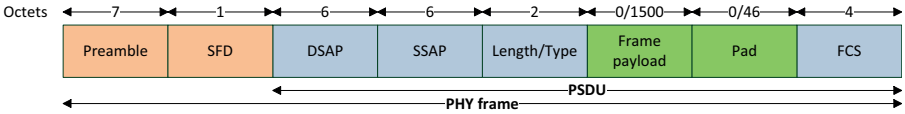

Figure 4.4: Ethernet frame format.

which is used for synchronization purposes, is followed by the starting frame delimiter (SFD). Then, destination service access point (DSAP) and source service access point (SSAP) respectively represent the destination and source MAC address. Since the frame payload can vary between 0 and 1500 bytes, there is padding field in order to ensure the minimum PHY payload length, i.e., 64 bytes. The frame is ended by a FCS for error detection.

Although Ethernet provides specifications for different communication media, when showing simulation results we consider the Fast Ethernet 100BASE-TX over Cat 5 cables (IEEE 802.3u) since it is the most deployed in today's HANs. Furthermore, we assume the full duplex operation mode: the network is switched thus the connections are handled point-to-point and cannot be shared by multiple devices. Therefore, the full duplex mode eliminates CSMA with collision detection (CSMA/CD) mechanisms because there is no need to determine whether the connection is already being used. However, is mandatory to consider an additional network device, namely, the switch, that enables the full duplex point-to-point connection among Ethernet nodes. Further details about 100BASE-TX are listed in Table 4.2.

Table 4.2: 100BASE-TX reference parameters.

PHY data rate $[Mbps]$	100
Bit time $[ns]$	10
Minimum PHY payload dimension $[bytes]$	64
Maximum PHY payload dimension $[bytes]$	1518
Minimum PHY frame duration $[\mu s]$	5.76
Maximum PHY frame duration $[\mu s]$	121.44

4.4 Convergent Network Implementation

In order to reproduce the testbed presented in Chapter 3, we have to integrate an Ethernet network with a G3-PLC network. As previously mentioned, modern Ethernet networks are switched, hence, they exhibit a star topology. On the other hand, G3-PLC networks exhibit a bus topology. Therefore, the resulting network architecture can be thought as a combination of bus and star, i.e., a tree topology (see Figure 4.5).

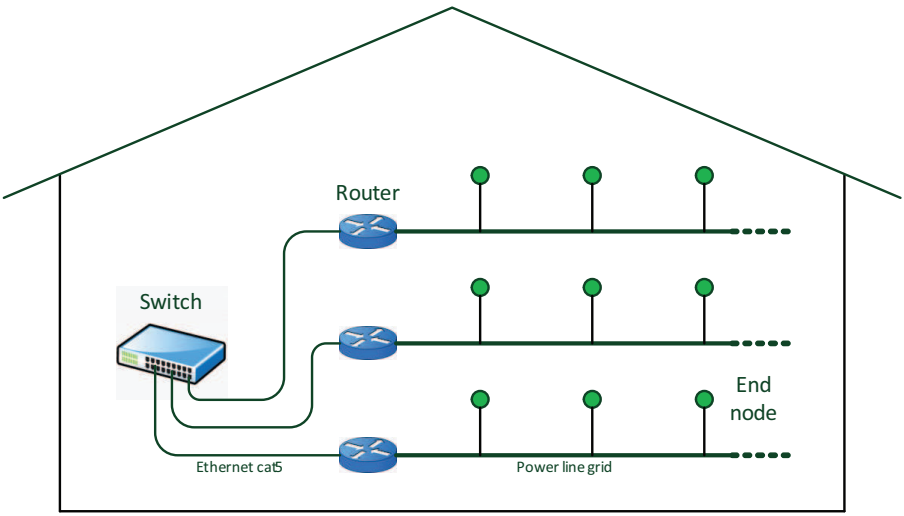

Figure 4.5: Convergent network architecture.

4.4.1 Network Devices

In this perspective, the integration between Ethernet and G3-PLC is achieved by means of the definition and the implementation of a shared common layer placed on top of DLL. In particular, a relevant role in achieving convergence and is played by the router and the switch as described in the following.

End Node

They represent the devices of the network that directly interact with the surrounding environment, e.g., sensors, actuators, switches, meters and so on. These nodes are grouped into subnetworks according to the same communication technology, i.e., G3-PLC. From a logical point of view, the end nodes can be all characterized by the same building blocks, i.e., a traffic generator (which is responsible of data packets generation) and the network adapter. The network adapter comprises a PHY, a MAC, and a buffer of data packets coming from the traffic generator.

Router

Since G3-PLC does not provide any specification for the integration in a switched Ethernet network, we need a network device that groups G3-PLC nodes into a subnetwork and integrates the subnetwork with the rest of the Ethernet network. To do that, we define a router that offers network adapters towards both Ethernet and G3-PLC. Beside the network adapters, the Router has a routing module that is responsible of translating and forwarding packets from one network adapter to the other and vice versa: this module is responsible of interconnectivity between Ethernet and G3-PLC. It is worth noting that since the maximum allowed G3-PLC PHY frame size is 251 bytes (corresponding to a payload of 235 data bytes both in DQPSK and DBPSK normal mode [28]), the router encapsulates each G3-PLC frame into one Ethernet frame, whose maximum frame payload dimension is 1500 bytes. On the other side, Ethernet frames exceeding 251 bytes are fragmented by the router in order to fulfill G3-PLC constraints. However, this assumption is not necessarily optimal.

As depicted in Figure 4.6, the routing module keeps trace of packets received from its subnetwork nodes, and it generates a forwarding table with *source address*, *insertion time*, and *link quality*. In this perspective, the router dynamically learns about the existence of nodes during reception of packets and modifies its table updating the link quality or removing aged entries, ac-

cording to the insertion time. It is worth noting that a given subnetwork can be managed by two (or more) routers in order to ensure a more reliable communication on harsh power line channels, or equally, to increase the network coverage. Furthermore, in order to prevent loops, the router is able to recognize and discard packets directly arrived from other routers.

Switch

The switch is a well-known network device. As depicted in Figure 4.7, the switch has been modified in order to work seamlessly with the routers. In particular, it is able to build and update a forwarding table exploiting nodes information harvested by each router. A forwarding table entry is composed by *source address*, *insertion time*, *link quality* and arrival *port number*. Therefore, the switch compares the information carried by a packet with the correspondent table entries and forwards the packet to the correct port (or broadcast if the destination address has no correspondence in the table). In this case, the insertion time parameter is exploited to remove aged entries from the table and thus increasing the system fault tolerance. Again, the switch is able to prevent packet loops. We also point out that since link quality is updated periodically, the switch is able to dynamically handle the network changes. It is now clear that the combination of the router and switch procedures enables the integration of heterogeneous communication technologies leading to a convergent network. Moreover, this combination provides the basis for satisfying quality of service (QoS) constraints.

It should be finally noted that the integration of G3-PLC with Ethernet easily allows for integrating the G3-PLC technology in IP networks.

4.5 Simulation Setup and Preliminary Results

In order to quantify the network performances, we exploit the representative metric defined in Equation 3.1, namely, the aggregate network throughput (THR). To this respect, we notice that it has been evaluated at MAC layer, thus considering the Equation 3.3. Moreover, in order to model the power

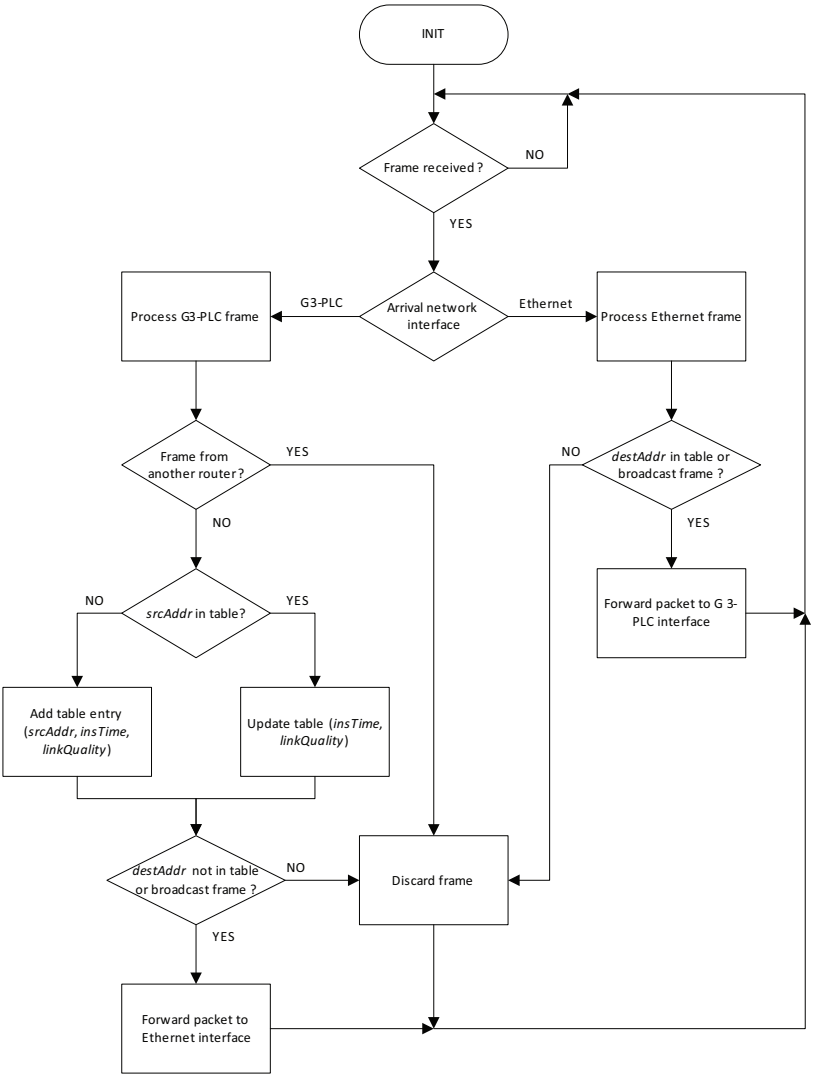

Figure 4.6: Router flow chart.

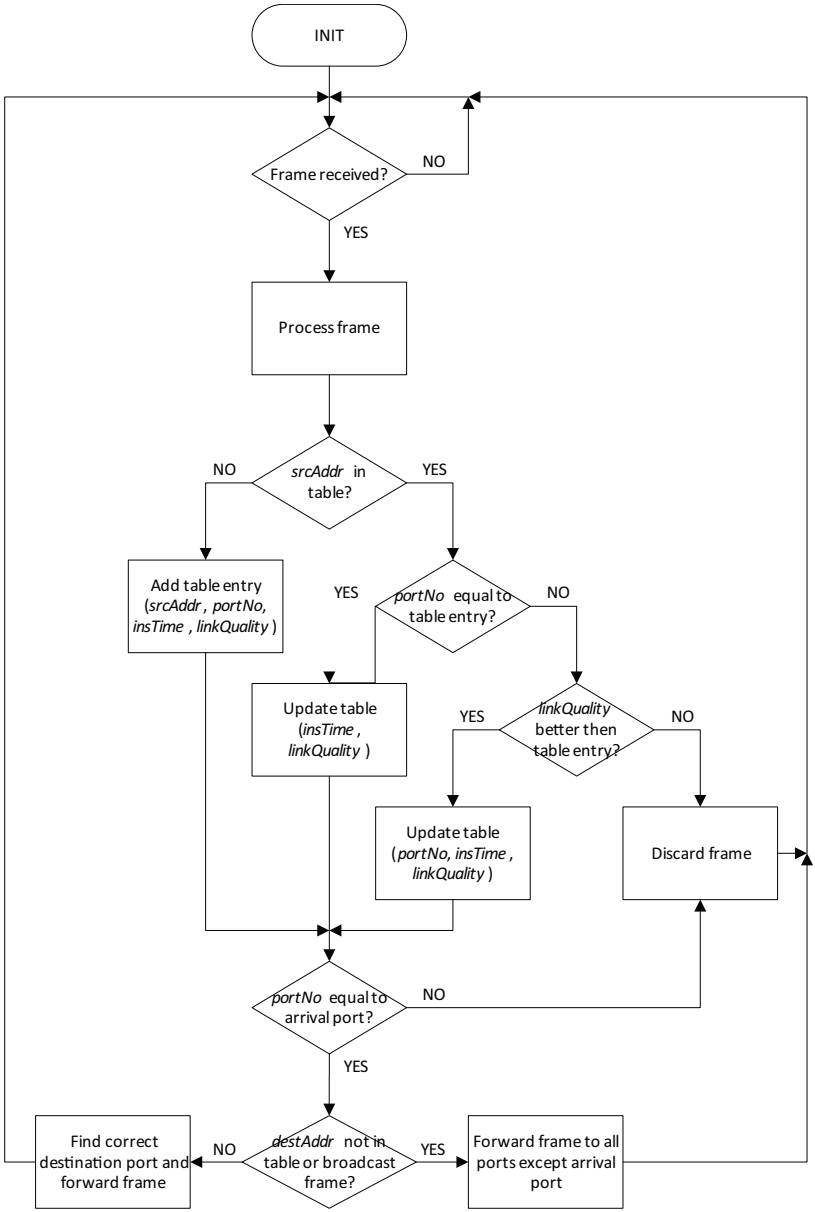

Figure 4.7: Switch flow chart.

line channel characteristics in the OMNeT++ implementation, we make use of FER obtained during field test campaign performed with the testbed.

Figure 4.8 shows the CDF of FER for normal and robust mode for single and multi floor house. From the obtained results, we computed the distribution of the FER. In particular, for the single floor house, the FER can be assumed to be exponentially distributed with mean equal to 0.0024 and 0.001, respectively for normal DQPSK and robust DBPSK mode. Regarding the multi floor house, we model the FER as uniformly distributed in the range (0.6429, 1) or (0.4615, 1), respectively for normal DQPSK and robust DBPSK mode. The obtained statistics are depicted in Figure 4.8 (red dotted lines). As regards

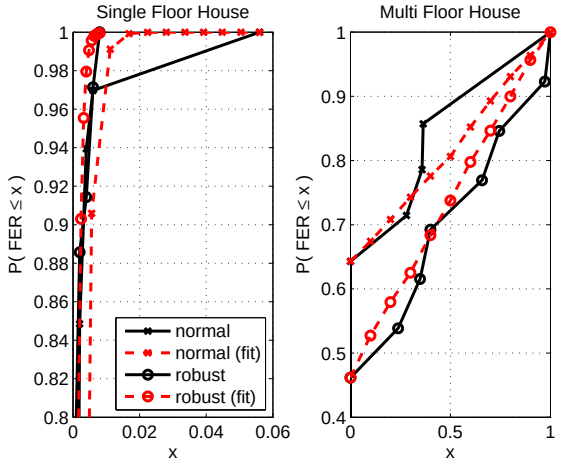

Figure 4.8: CDF of the measured FER for G3-PLC technology. The distribution fitting is also shown.

Ethernet network, we assume cat5 cables ideal from the FER point of view, while the propagation delay is assumed 500 *ns*.

It is important to note that in the case of a multi floor house, the G3-PLC network can be naturally split into several subnetworks, one for each floor. The subnetworks can afterwards be interconnected through Ethernet. The same architecture can be used in large buildings that may already have a wired Ethernet deployment.

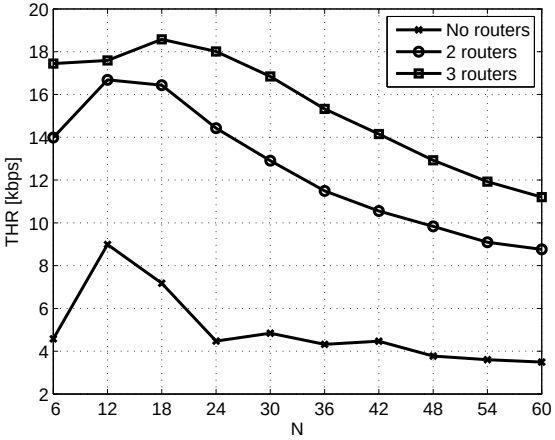

Figure 4.9: Simulated THR for different network configurations.

We now turn our attention to the convergent network behavior. To do that, we consider the THR in saturation condition, which is defined as the limit reached by the THR when the offered load increases, and it represents the maximum load that the system can carry [51]. In saturation conditions, each node has immediately a packet available for transmission, after the completion of each successful transmission. We build the simulation scenario using from 6 up to 60 G3-PLC nodes and we evaluate the THR when no routers are introduced, and when two and three routers – e.g., one per each floor, – are considered. The traffic is point-to-point and is generated such as the destination address belongs to a node inside the same subnetwork or to a different subnetworks with respect to source node (when routers are present). In this perspective the traffic model can be considered peer-to-peer. Figure 4.9 shows the THR. As we can see, the introduction of 2 and 3 routers substantially improves the performance. It is worth noting that the THR improvements directly translates in a coverage increase.

4.6 Further Improvements Using Time Division Multiple Access

Despite the THR improvements related to the introduction of routers, the bottleneck of the network is represented by the degradation of the performance with the increasing number of G3-PLC nodes within each subnetwork (see Figure 4.9). To prevent this occurrence, we envision the G3-PLC communication technology proposing a different channel access method that provides a higher QoS, namely, time division multiple access (TDMA). To do this, we implement the *beacon-enabled* mode of the IEEE 802.15.4–2006 specifications [42]. It defines a *superframe* structure as depicted in Figure 4.10. Each superframe is de-

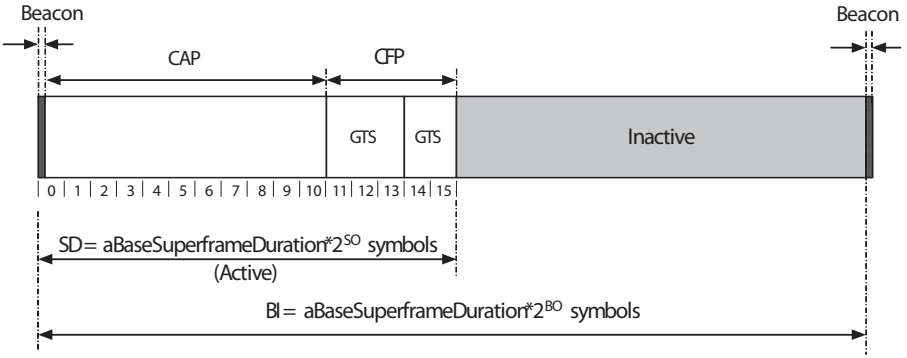

Figure 4.10: An example of superframe structure [42].

fined by the beacon order (BO), it lasts $BI = aBaseSuperframeDuration * 2^{BO}$ OFDM symbols, and it is characterized by an active and an inactive part. The active part, which is defined by the superframe order (SO), lasts $SD = aBaseSuperframeDuration * 2^{SO}$ OFDM symbols, and it consists of a contention access period (CAP) and a contention-free period (CFP). The BO, and the SO values are related according to $0 \leqslant SO \leqslant BO \leqslant 14$. In the CAP, the channel access is based on CSMA/CA, while during the CFP, it is based on TDMA. The active portion of each superframe is divided into a number of time slots equally spaced, whose duration is given by $aBaseSlotDuration = N_s + aInterFrameSpacing$, where N_s is the number of OFDM symbols in a G3-PLC frame (see Table 4.1), and $aInterFrameSpacing$

is the interframe space within two time slots. The CFP grows or shrinks dynamically fulfilling the minimum CAP length of 440 OFDM symbols. We denote with N_{TStot} the number of time slots present in the CFP. It is worth noting that the beacon frame, which is periodically sent by a WPAN coordinator for synchronization purposes, can be replaced by the synchronization with the mains cycle.

Table 4.3 reports the values of the parameters used for the beacon-enabled mode simulations.

Table 4.3: Superframe parameters and values.

Parameters	Value
$SO = BO$	1, 2, 5
$aBaseSuperframeDuration$	$aBaseSlotDuration * aNumSuperframeSlots$
$aBaseSlotDuration$	$N_s + aInterFrameSpacing$
$aInterFrameSpacing$	10
$aNumSuperframeSlots$	16

Now, in order to maximize the THR, each subnetwork coordinator, represented by a router, assigns a guaranteed time slot (GTS) – which lasts one or more time slots, – to each node that wants to transmit, by solving the following optimization problem

$$\begin{aligned} \max_{\underline{N}_{TS}} \quad & \sum_{u=1}^{N} \frac{N_{TS}^{(u)}}{N_{TS_{tot}}} THR^{(u)} \\ \text{s.t.} \quad & \sum_{u=1}^{N} \frac{N_{TS}^{(u)}}{N_{TS_{tot}}} = 1, \\ & \frac{N_{TS}^{(u)}}{N_{TS_{tot}}} THR^{(u)} \geq p^{(u)} THR^{(u)} \quad \forall u = 1, \ldots, N, \end{aligned} \tag{4.1}$$

where N is the number of nodes, $N_{TS}^{(u)}$ is the number of time slots assigned to node u, and $\underline{N}_{TS} = \left[N_{TS}^{(1)}, N_{TS}^{(2)}, \ldots, N_{TS}^{(N)}\right]$. Furthermore, $THR^{(u)}$ is considered as the MAC throughput of node u in *bps*, according to Equation 3.3. It can also be obtained as $THR^{(u)} = 8n\left(1 - FER^{(u)}\right)/T_s$, where T_s denotes the time slot duration in seconds and $FER^{(u)}$ is according to Equation 3.4.

$p^{(u)} \in [0, 1]$ are QoS coefficients, each indicates the percentage of the throughput that the u-th node has to achieve w.r.t. the one that it would achieve in the corresponding single user scenario. Finally, the condition in the second line of (6.1) forces all the time slots in a CFP to be used.

Problem (6.1) is an integer linear programming problem. Therefore, it is, in general, NP hard. To simplify the problem, we solve (6.1) using linear programming (LP) and we round the obtained coefficients to the lower closest integer value. Clearly, there could be cases where the number of slots assigned to one or more nodes is zero. In these cases, the correspondent nodes are deferred to transmit in the CAP. Furthermore, when some time slots are not occupied as result of the rounding of the coefficients, these will be assigned to the nodes that have the highest throughput, leaving the CAP free of transmissions. Finally, we assume $\sum_{u=1}^{N} p^{(u)} \leq 1$. The latter assures that the LP always give a feasible solution if $N \leq N_{TS_{tot}}$.

It is easy to prove (see Appendix 8.1) that when $\sum_{u=1}^{N} p^{(u)} = 1$, e.g., $p^{(u)} = 1/N$, the optimal solution to (6.1) can be found imposing the Karush Kuhn Tucker (KKT) conditions [52] and is given by $N_{TS}^{(u)} = N_{TStot}/N, \quad \forall u = 1, \ldots, N$. In the following, we assume the last condition holds true.

Now, in Figure 4.11, we show the THR, when no router is present, obtained using CSMA/CA and the proposed TDMA with $FER^{(u)} \sim \mathcal{U}\,(0.6429,\ 1)$ (top) and $FER^{(u)} \sim \mathcal{E}\,(0.0024)$ (bottom), respectively corresponding to multi and single floor hose. The results are shown for $SO = BO = \{1,\ 2,\ 5\}$, namely for superframe duration of $\{1.72,\ 3.43,\ 27.47\}\,s$, or equally for a number of allocable GTS equal to $\{23,\ 55,\ 503\}$. We notice that we have not found any substantial improvement for value of SO greater than 5.

Figure 4.12 and Figure 4.13 show the comparison between TDMA and CSMA/CA when 2 and 3 routers are used. In this case, it is assumed $FER^{(u)} \sim \mathcal{E}\,(0.0024)$.

From Figs. 4.11, 4.12, 4.13 we derive the following observation.

- In general, the TDMA scheme allows a substantial increase of the aggregate network throughput w.r.t. CSMA, even when SO is equal to 1.

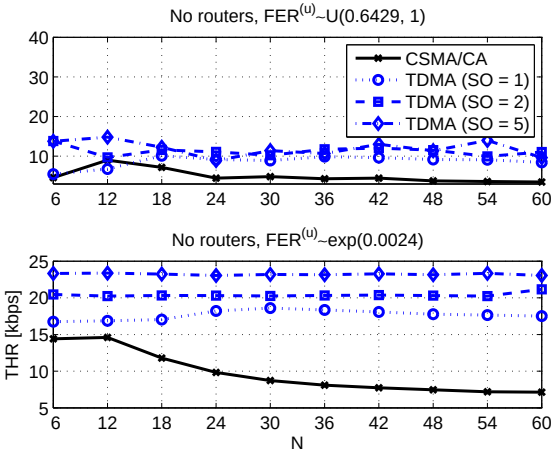

Figure 4.11: THR comparison between CSMA/CA and TDMA for a network configuration without routers.

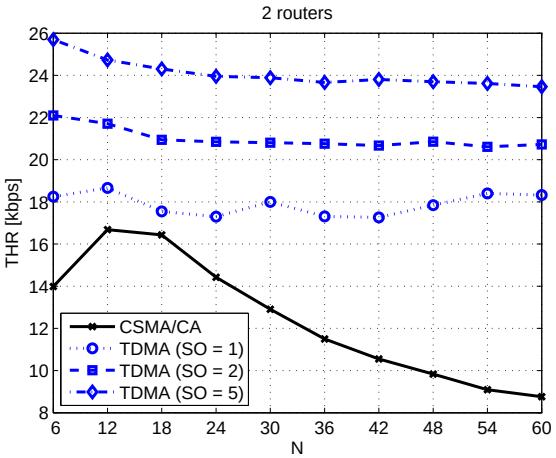

Figure 4.12: THR comparison between CSMA/CA and TDMA for a network configuration with 2 routers.

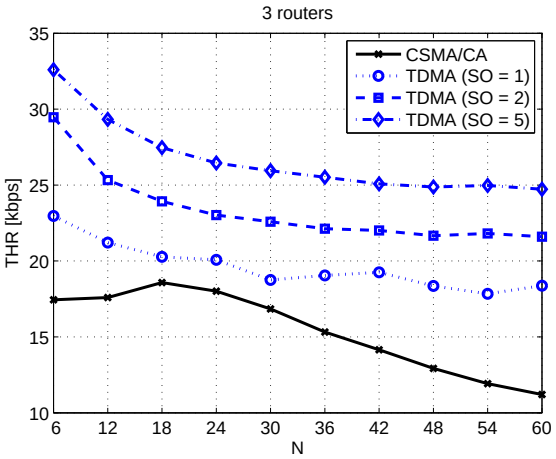

Figure 4.13: THR comparison between CSMA/CA and TDMA for a network configuration with 3 routers.

- The use of TDMA solves the bottleneck problem of CSMA represented by the considerable degradation of the performance with the increasing number of nodes within each subnetwork.

- The minimum CAP length constraint, specified by the 802.15.4 standard, affects the behavior of the aggregate throughput in two ways. Firstly, there is an improvement of the throughput increasing the number of time slots (namely SO). This is because, in many cases the largest part of the CAP is not used and thus by increasing the duration of the superframe, the impact of the CAP on the throughput decreases. Secondly, the throughput exhibits a faster decay when considering 2 and 3 routers w.r.t. the no router case. This is because the negative effect of the CAP is present in each sub-network, namely twice or three times, respectively.

- The aggregate network rate increases by increasing the number of routers. This is because the same resources are shared within each subnetwork by a smaller number of nodes.

We now focus on the $THR^{(u)}$, i.e., the throughput achieved by the single network nodes at MAC layer, according to Equation 3.3. Figure 4.14 shows the throughput achieved by each network node when three routers are deployed (see Figure 4.13). From Figure 4.14, we note the following.

- The throughput achieved by each network node with TDMA is always higher than that of CSMA.
- CSMA appears more fair than the considered contention-free approach. In fact, in TDMA, the variance of $THR^{(u)}$ is higher than in CSMA.

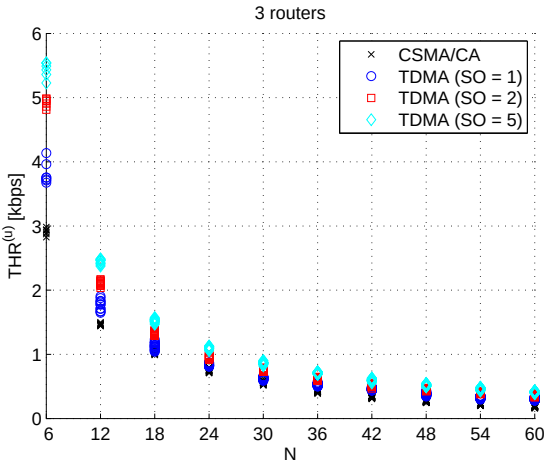

Figure 4.14: Throughput achieved by each node in a 3 routers network using CSMA/CA or TDMA.

4.7 Main Findings

In this chapter, we have found that the performance of G3-PLC can be substantially improved in-home/building scenarios by enhancing its MAC sublayer. In particular, we propose a convergent network architecture that allows the integration of G3-PLC with Ethernet in order (a) to cope with the strong channel attenuation that is present in houses/buildings where the signal crosses

circuit breakers, and (b) to increase the available resources by splitting the network in sub-networks. Although the convergent network leads to a substantial increase of the aggregate network throughput, its performance appreciably decrease with the increase of the number of network nodes. This is mainly due to the use of the CSMA/CA MAC scheme of G3-PLC. Therefore, we propose and implement a contention-free MAC scheme, namely a TDMA, based on an optimized version of the beacon-enable mode of the IEEE 802.15.4. Numerical results show that TDMA allows to solve the problem of CSMA related to the increasing number of nodes, and further allows to increase the THR.

Chapter 5

Cross-Platform Simulator for In-home G3-PLC Evaluation

In this chapter, an innovative cross-platform simulator that allows to realistically simulate the G3-PLC technology up to the network layer is presented. The proposed cross-platform consists of two different simulators jointly connected: one for the physical (PHY) layer and one for the data link layer (DLL)/ network layer (NL). The PHY layer simulator is implemented in MATLAB, while the DLL/network simulator in OMNeT++. A convergent network architecture that permits the integration of the G3-PLC technology within a switched Ethernet network is also presented with the aim of improving the G3-PLC performance in large scale houses/buildings. The performance of the considered communication technology are presented through extensive numerical results for the in-home application scenario.

5.1 Introduction

In the last years, we have observed a widespread deployment of distributed renewable energy sources (DRESs). These are meant to accommodate the future growth of electricity demand, to produce clean energy, to save power and to lower carbon emissions. However, the presence of DRESs has also a direct impact on the electricity grid. In fact, the electricity grid model is

changing: from a grid where electricity was distributed from the bulk generation to the customers, the electricity grid is becoming a smart grid (SG), namely a large-scale system of systems that needs to smartly manage flows of electricity produced by big or small plants. As a consequence, in addition to the use of more advanced electrical power components, the modernization of the power grid involves an extensive use of information and communication technology (ICT) tools over different domains [53]: *generation*, *transmission*, *distribution*, and *customer*. Therefore, from a communication point of view, the SG can be seen as a communications network that needs to deliver flows of data to offer several services over these domains [54]. Some representative examples of services are: automatic meter reading (AMR), meter events and alarms, substations automation, microgrids integration, demand response through the smart management and monitoring of household appliances, control of local renewable energy plants (e.g., photovoltaic generators), managing the charge of plug-in electric vehicles, etc.. To offer this plethora of services is fundamental to adopt/develop adequate communication technologies capable of satisfying the communication requirements of each service, e.g., throughput, packet error rate, end-to-end delay, etc..

Although finding the best communication technology for SG applications is not straightforward, recently, industries and standardization organizations have proposed the use of narrow band (NB) power line communication (PLC) technology as a cost-effective solution to support the development of the SG concept. Several solutions and standards have been conceived and developed for this scope. Among them, G3-PLC [28] is playing a significant role inasmuch it has been used as the basis for the development of the IEEE P1901.2 [32] and the ITU-T G.hnem [33] standards for SG applications. G3-PLC is thought to facilitate "high-speed", highly-reliable, long-range communication over the existing power line grid for grid asset management, meter management, in-home energy display/management, electric vehicle charging, lighting automation, and factory automation. Therefore, it has been developed to be used either for indoor or outdoor applications. In this context, it is fundamental to have a tool that enables the simulation and thus the prediction of the behavior of

such a technology over different scenarios.

In this chapter, we propose the use of a cross-platform simulator that allows to realistically simulate the G3-PLC technology. We consider the customer's domain as application scenario, and in particular the in-home scenario. The choice of the application scenario is dictated by its challenging nature. In fact, apart from energy management services, the customer's domain requires the joint delivery of home networking and automation services in order to realize the so called smart home (SH) concept, where different communication technologies need to be integrated in a convergent manner and be interoperable.

Although several network simulators are nowadays available, e.g., ns-2, ns-3, OMNeT++, JiST and SimPy, a comprehensive implementation and simulation of a G3-PLC system has not been performed yet. This is because of the implementation issues related to physical (PHY) layer modeling within a network simulator, which has not been thought for these purposes. In fact, PHY modeling exploits signal processing techniques whose integration in network simulators is rather costly from a computational point of view. Furthermore, the computational complexity grows with the number of considered communication technologies and network devices. On the other hand, network simulators are well suited for higher layers simulation, e.g., medium access control (MAC) algorithms, network procedures and transport protocols, and are optimized for these purposes [48].

The proposed cross-platform consists of two different simulators: one for the PHY layer and one for the data link layer (DLL)/network layer (NL). The PHY layer simulation is performed using MATLAB and is meant to estimate the frame error rate (FER). The obtained FER is used to abstract the PHY layer within the DLL/NL simulator. The network architecture and devices have been implemented using OMNeT++ [43] and its extension, the INET-Framework [49].

The chapter contributions are summarized as follows:

- A simulation procedure is proposed. To be more precise, the proposed model allows its application to any system, despite its initial focus on a given application technology.

- A convergent network architecture that enables the integration of the G3-PLC technology within a switched Ethernet network is suggested to increase the network performance in large scale houses/buildings.

- The evaluation of the performance for the considered technology are presented considering a real scenario. In particular, the PHY layer simulation adopts the results of a channel/noise measurement campaign that has been carried out in a house.

- Several metrics are considered to present the results: (i) aggregate network throughput, (ii) end-to-end delay, (iii) frame drop rate, and (iv) number of corrected received frames.

The remainder of the chapter is as follows. In Section 5.2, the G3-PLC technology is described. Then, the cross-platform simulator is presented in Section 5.3. Extensive numerical results are reported in Section 5.4. Finally, the main findings follow in Section 5.5.

5.2 G3-PLC Communication Technology Further Details

The PHY and MAC layer specification of G3-PLC has been previously discussed in Chapter 4 focusing on CENELEC band A. However, the G3-PLC technology has been designed to support CENELEC bands in the frequency range 3–148.5 kHz as well as FCC band in the frequencies range 9–490 kHz. In detail, CENELEC specifies four frequency bands: the band A (3–95 kHz) that is reserved exclusively to power utilities, the band B (95–125 kHz) can be used for any application, the band C (125–140 kHz) is dedicated to in-home networking systems, the band D (140–148.5 kHz) is reserved to alarm and security systems. Besides this classification, G3-PLC is able to work in a combination of two or more CENELEC bands, i.e., BC, BCD and BD.

Figure 5.1 shows the block diagram of the implemented version of the G3-PLC transceiver. Input data bits are initially scrambled and encoded with a Reed-Solomon (RS) encoder that adds 16 or 8 parity bytes respectively in "normal" or "robust" mode. Afterwards, a given number of frame control

header (FCH) symbols is put before data bits in order to be encoded with a convolutional encoder. The resulting bits are combined in "normal" mode (i.e., no further operation is done) or in "robust" mode (i.e., each bit is repeated 4 times) before being mapped into DQPSK or DBPSK symbols. Three operating modes are available, namely, "normal" DQPSK, "normal" DBPSK, and "robust" DBPSK. It is worth noting that the differential modulation is performed in the time domain (across the data stream of each sub-channel). Finally a pulse shaped OFDM (PS-OFDM) is used with a cyclic prefix (CP) extension. Although the receiver is not specified by the standard, in the following, we implement a receiver that makes the following operations: after synchronization, a serial to parallel conversion is applied, CP samples are discarded and fast Fourier transform (FFT) is applied on the remaining samples. Then zero forcing equalization, differential PSK (DPSK) and channel decoding are applied.

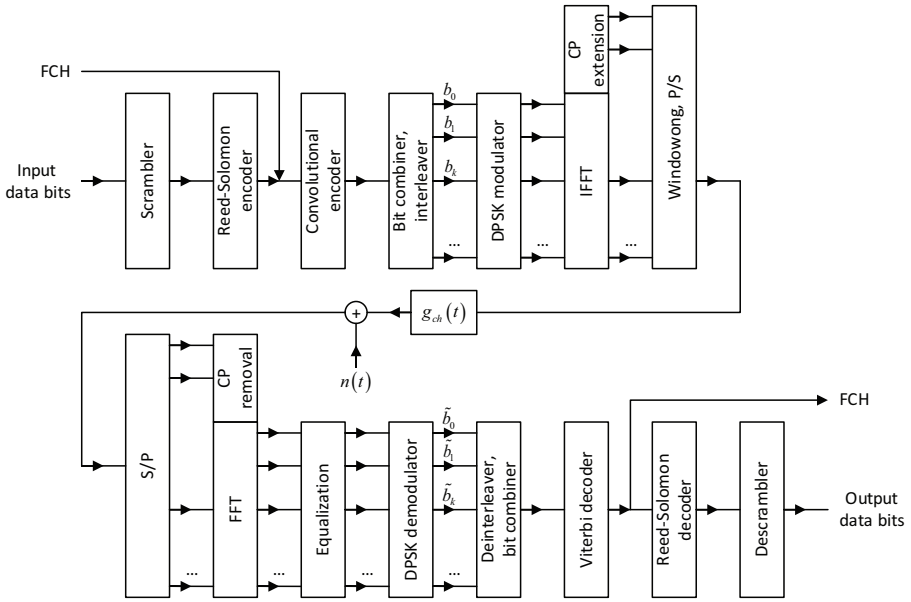

Figure 5.1: Block diagram of the implemented version of G3-PLC transceiver.

The PHY frame format (see Figure 4.3 (bottom)) starts with the preamble, which is a fixed number of symbols used for synchronization and detection, in addition to automatic gain control (AGC) adaptation. Preamble symbols are transmitted using PS-OFDM without cyclic prefix. The preamble is followed by a given number of symbols allocated to FCH and, finally, by data payload (PSDU). FCH brings important control information required to demodulate the data frame.

The MAC sub-layer is based on the IEEE 802.15.4–2006 specifications for low-rate wireless personal area network (WPAN) [42]. Basically, the channel access method is based on CSMA with collision avoidance (CSMA/CA) mechanism and a random backoff time. The general MAC frame format (see Figure 4.3 (top)), is substantially based on the 802.15.4–2006 specifications, except for the *segment control* field, which is defined in [40] and is used for tone mapping, contention handling and segmentation purposes.

When showing simulation results, we consider G3-PLC working in CENELEC A, C, BC bands and in the FCC band. The representative PHY layer parameters are listed in Table 6.2.

Table 5.1: G3-PLC system parameters.

	CENELEC A	CENELEC C	CENELEC BC	FCC
Number of IFFT/FFT points (M)	256	256	256	256
Number of modulated carriers (N_c)	36	7	26	72
First modulated carrier frequency (f_1) $[kHz]$	35.938	128.125	98.438	145.3
Last modulated carrier frequency (f_2) $[kHz]$	90.625	137.5	137.5	478.125
Available bandwidth ($f_2 - f_1$) $[kHz]$	54.688	9.375	39.063	342.2
Sampling frequency (f_s) $[MHz]$	0.4	0.4	0.4	1.2
Frequency spacing (f_s/M) $[Hz]$	1562.5	1562.5	1562.5	4687.5
Number of overlapped samples (N_o)	8	8	8	8
Number of cyclic prefix samples (N_{CP})	30	30	30	30
Number of FCH symbols (N_{FCH})	13	52	18	12
Number of preamble symbols (N_{pre})	9.5	9.5	9.5	9.5
Preamble duration $[ms]$	6.08	6.08	6.08	2.0267
PS-OFDM symbol duration $[\mu s]$	695	695	695	231.7

5.3 Cross-Platform Simulator

As previously discussed, G3-PLC has been proposed for different applications. In order to statistically characterize its performance and thus to asses whether or not it can be a valid solution for a given application scenario, we propose to implement a cross-platform simulator that makes use of two simulators: one for the PHY layer and one for the DLL/NL. As explained above, this approach is dictated by the fact that in general network simulators are not thought to implement the PHY layer, rather they abstract the PHY layer by using the information regarding the frame error rate (FER). Then, the performance assessment can be evaluated. It is worth noting that the proposed approach allows for statistically characterizing different scenarios by only changing the channel and noise model in the PHY layer simulator. Furthermore, as it will be explained in the following, particular topologies, as for example a given house or a part or a whole access grid, can be also precisely simulated.

In the following, sub-sections 5.3.1 and 5.3.2 respectively describe the PHY layer and the DLL/NL simulators.

5.3.1 PHY Layer Simulator

The first step towards the cross-platform realization is represented by the PHY layer implementation. To this end, we decided to use MATLAB together with data collected from a channel and noise measurement campaign.

First of all, we implemented the G3-PLC transceiver in Figure 5.1. Then, in order to validate the transceiver implementation, we computed the bit error rate (BER) for the k-th modulated subcarrier as follows

$$BER_{\text{simul}} = \text{Prob}\left[\tilde{\text{b}}_{\text{k}} \neq \text{b}_{\text{k}}\right], \tag{5.1}$$

where $\tilde{b}_k$ denote the demodulated bit for the k-th subcarrier, according to Figure 5.1, and we compare it with the theoretical BER of DBPSK and DQPSK (according to the corresponding transmitted symbols), which can be written

in closed form as [55, Chapter 5]

$$BER_{\text{theor}}^{DBPSK} = \frac{1}{2}\exp\left(-\frac{E_b}{N_0}\right), \tag{5.2}$$

$$BER_{\text{theor}}^{DQPSK} = Q_1(a,b) - \frac{1}{2}I_0(ab)\cdot\exp\left[-\frac{1}{2}\left(a^2+b^2\right)\right], \tag{5.3}$$

where $Q_1(a,b)$ is the Markum Q function, $I_0(\cdot)$ is the modified Bessel function of zero order, a and b are related to the signal-to-noise ratio per bit (E_b/N_0) as follows

$$a = \sqrt{\frac{2E_b}{N_0}\left(1-\sqrt{1/2}\right)}, \quad b = \sqrt{\frac{2E_b}{N_0}\left(1+\sqrt{1/2}\right)}. \tag{5.4}$$

Figure 5.2 shows the results of the theoretical and simulated model behavior. As we can see, the comparison validates the accuracy of the implemented transceiver.

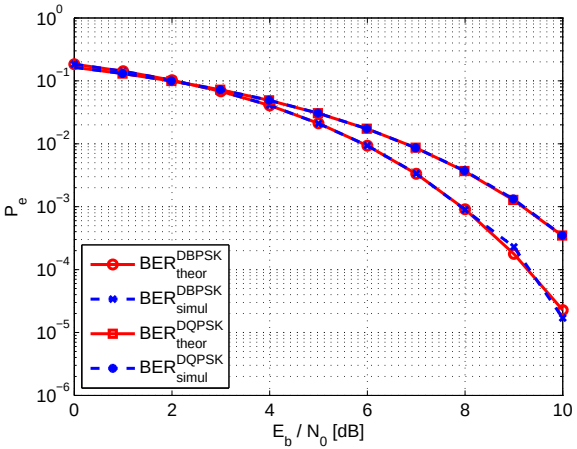

Figure 5.2: Theoretical and simulated BER for DBPSK and DQPSK modulations.

Channel and Noise Modeling

In the following, we consider the adoption of G3-PLC system for in-home applications. To this end, the last step to complete the PHY layer simulator and therefore to derive the FER to be used by the DLL/NL simulator is the choice of a right channel and noise model. At this point, it should be noticed that differently from the broadband case where validated channel and noise models are present in the literature, e.g., [18, Chapter 2] and [56–58], the knowledge of the in-home PLC channel and noise in the narrow band 30–500 kHz is very limited. Therefore, in order to obtain some useful results, we decided to carry out a measurement campaign in a single floor apartment. The topology of the considered scenario is depicted in Figure 5.3. In detail, the channel frequency response of the links that connect 11 different outlets have been measured in the frequency range 30–500 kHz with a resolution bandwidth of 3 kHz. A total of 110 channel frequency responses have been measured (see Figure 5.4a). Regarding the noise, it has been measured for each of the 11 outlets. In particular, 100 noise acquisitions in a mains cycle, i.e., 20 ms, have been acquired, so that it was possible to estimate the power spectral density (PSD) via the periodogram (see Figure 5.4b).

PHY Layer Abstraction

Combining the PHY layer simulator and the measurement campaign results, we are now able to derive the FER for the G3-PLC system in the considered scenario. At this point, it is important to note that there are two possibilities for the abstraction of the PHY layer to the DLL layer. The first consists in computing the FER for a given link while the second consists in computing the statistics of the FER for a given scenario, e.g., in-home. The former choice allows for making a topological performance analysis and it can be useful in the phase of coverage planning, e.g., for the deployment of smart meters, sensors, etc.. The latter choice allows for deriving a statistical characterization of the system performance and thus it is useful for those applications such as consumer electronics that do not foresee a design phase. In the following,

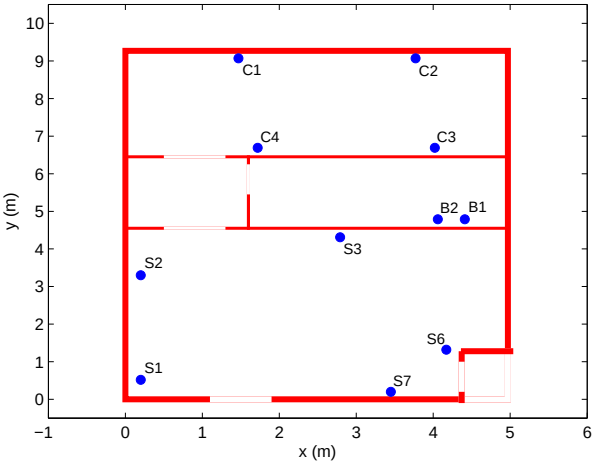

Figure 5.3: Single floor house topology.

we focus on the statistical analysis of the FER since we have considered the in-home application scenario. To this end, exhaustive simulations have been performed for CENELEC A, C, BC bands and for the FCC band, taking into account all the combination of transmission modes, i.e., normal DQPSK, normal DBPSK and robust DBPSK, and considering all the allowed number of PS-OFDM symbols per PHY frame (N_s), according to [28]. Moreover, we have transmitted 10^5 frames and we have considered all the 110 channel frequency responses and the correspondent noise power spectral density (PSD) at the receiver side. This means that for each transmission, the simulator randomly extracts one channel response, which is identified by the source and destination outlet index, and adds the noise. We eventually assume the transmitter and the receiver to be synchronized and perfect channel estimation.

Figures 5.5, 5.6 and 5.7 depict the CDF of the FER respectively for CENELEC band A, C and BC. Regarding the results for the FCC band, although not show, we notice that no corrupted bits/frames have been observed. Therefore, the PLC channel can be considered ideal in the last case.

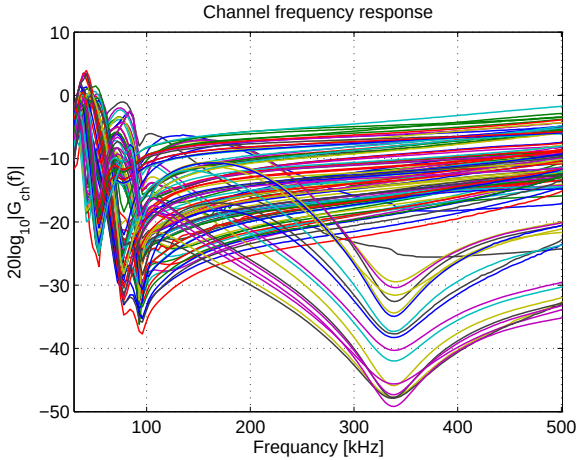

(a) Channel frequency responses for 110 combinations of outlets.

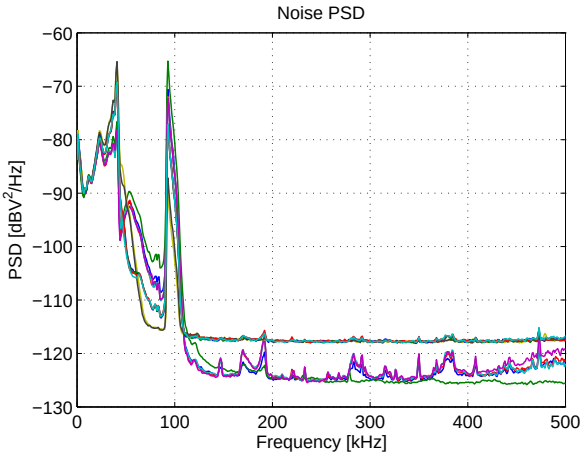

(b) Noise PSD for the 11 outlets.

Figure 5.4: Measurement campaign results.

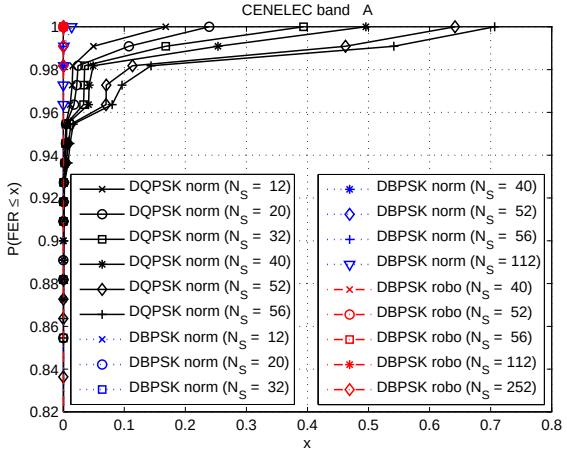

Figure 5.5: CDF of FER for CENELEC band A.

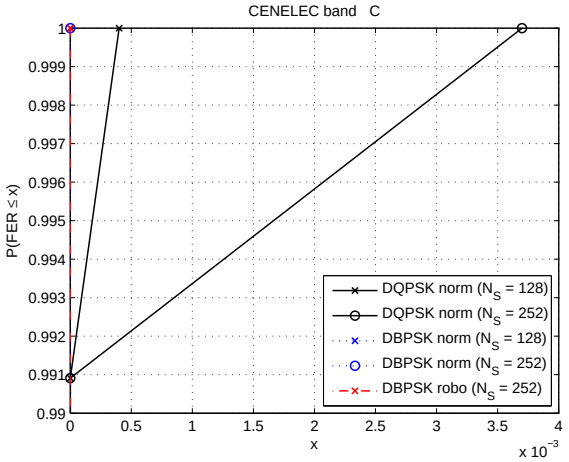

Figure 5.6: CDF of FER for CENELEC band C.

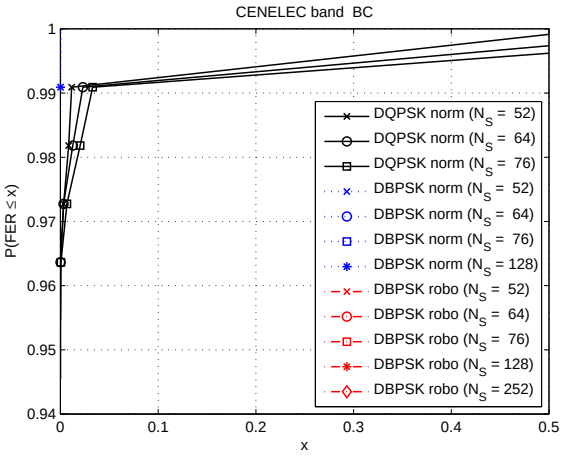

Figure 5.7: CDF of FER for CENELEC band BC.

5.3.2 Data Link and Network Layer Simulation

Once characterized the PLC channel from the FER point of view, we are able to exploit the simulation results for DLL and NL simulation.

To this aim, we decided to use the OMNeT++ network simulator to implement a network model based on G3-PLC communication technology combined with a switched Ethernet network. The benefits deriving from this approach have been discussed in Chapter 4, and can be summarized in:

- The possibility to extend the network coverage in large buildings/houses. This is because the G3-PLC network can be split into subnetworks that are connected through Ethernet.
- The possibility to interconnect devices compliant to different technologies, standards an protocols by exploiting the Ethernet connectivity.
- The overall network improvement in terms of reliability and performance.
- The network scalability.

Since modern switched Ethernet networks exhibit a star topology and the power line channel can be considered as a bus, we adopt a tree like topology – as a combination of bus and star topologies – to implement the convergent network (see Figure 4.5). However, G3-PLC does not provide any specification for the integration in switched Ethernet network. Since the convergence between Ethernet and G3-PLC is a prerequisite of the whole network implementation, we need to define a shared common layer that provides interconnectivity among heterogeneous lower layers.

In this perspective, a fundamental role is played by the network devices presented in Chapter 2 and detailed in Chapter 4, particularly the *router* and the *switch*. According to the general architecture depicted in Figure 2.6, the router is a network device characterized by network adapters towards both Ethernet and G3-PLC. Network adapters exhibit PHY and DLL specification, whereas on top of these layers we define a convergent network layer responsible of relaying frames from one network adapter to the other and vice versa. The router dynamically learns about the existence of end nodes during reception of frames and updates a forwarding table with link quality information in order to ensure a more reliable communication on harsh power line channels, or equally, to increase the network coverage. On the other hand, the switch behavior, which is well-known since its large deployment in nowadays local area network (LAN) and home area network (HAN), has been modified in order to work seamlessly with the routers. In particular, it is able to exploit information harvested by routers to build and update its own forwarding table. Therefore, the combination of router and switch procedures enables the integration of heterogeneous communication technologies leading to a convergent network and providing the basis for satisfying QoS constraints.

5.3.3 Performance Metrics

In order to quantify the network performance, we take into account four representative metrics. Beside aggregate network throughput (THR), we define three additional metrics: the average *end-to-end delay*, the average *frame drop rate* and the average number of corrected received frames. It is worth not-

ing that THR is given by Equation 3.1, and is evaluated at the MAC layer according to Equation 3.3

According to [59], the average end-to-end delay (t_{e2e}) is computed as the time lapse between the instant when a frame is sent from the source and the instant when the frame is received at the destination. As depicted in Figure 2.6, it is measured between the two higher layers running at the source and destination nodes and it is equal to the sum of all the time intervals spent by the frame during its queuing, transmission and propagation at every traversed node. It is worth noting that the delay is strongly dependant on the channel access method, which is taken into account within the transmission delay term. In particular, G3-PLC technology exploits CSMA/CA algorithm, hence, the transmission delay is affected by the random backoff time. Furthermore, each intermediate forwarding node, i.e., the router, adds extra delay to relay the frame. In details, the average end-to-end delay is computed as follows

$$t_{e2e} = \frac{1}{N} \sum_{u=1}^{N} \left(\frac{1}{N_{RX}^{(u)}} \sum_{i=1}^{N_{RX}^{(u)}} n_{\text{sn}}^{(i)} \left(t_{\text{queue}}^{(i)} + t_{\text{transmission}}^{(i)} + t_{\text{propagation}}^{(i)} \right) \right), \quad (5.5)$$

where N is the number of nodes, and $N_{RX}^{(u)}$ is the total number of correct frames received by u-th node. Moreover, queuing ($t_{\text{queue}}^{(i)}$), transmission ($t_{\text{transmission}}^{(i)}$) and propagation ($t_{\text{propagation}}^{(i)}$) delays for the i-th frame are weighted for the factor $n_{\text{sn}}^{(i)}$, which is the number of subnetworks the i-th frame has to cross in order to reach the u-th node. We notice that processing delays at the transmitter and receiver have been assumed ideal. Furthermore, since the propagation delay in electric cables is 5.775 $\mu s/km$ [28], we neglect its contribution due to small length of cables within households.

The third considered metric is the average frame drop rate (R_{FD}). This quantity is representative of the efficiency of the channel access method. It is computed as

$$R_{FD} = \frac{1}{N} \sum_{u=1}^{N} \frac{N_{FD}^{(u)}}{N_{TX}^{(u)}}, \quad (5.6)$$

where N is the number of nodes, $N_{FD}^{(u)}$ is the number of dropped frames by the u-th node due to exceeding the backoff attempt limit, and $N_{TX}^{(u)}$ is the number of correct transmitted frames by the u-th node.

Finally, we take into account the average number of corrected frames received that is computed as follows

$$N_{RX} = \frac{1}{N} \sum_{u=1}^{N} N_{RX}^{(u)}. \tag{5.7}$$

We notice that this parameter is strictly related to the network coverage. In fact, for a fixed number of nodes, the greater N_{RX}, the larger the network coverage is.

5.4 Smart Home Network Simulation Results

5.4.1 Simulation Setup

In order to obtain numerical results, we consider the G3-PLC system working in the CENELEC A, C, BC bands and in the FCC band using the "normal" DQPSK transmission mode. We assume each PHY frame to be composed of 40, 64, 128 and 20 PS-OFDM symbols respectively for CENELEC A, C, BC and FCC bands. Furthermore, with reference to Figure 4.3, a fixed overhead of 20 bytes is assumed as the result of the minimum MAC overhead (8 bytes) in addition to source and destination MAC addresses (6 bytes each). Therefore, the resulting MAC payloads are 143, 75, 171 and 135 bytes for the above mentioned bands. It is worth noting that source and destination personal area network (PAN) addresses, shown in Figure 4.3, have been disregarded since router and switch are designed to manage the network dealing with MAC addresses of nodes, as described in Chapter 4.

The simulation parameters are listed in Table 5.2, where we highlight the shortest PHY frame duration for FCC band due to the sampling frequency (see f_s in Table 6.2), i.e., three times greater than CENELEC bands.

Table 5.2: G3-PLC simulation parameters.

	CENELEC A	CENELEC C	CENELEC BC	FCC
Number of PS-OFDM symbols per PHY frame (N_s)	40	128	64	20
PHY frame duration [ms]	42.9	131.2	63.1	9.4
PHY payload dimension (n) [bytes]	163	95	191	155
MAC overhead [bytes]	20	20	20	20
MAC payload dimension [bytes]	143	75	171	135
Maximum PHY data rate [kbps]	30.4	5.8	24.2	131.4

In order to model the power line transmission channel in OMNeT++, we exploit the inversion method applied to the cumulative distribution function (CDF) of the FER (see Section 5.3.1). Regarding the Ethernet network, we model 100BASE-TX over cat5 cables assuming ideal the FER and the delays.

We build the simulation scenario using from 6 up to 60 G3-PLC nodes and we evaluate the THR, the t_{e2e}, R_{FD} and N_{RX} without routers, or when two and three routers are considered. The point-to-point traffic is randomly generated among G3-PLC nodes, i.e., each node generates traffic destined to any other node (belonging to the same subnetwork or to different subnetworks) according to a peer-to-peer model. Furthermore, we take into account different network load conditions:

Saturation traffic happened when each node has immediately a packet available for transmission, after the completion of each successful transmission [51].

Heavy load traffic generated by each node according to an exponential distribution with mean equal to 1 second.

Medium load traffic generated by each node according to an exponential distribution with mean equal to 10 second.

Light load traffic generated by each node according to an exponential distribution with mean equal to 60 second.

In this perspective, we consider a buffer queue for each network node equal to 1 frame. Furthermore, we assume that the transmission does not wait for any acknowledgement receipt.

5.4.2 Numerical Results

Figures 5.8, 5.9, 5.10 and 5.11 show the THR according to different network traffic conditions. From these figures, we derive the following observations:

- The introduction of 2 and 3 routers is beneficial in saturation (see Figure 5.8) and heavy load (see Figure 5.9) conditions while it almost leads

to the same THR as the no router case in medium (see Figure 5.10) and light load (see Figure 5.11) conditions. However, we notice that in larger environments, e.g., large buildings, we can expect that the use of routers is beneficial to increase the coverage and thus the throughput.

- There is a performance decay with the increasing number of network nodes in saturation (see Figure 5.8) and heavy load (see Figure 5.9) conditions due to the CSMA algorithm.

- FCC band offers higher THR in saturation (see Figure 5.8) and heavy load (see Figure 5.9) conditions, while it is underutilized when dealing with medium (see Figure 5.10) and light (see Figure 5.11) loads.

Furthermore, although not inferable from Figures 5.8, 5.9, 5.10 and 5.11, the THR depends on the number of correct received frames, which, in turn, is dependent on both CSMA and the power line channel characteristic, i.e., the FER.

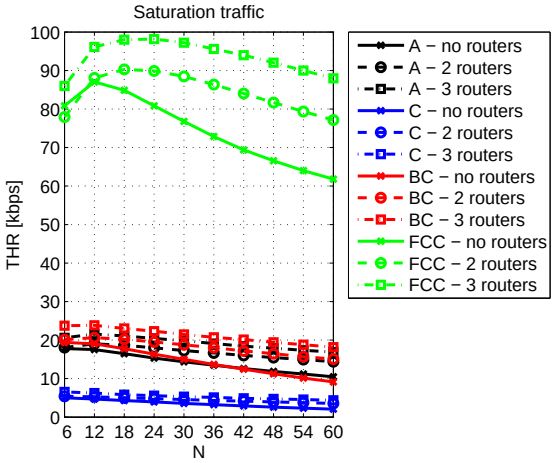

Figure 5.8: THR in saturation traffic conditions.

Figures 5.12, 5.13, 5.14 and 5.15 show the average end-to-end delay. From the comparison of the delays for different traffic loads we make the following

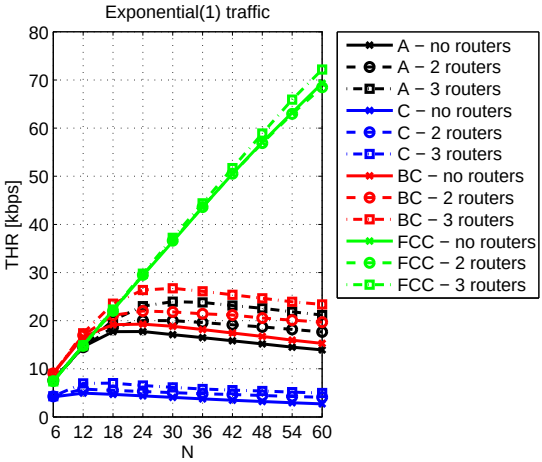

Figure 5.9: THR in heavy load traffic conditions.

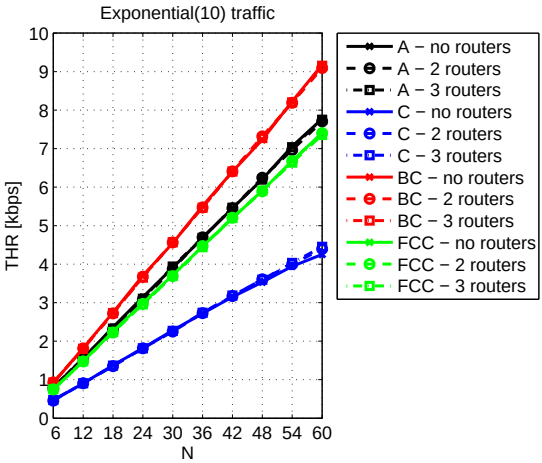

Figure 5.10: THR in medium load traffic conditions.

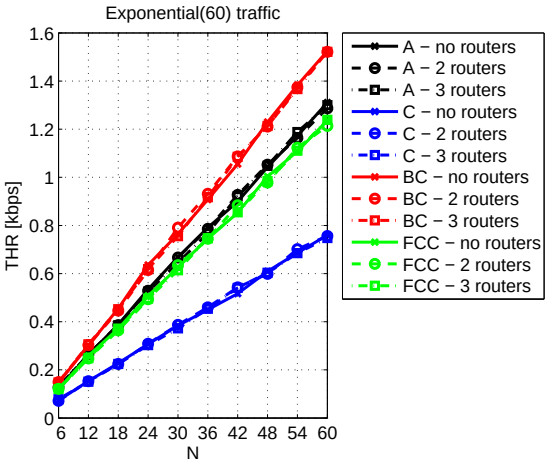

Figure 5.11: THR in light load traffic conditions.

observations:

- The introduction of 2 and 3 routers slightly increases the delays since the CSMA has to be performed twice whenever source and destination nodes belong to different subnetworks.

- The delays in FCC band are always smaller than those in CENELEC bands. This behavior is due to the higher transmission rate and lower frame duration in FCC band.

- The delays tend to be constant with the increasing number of nodes in saturation (see Figure 5.12) and heavy load (see Figure 5.13) conditions. This is because the delay is computed on the correct received frames. Clearly, the average frame drop rate increases with an increasing number of nodes (see Figures 5.16, 5.17, 5.18 and 5.19).

- The delays decrease with the decreasing network traffic load since the higher probability to find the channel idle and the lower number of collisions.

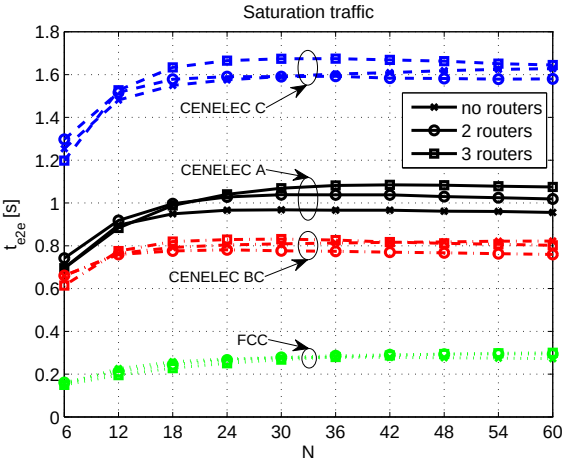

Figure 5.12: Average end-to-end delay in saturation traffic conditions.

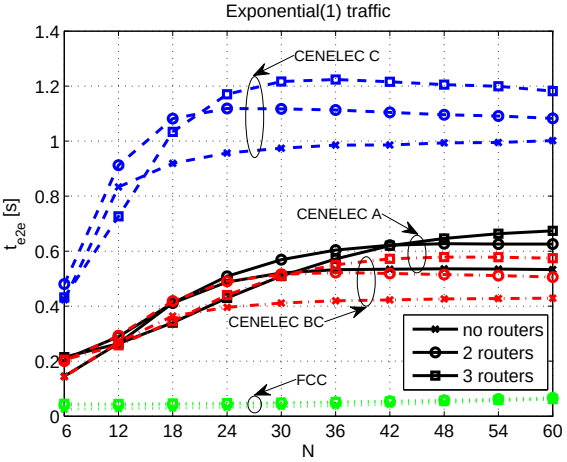

Figure 5.13: Average end-to-end delay in heavy load traffic conditions.

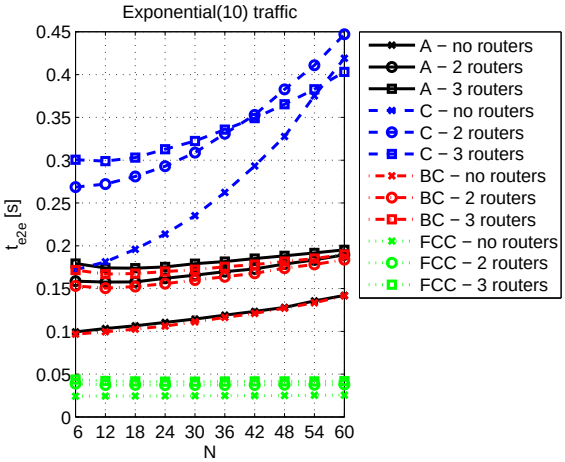

Figure 5.14: Average end-to-end delay in medium load traffic conditions.

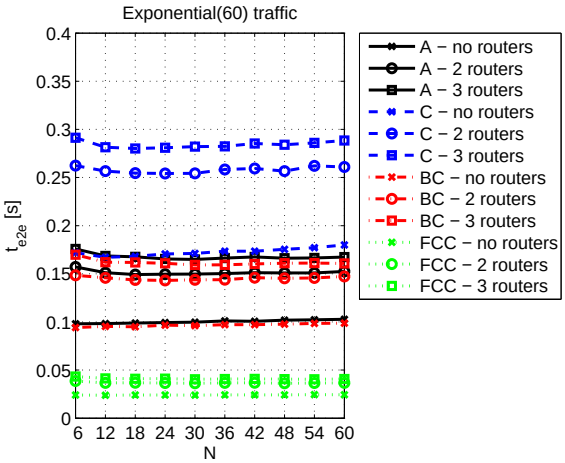

Figure 5.15: Average end-to-end delay in light load traffic conditions.

Figures 5.16, 5.17, 5.18 and 5.19 show the average frame drop ratio for different traffic conditions. This performance metric is related to the efficiency of the CSMA method. In this perspective, we make the following observations.

- The introduction of 2 and 3 routers is always beneficial since it splits the whole network in 2 or 3 subnetworks where the CSMA performs more efficiently since there is a smaller number of nodes per subnetwork.
- CSMA is more efficient in FCC band than CENELEC bands since it shows the lowest drop ratio in all network traffic conditions due to the shortest PHY frame duration.
- The drop ratio grows faster in absence of routers when considering the increasing number of nodes.

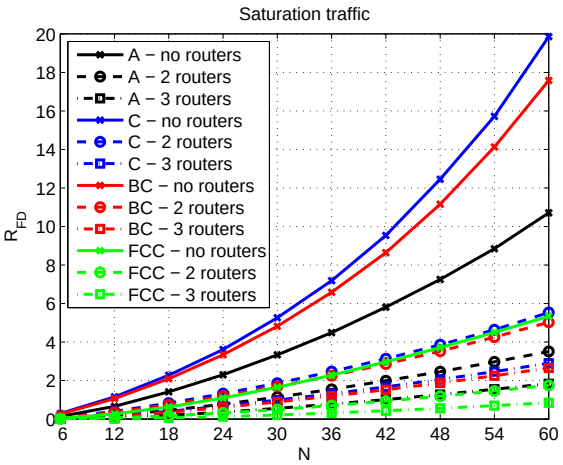

Figure 5.16: Average frame drop rate in saturation traffic conditions.

Finally, the average number of correct receptions is depicted in Figures 5.20, 5.21, 5.22 and 5.23. We derive the following observations:

- The introduction of 2 and 3 routers provides a greater number of corrected received frames (thus a better network coverage) when consider-

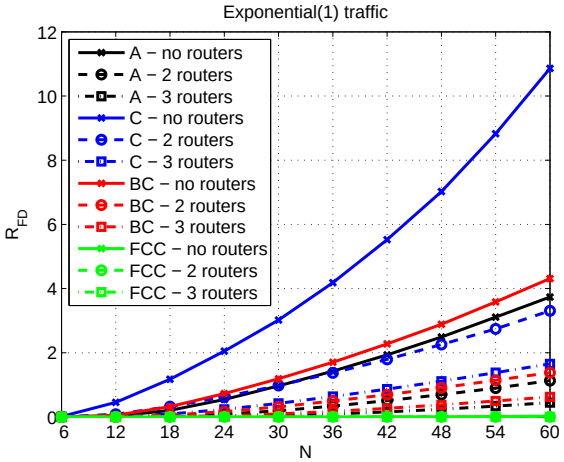

Figure 5.17: Average frame drop rate in heavy load traffic conditions.

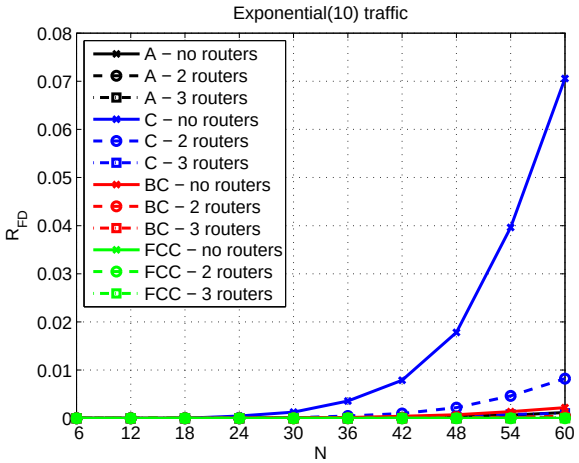

Figure 5.18: Average frame drop rate in medium load traffic conditions.

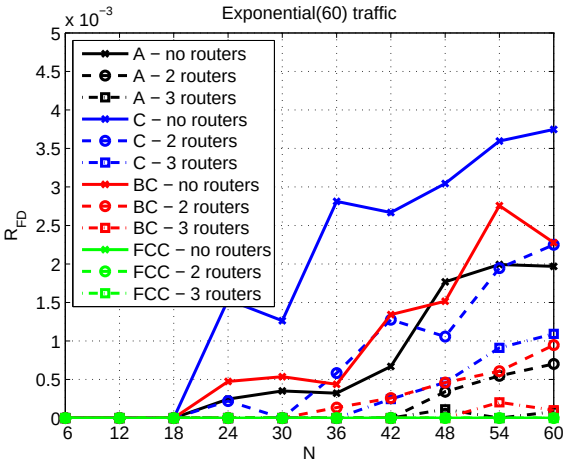

Figure 5.19: Average frame drop rate in light load traffic conditions.

ing saturation (see Figure 5.20), heavy (see Figure 5.21) and partially medium load (see Figure 5.22) traffic conditions.

- In light load conditions (see Figure 5.23), the benefit deriving from the introduction of 2 or 3 routers cannot be appreciated since the small number of frames received and the small area of the considered house.
- The number of correct receptions is affected both by the channel conditions and the CSMA algorithm.

5.4.3 Obervations on the Usability of the Cross-Platform

The cross-platform simulator can be used to verify whether a communication technology, e.g., G3-PLC, satisfies a given set of requirements for a certain application scenario. As an example, we can reconsider the traffic profile classification, presented in [60], within the customer's domain. In detail, we focus on mission-critical, soft real-time, and non-real-time traffic profiles. Mission-critical traffic represents alarm-response commands and it is classified into LOW-LOW (3 ms), LOW (16 ms), MEDIUM (160 ms), and HIGH ($>$ 160 ms)

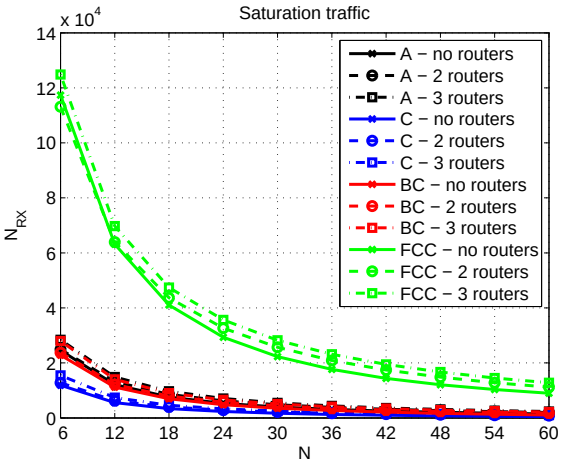

Figure 5.20: Average number of corrected received frames in saturation traffic conditions.

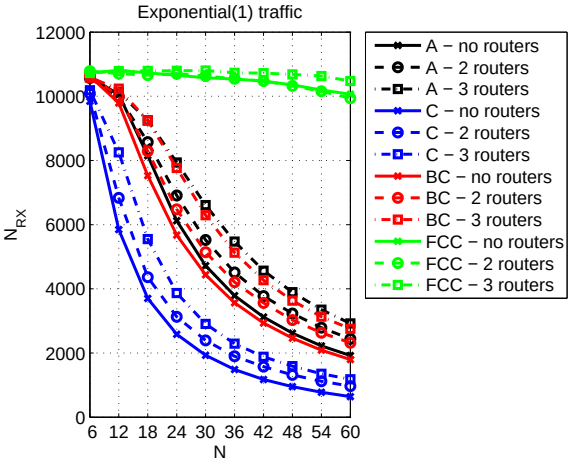

Figure 5.21: Average number of corrected received frames in heavy load traffic conditions.

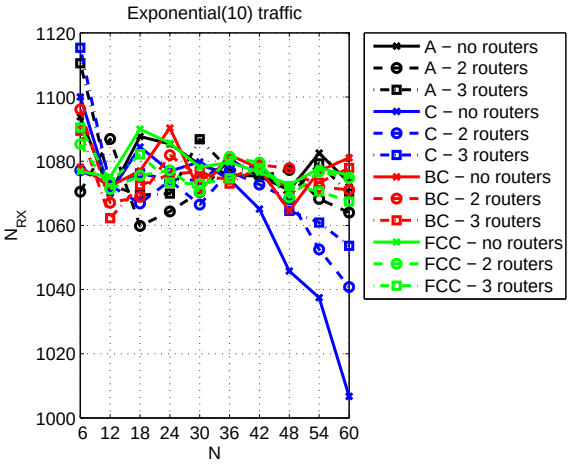

Figure 5.22: Average number of corrected received frames in medium load traffic conditions.

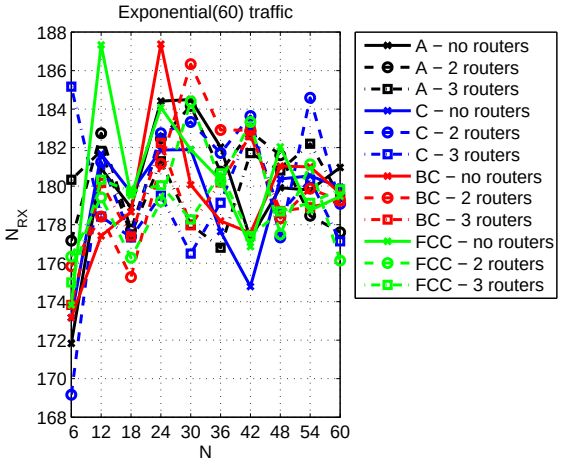

Figure 5.23: Average number of corrected received frames in light load traffic conditions.

latency classes [61]. Soft real-time traffic regards interactive maintenance commands, periodic smart plug readings and other sensor measurements. In this case, commands and measurements are sporadic (with periods in the order of 1–15 min [62]), and latency requirements are soft ($\sim 1\ min$). Finally, non-real-time traffic profile refers to the planning of services to exchange information, e.g, firmware updates and similar file-transfer operations. It requires higher information rates than the previous traffics, but it is delay-tolerant.

Now, we can exploit the numerical results obtained with the cross-platform simulator to infer that (see Figures 5.12, 5.13, 5.14 and 5.15) the G3-PLC technology may support part of the mission-critical traffic profile, while it fully supports soft real-time and non-real-time traffic profiles.

5.5 Main Findings

This chapter has presented a cross-platform simulator for G3-PLC systems. The cross-platform simulator consists of two simulators: one for the physical layer, and one for the higher layers. The physical layer simulator has been implemented in MATLAB and it is meant to compute the frame error rate of a given communication link. The higher layers simulator has been implemented in OMNeT++ and it makes use of the frame error rate to abstract the physical layer. The cross-platform simulator enables the computation of the performance of the system considering either a given communication link or a given communication scenario. In order to improve the performance of G3-PLC systems, a convergent network architecture where G3-PLC devices are integrated into a switched Ethernet network has been presented. The convergent network has been realized by defining router and switch devices. The platform has been used to derive the network performance in terms of throughput, end-to-end delay, frame drop rate, and coverage. The results have been exploited to test the requirements meeting of G3-PLC for a certain application scenario.

Chapter 6

Cross-Platform Simulator for G3-PLC Evaluation in Access Networks

In this chapter the cross-platform simulator is used to evaluate G3-PLC systems for SG applications in the access network scenario. This is fundamental since the interaction of the outside world, i.e., the access network, with the SH is mandatory in order to achieve and exploit the SG concept. Moreover, to improve the performance and coverage of G3-PLC, a simple adaptive tone mapping algorithm together with a routing algorithm are also presented.

6.1 Introduction

The SG can be seen as a communications network that needs to deliver flows of data to offer several services over different domains [53]: *generation*, *transmission*, *distribution*, and *customer*. Some examples of services are: AMR, meter events and alarms, substations automation, microgrids integration, demand response through the smart management and monitoring of household appliances, control of local renewable energy plants, integration of plug-in electric vehicles, etc.. To offer this plethora of services, it is fundamental to adopt/develop adequate communication technologies capable of satisfying the communication requirements of each service, e.g., throughput, FER, end-to-end delay, etc..

Although finding the best communication technology for SG applications is not straightforward, recently, industries and standardization organizations have proposed the use of NB-PLC as a cost-effective solution to support the development of the SG concept. Several solutions and standards have been conceived and developed for this scope. Among them, G3-PLC [28] is playing a significant role inasmuch it has been used as the basis for the development of the IEEE P1901.2 [32] standard and the ITU-T G.hnem [30, 33] standard for SG applications.

In this context, it is important to have a simulation tool that permits to predict the performance of such a technology over different scenarios.

In this paper, we present a cross-platform simulator that allows for simulating the G3-PLC technology. We consider the distribution domain as application scenario, and in particular the access network.

The proposed cross-platform consists of two different simulators: one for the PHY layer and one for the DLL/adaptation (ADP) layer. The PHY layer simulator is implemented MATLAB and it is meant to estimate the FER of a given link. The obtained FER is used to abstract the PHY layer within the DLL/ADP layer simulator, which is implemented in OMNeT++.

To improve the reliability of G3-PLC, beside the cross-platform simulator, we also propose a simple bit loading algorithm and a routing algorithm.

The remainder of the chapter is as follows. Section 6.2 describes the application scenario. Then, Section 6.3 overviews the G3-PLC technology and presents the bit-loading algorithm. The cross-platform simulator is presented in Section 6.4. Extensive numerical results are reported in Section 6.5. Finally, the conclusions follow in Section 6.6.

6.2 Application Scenario

We consider the application of G3-PLC in the low voltage (LV) power distribution grid, and in particular between the medium voltage medium voltage (MV)/LV transformer stations and the house meters, i.e., in the access network [18, §2.3].

In the following, sections 6.2.1 and 6.2.2 respectively describe the considered network topology and the SG services that that will be adopted in the rest of the paper to evaluate the performance of G3-PLC.

6.2.1 Network Topology

A general description of the characteristics of the EU access network topology can be found in [18,63,64]. Beside the previous works, [65] proposes a topology model that is mainly developed for US grids. According to the previous works, there is a distinction between European and US/Asia networks. These differ for the density of households (higher in EU) and for the way the current feeds the house, e.g., in US is not difficult to find houses which are fed with different phases, while in EU the latter case is not frequent, although possible. However, in general, there is an agreement on the characteristics of the network topologies. Regarding the EU network, which will be considered from now on, it is agreed that from the MV-LV transformer a three phase backbone starts. Then, from the backbone one or more branches (up to 10) can be present where tens of households per branch can be connected (see [64, §3], [18, §3], [63, §2]). The network length, namely the maximum distance between the MV-LV transformer and the households, is up to 1 Km, while the number of houses that are fed by a given MV/LV transformer station varies between some tens to one/two hundreds.

In order to simulate an access network, we made use of the bottom-up channel generator presented in [56]. Briefly, this simulator generates the channels frequency response between pairs of network nodes from the physical description of the network, namely from knowledge of the topology, cables and loads. Therefore, beside the network topology, another important parameter to model the network and in particular to compute the channel response between pairs of network nodes is the access impedance, i.e., the impedance seen at the input of each household. To this respect, we highlight that the literature is really poor, and we only found the work of Sigle [66] that reports three examples of measured access impedance up to 500 kHz. Among these examples, we used the two access impedances measured in households of a residential scenario to

model the households in our network. Finally, we consider NAYY150SE cables for the backbone and the branches (150 mm^2 area for each of the four cores), and NAYY50SE cables to connect the household to the branches (50 mm^2 area of each of the 2 cores).

Figure 6.1 shows the access network topology that will be used in this work to obtain numerical results. It represents a residential area of about 92,000 m^2 where 25 houses connected to 7 branches are fed by a single MV/LV transformer. Each house is identified by a number between 13 and 58, and the MV/LV transformer station is identified by the number 1.

For the considered topology, 650 channel frequency responses within 30–500 kHz have been generated. Some examples are reported in Figure 6.2.

Regarding the noise, we model it according to [67] as a background noise in the narrow band (3–500 kHz). In particular, we assume the PSD of the noise to decrease exponentially as it is shown in Figure 6.2. We notice that the exponential behavior of the NB background noise has also been experienced in US distribution grids [68].

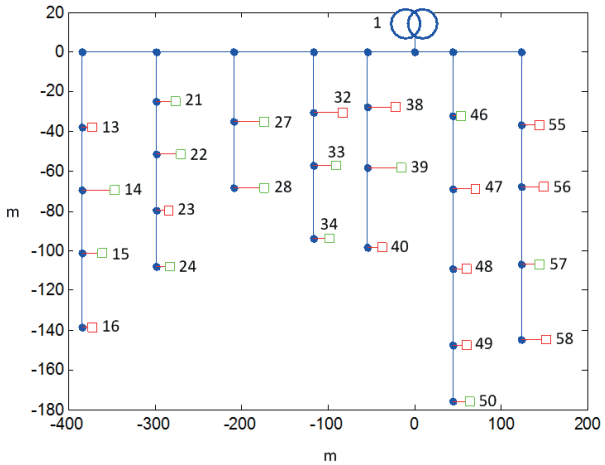

Figure 6.1: Physical network topology and host ID.

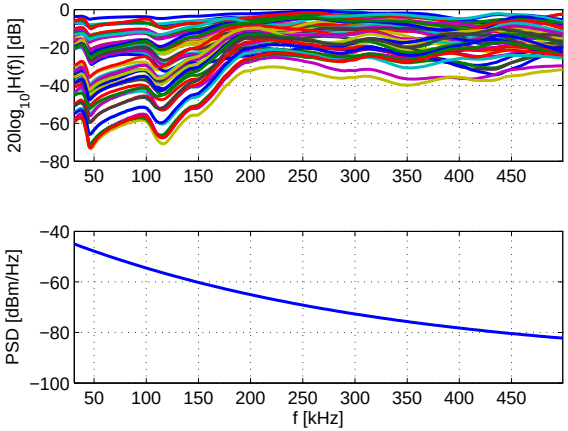

Figure 6.2: Top: example of channel frequency response realizations. Bottom: PSD profile of the background noise.

6.2.2 Network Traffic

In order to simulate the behavior of G3-PLC in the access network, we need to model the traffic that is required by SG application. To this end, we consider the work [60] according to which SG applications generate traffic that can be classified into three categories: mission-critical, soft real-time, and non-real-time traffic profiles. Mission-critical traffic represents alarm-response commands and it is classified into LOW-LOW (3 ms), LOW (16 ms), MEDIUM (160 ms), and HIGH ($>$ 160 ms) latency classes [61]. Soft real-time traffic regards interactive maintenance commands, periodic meter readings and other sensor measurements. In this case, commands and measurements are sporadic (with periods in the order of 1–15 min [62]), and latency requirements are soft ($\sim$ 1 min). Finally, non-real-time traffic profile refers to the planning of services to exchange information, e.g, firmware updates and similar file-transfer operations. It requires higher information rates than the previous traffics, but it is delay-tolerant.

The previous traffic categories provide a description of SG application

requirements, but they are not sufficient for testing network performances. Therefore, an exhaustive traffic model is needed in order to model the generation of packets within the simulator. To this aim, according to [60], we consider the traffic generated by energy services interfaces (ESIs), i.e., network nodes, to be directed to the distribution access point (DAP), i.e., the MV/LV transformer station. In Table 6.1, we detail the considered traffic models.

Table 6.1: Smart Grid traffic model.

Traffic description	Traffic generation	Mean value [s]	Packets / dimension [bytes]
Alarm signals	Exponential	240	1 / 1000
Network joining	Exponential	3600	1 / 1000
Metering data	Exponential	60	1 / 1000
Telemetry signals	Exponential	60	1 / 1000
Information reports	Exponential on-off traffic	$T_{on} = 0.2$ $T_{off} = 10$	–

6.3 G3-PLC Technology Overview

Exhaustive details about G3-PLC technology have been provided in previous chapter. Since we are interested in SG applications in the LV distribution grid, when showing numerical results, we consider G3-PLC working in CENELEC A and FCC bands. The corresponding PHY layer parameters are listed in Table 6.2. We also assume that each PHY frame is composed of 20 and 56 PS-OFDM symbols, respectively for CENELEC A and FCC, each carrying data modulated with robust DBPSK. This assumption respectively leads to 22 and 12 bytes of payload dimension. Consequently, the maximum achievable bit-rates is 3.26 *kbps* and 10.17 *kbps* for CENELEC A and FCC band, respectively. Table 6.3 reports other reference PHY layer parameters that will be used for the simulations. A detailed set of PHY layer parameters for G3-PLC can be also found in [30].

Table 6.2: G3-PLC system parameters.

	CENELEC A	FCC
Number of IFFT/FFT points (M)	256	256
Number of modulated carriers (N_c)	36	72
First modulated carrier frequency (f_1) $[kHz]$	35.938	145.3
Last modulated carrier frequency (f_2) $[kHz]$	90.625	478.125
Available bandwidth ($f_2 - f_1$) $[kHz]$	54.688	342.2
Sampling frequency (f_s) $[MHz]$	0.4	1.2
Frequency spacing (f_s/M) $[Hz]$	1562.5	4687.5
Number of overlapped samples (N_o)	8	8
Number of cyclic prefix samples (N_{CP})	30	30
Number of FCH symbols (N_{FCH})	13	12
Number of preamble symbols (N_{pre})	9.5	9.5
Preamble duration $[ms]$	6.08	2.0267
PS-OFDM symbol duration $[\mu s]$	695	231.7

Table 6.3: G3-PLC simulation parameters.

	CENELEC A	FCC
Transmitted PSD [dBm/Hz]	-13	
Carrier modulation	robust DBPSK	robust DBPSK
Number of PS-OFDM symbols per PHY frame (N_s)	56	20
PHY frame duration $[ms]$	54	9.4
PHY payload dimension n [bytes]	22	12
Maximum PHY data rate [kbps]	3.26	10.17

6.3.1 Adaptive Tone Mapping

G3-PLC permits the use of bit and power loading algorithms. According to [28], the transmitter performs a tone map request exploiting the FCH, which is a multi symbol field following the preamble. Upon reception of tone map request, the receiver estimates the signal to noise ratio (SNR) of the received signal for each modulated carrier, and informs the remote transmitter with a tone map response. At this point, the transmitter is able to adaptively select the usable tones, optimum modulation and code rate to ensure a reliable communication. In particular, the transmitter selects the tones to send data symbols, and the ones to send dummy data symbols (noise) that have to be discarded at the receiver. At this point, it is important to note that the choice of the loading algorithm to be implemented is up to the chip maker.

To this respect, we propose to use a very simple on-off loading algorithm. The proposed bit-loading algorithm targets the bit rate maximization under a BER and a power constraint on each carrier, and a constraint on the constellation to be employed. It can be formulated as follows

$$\max \quad R = \sum_{k \in \mathbb{N}_C} b^{(k)}, \tag{6.1}$$

$$\text{s.t.} \quad BER^{(k)} \leq \gamma, \tag{6.2}$$

$$b^{(k)} \in \{0, 1\}, \tag{6.3}$$

$$P^{(k)} \leq \bar{P}, \quad \forall k \in \mathbb{N}_C, \tag{6.4}$$

where $b^{(k)}$, $BER^{(k)}$, $P^{(k)}$, and $\bar{P}$ respectively represent the bits loaded, the BER and the transmitted power on carrier k, and the maximum transmit power on each carrier, which is assumed to be constant, e.g., it is given by a PSD mask constraint. Furthermore, $\mathbb{N}_C$ denotes the set of modulated carriers. It is well known that for uncoded systems the BER constraint is equivalent to an SNR constraint [69]. Furthermore, an SNR gap can be considered for a given channel coding scheme [69]. In our case, we decided to choose the SNR gap, or equally the SNR threshold from the curves of the average BER (averaged across carriers) obtained for uncoded and coded DBPSK (see Figure 6.3).

In particular, we set the SNR threshold equal to 2 dB, so that the BER of the coded system is of about 10^{-4}. Figure 6.3 has been obtained using the G3-PLC system in CENELEC A band with the parameters of Tables 6.2, and 6.3. We notice that although not shown, similar results have been obtained for the FCC band. Furthermore, in Figure 6.3, the curve labeled with "theoretical" shows the theoretical BER for the uncoded DBPSK system, computed as described in [55, § 5].

Now, once the SNR threshold is set, problem (6.1) is solved by loading DBPSK symbols only in those carriers whose SNR is higher or equal to the threshold.

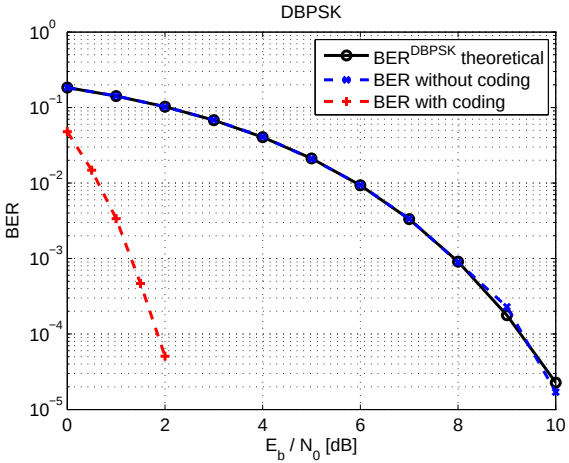

Figure 6.3: BER vs E_b/N_0 for DBPSK modulation with or without coding techniques.

6.4 Cross-Platform Simulator

In order to test the performance of G3-PLC in the access networks, and thus to asses whether or not it can be a valid solution for a given SG application scenario, we implemented a cross-platform simulator composed by two simulators: one for the PHY layer and one for the DLL and ADP layers. They are

briefly described n the following.

6.4.1 PHY Layer Simulator

The PHY layer simulator makes use of the channel generator described in section 6.2.1 and of a PHY layer simulator of G3-PLC developed in MATLAB. From these two simulators, we are able to compute the FER that characterize every link of the network topology. The FER is then used as an abstraction of the PHY layer by the DLL and ADP layers simulator.

6.4.2 DLL and ADP Layer Simulator

The DLL and ADP layers simulator is implemented using OMNeT++ which is an event based simulator that allows for implementing channel access policies, routing algorithms and traffic models.

G3-PLC specifies an ADP layer which is based on the IPv6 over low power wireless personal area networks (6LoWPAN) [70]. Furthermore, 6LoWPAN ad-hoc (LOAD) routing protocol LOAD, which is a simplified form of ad-hoc on-demand distance vector (AODV) for 6LoWPAN, is selected as an effective routing protocol to handle changing link conditions. LOAD operates on ADP layer creating a logical network topology below IPv6 network layer. For the IPv6 layer, the 6LoWPAN adaptation layer is considered as a single link. LOAD is designed to find the optimized route that minimizes the route cost (RC) as follows

$$\min_{i} \left\{ \mathrm{RC}\left(p^{(i)}\right) \right\}, \tag{6.5}$$

where p_i denotes the i-th route from the source to the destination. We decide to define it as follows

$$\mathrm{RC}\left(p^{(i)}\right) = -\frac{1}{N_H^{(i)}} \prod_{h=0}^{N_H^{(i)}-1} C\left\{[D_h, D_{h+1}]\right\}, \tag{6.6}$$

where the i-th route goes through the nodes $D_0, D_1, \ldots, D_{N_H^{(i)}}$. $N_H^{(i)}$ denotes the number of hops ($0 < N_H^{(i)} \leq$ adpMaxHops), and $C\left\{[D_x, D_y]\right\}$ is the link

cost between device D_x and D_y. We notice that, according to [40], we consider adpMaxHops = 4. As regards the link cost, we propose to take into account PHY transmission parameters and to model it as follows

$$C\left\{[D_x, D_y]\right\} = \left(1 - FER\left\{[D_x, D_y]\right\}\right) \frac{N_c^{ON}\left\{[D_x, D_y]\right\}}{N_c}, \tag{6.7}$$

where $FER\{[D_x, D_y]\}$ is the FER associated to the link between nodes D_x and D_y. $N_c^{ON}\{[D_x, D_y]\}$ is the number of *on* carriers (see section 6.3.1), and N_c the total number of modulated carriers. The proposed route cost takes into account the delay of the route with the term $1/N_H^{(i)}$ (by assuming the delay of each link to be constant), while the link cost computes the probability of receiving correct bits.

Now, in order to evaluate the G3-PLC performances, we consider the throughput and the average end-to-end delay of each node. The throughput is computed according to Eq. 3.3, while the average end-to-end delay is computed as the time lapse between the instant when a frame is sent from the source and the instant when the frame is received at the destination. It is computed as follows

$$t_{e2e}^{(u)} = \frac{1}{N_{RX}^{(u)}} \sum_{i=1}^{N_{RX}^{(u)}} N_H^{(i)} \left(t_q^{(i)} + t_{tx}^{(i)} + t_p^{(i)}\right), \tag{6.8}$$

where $N_{RX}^{(u)}$ is the total number of correct frames received by the coordinator and sent by the u-th node. Moreover, queuing ($t_q^{(i)}$), transmission ($t_{tx}^{(i)}$) and propagation ($t_p^{(i)}$) delays for the i-th frame are weighted for the factor $N_H^{(i)}$, which is number of hops ($N_H^{(i)} > 0$) the frame has to do in order to reach the destination. We notice that processing delays at the transmitter and receiver have been assumed ideal. Furthermore, since the propagation delay in electric cables is 5.775 $\mu s/km$ [28], we neglect its contribution.

6.5 Numerical Results

In order to show the functionality of the proposed cross-platform simulator, we consider the network of Figure 6.1 where we assume the communication to be from the network nodes 13–53 to the network coordinator (node 1).

The first scenario that we consider consists of the transmission of 10^4 frames from each node to the coordinator. It is meant to show the functionality of adaptive tone mapping (see section 6.3.1). Figure 6.4 shows the BER, the FER, and the throughput for the considered scenario with and withouth the use of tone mapping, when no relay is used, namely when the communication exploits the direct link between transmitter and receiver. The considered frequency band is the CENELEC A. Although not shown, we report that no errors have been experienced for transmission over the FCC band for all nodes, and further their correspondent throughput is equal to the maximum PHY data rate shown in Table 6.3, i.e., 10.17 *kbps*. From Figure 6.4, we can see that the use of tone

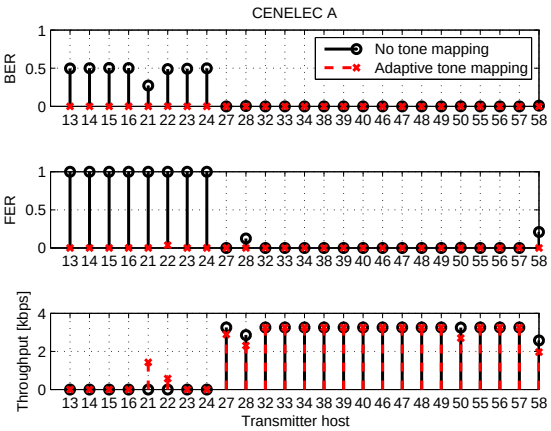

Figure 6.4: BER, FER, and throughput for direct link communication between each network node and the coordinator.

mapping decreases the BER to the expected value of about 10^{-4} and in some cases also increases the throughput, e.g., node ID 21 and 22. Furthermore, it is

worth noting that nodes 13, 14, 15, 16, 23 and 24 exhibit BER and FER equal to 0, but they are not visible from the coordinator since their correspondent throughput is 0. We highlight that this behavior is due to the fact that none of these node experience in their modulated carriers an SNR that is higher than the threshold, therefore they do not transmit data at all (see section 6.3.1).

6.5.1 MAC/ADP Layer Simulation

The second scenario that we consider is the following. We assume a metering scenario. In detail, a smart meter, represented by a G3-PLC node, is placed in every house and it transmits 1 frame of data per reading to the coordinator. The generation of this traffic represents a deterministic periodic transmission of frames from the meter to the coordinator. In this perspective, according to the worst case in [71], we assume that each node generates traffic according to an exponential distribution with mean equal to 60 s.

Figure 6.5 shows the logical network topology as the result of the application of the routing algorithm for CENELEC A band. It is worth noting that few nodes (yellow circles) act as relay, in order to allow the communication between all network nodes and coordinator. Regarding the FCC band, we notice that no relay turns out to be used.

Figure 6.6 reports the throughput and the end-to-end delay for both frequency bands. Furthermore, regarding CENELEC A, the results are reported either for the case when the routing algorithm (LOAD) is adopted or when it is not. It is interesting to note that, when LOAD is applied, all network nodes reach almost the same throughput (this is because the network is overloaded) and the network coverage is improved. However, the delays of relayed frames are proportional to the number of hops, according to Eq. 6.8.

As last scenario, we consider the case where different SG applications run over the network.

From Table6.1, we notice that, alarm signals, network joining, metering data and telemetry signals are characterized by a single packet of 1000 bytes. However, there is not any configuration of G3-PLC parameters which supports a single PHY frame with a dimension of 1000 bytes. Therefore, to cope with

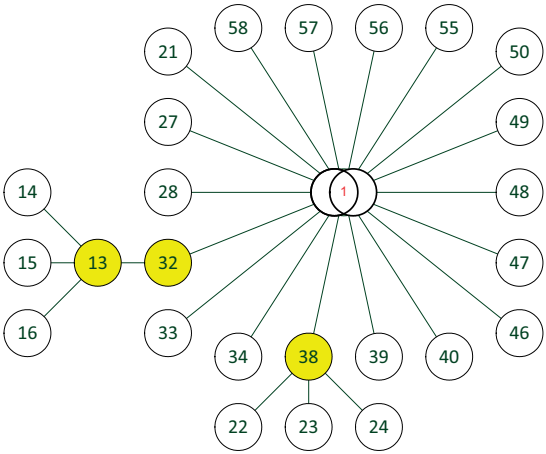

Figure 6.5: Logical network topology for CENELEC A band.

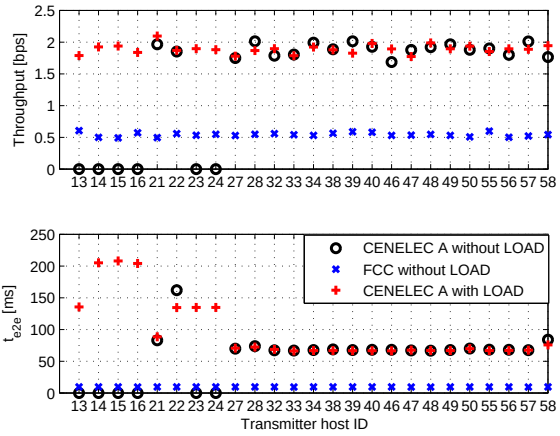

Figure 6.6: Throughput and end-to-end delay for metering traffic.

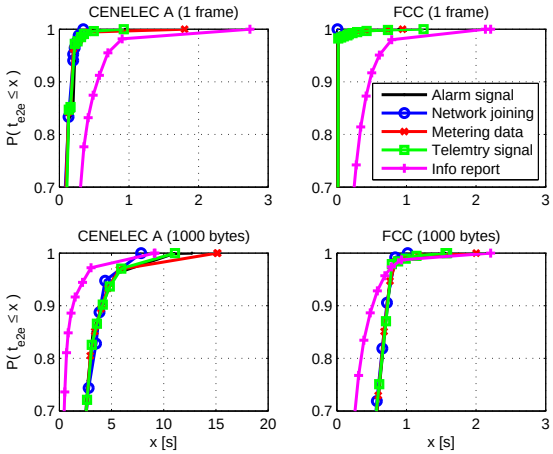

Figure 6.7: CDF of different traffic profiles for CENELEC A and FCC bands.

this problem, we consider two cases: (i) the transmission of a single frame with maximum dimension of 22 and 12 bytes, respectively for CENELEC A and FCC, and (ii) the transmission of a frame burst whose total dimension is 1000 bytes. The traffic model has been applied so that every network node transmits to the coordinator. A total of 6 hours of simulations have been performed.

Figure 6.7 shows the CDF of the end-to-end delay of each traffic profile. In particular, top-left and top-right figures show the CDF for a single frame transmission, respectively for CENELEC A and FCC bands. Bottom-left and bottom-right figures show the CDF for a frame burst of 1000 bytes, respectively for CENELEC A and FCC bands.

From Figure 6.7 one can assert whether or not a given class of service can be offered. As an example, we can assert that LOW (16 ms) and MEDIUM (¡160 ms) latency class services of alarm-response command could not be offered in both CENELEC A or FCC bands assuming 1000 bytes of data. Nevertheless they could with high reliability considering FCC band and 1 frame of data.

6.6 Main Findings

The use of a cross-platform simulator can be beneficial to predict the performance of a given communication technology in a certain application scenario. Adaptive bit-loading and routing algorithms are needed to make the communication network reliable and improve the network coverage.

Chapter 7

Conclusions

In this thesis, we have focused on the SH networks. In particular, we have defined a general SH network architecture and its main devices that should be used to overcame coexistence, interconnectivity and interoperability problems. In this scenario, we have focused on a representative technology, i.e., PLC, trying to characterize its behavior within a home scenario. We have performed field trials where the results have highlighted some disadvantages related to the use of the NB-PLC technology for SH application purposes. Therefore, exploiting a network simulator, we have modeled NB-PLC technology PHY and MAC layers in order to evaluate its performance in peculiar conditions and analyze potentialities and boundary conditions of the network. Moreover, we have proposed an innovative contention-free MAC scheme that allows performance improvements. Finally, we have presented a cross-platform simulator which allows to realistically simulate the PLC technology within in-home scenarios.

The main achievements are summarized in the following.

7.1 The Smart Home Network

Several communication technologies, suitable for in-home applications, have been surveyed, focusing on wireline, wireless and PLC. Nevertheless, they make use of different standards, protocols and even different media to com-

municate, and consequently, they are not interoperable/interconnected and/or can not even coexist. To this respect, we have focus on coexistence, interconnectivity and iteroperability issues as the major obstacles to the realization of the SH. Then, we have presented a convergent network architecture in order to achieve the interconnectivity. This has been done through the definition of a of a shared common layer that is able to manage heterogeneous lower layers allowing network convergence. Furthermore, we have discussed in detail the features of the main network devices.

7.2 PLC Network Testbed for In-home Performance Evaluation

Focusing on PLC technologies, we have tested, in single and multi floor houses, two representative NB-PLC devices, i.e., one based on FSK and the other based on OFDM. Test results have shown that, although OFDM, in general, allows for higher peak throughput than FSK, it exhibits poor performance in terms of FER, thus throughput, when working in the multi-floor house. This issue has been solved developing a network testbed where BB-PLC devices are used to provide an Ethernet backbone that allows for (i) connectivity between NB-PLC and BB-PLC devices, and (ii) range extension.

7.3 Enhancements of G3-PLC Technology for Smart Home Applications

In order to cope with OFDM poor performances, we have focused on G3-PLC technology where we have found that performances can be substantially improved by enhancing its MAC sub-layer. In particular, we have proposed a convergent network architecture that allows the integration of G3-PLC with Ethernet in order (a) to cope with the strong channel attenuation that is present in houses/buildings where the signal crosses circuit breakers, and (b) to increase the available resources by splitting the network in sub-networks. Although the convergent network has shown a substantial increase of the aggregate network throughput, its performance is appreciably decreased with the increase of the number of network nodes. This is mainly due to the use

of the CSMA/CA MAC scheme of G3-PLC. Therefore, we have proposed and implemented a contention-free MAC scheme, namely a TDMA, based on an optimized version of the beacon-enable mode of the IEEE 802.15.4. By means of numerical results we have shown that TDMA allows to solve the problem of CSMA related to the increasing number of nodes, and further allows to increase the THR.

7.4 Cross-Platform Simulator for In-home G3-PLC Evaluation

Finally, we have presented a cross-platform simulator for G3-PLC systems. The cross-platform simulator consists of two simulators: one for the PHY layer, and one for the higher layers. The physical layer simulator has been implemented in MATLAB and it is meant to compute the frame error rate of a given communication link. The higher layers simulator has been implemented in OMNeT++ and it makes use of the frame error rate to abstract the physical layer. We have pointed out that the cross-platform simulator enables the computation of the performance of the system considering either a given communication link or a given communication scenario. Furthermore, in order to improve the performance of G3-PLC systems, a convergent network architecture where G3-PLC devices are integrated into a switched Ethernet network has been presented. We have realized the convergent network by providing a shared common layer and by defining networking rules for router and switch devices. The platform has been used to derive the network performance in terms of throughput, end-to-end delay, frame drop rate, and coverage. The results have been exploited to test the requirements meeting of G3-PLC for a certain application scenario.

7.5 Cross-Platform Simulator for G3-PLC Evaluation in Access Networks

The cross-platform simulator have been also used to evaluate G3-PLC systems for SG applications in the access network scenario. Moreover, to improve the performance and coverage of G3-PLC, a simple adaptive tone mapping

algorithm together with a routing algorithm have been also presented.

7.6 Future Perspectives

As a final comment we would like to show some future perspectives which could represent further research topics. First of all, it would be interesting consider different traffic models. Although it has been done in Chapter 6 for the outdoor access network scenario, the traffic differentiation should be extended to the in-home scenario, where high data rate technologies are also present. Secondly, following the traffic differentiation, it would be interesting to statistically characterize the performance metrics, e.g., introducing the minimum and maximum throughput, with respect to different network topologies. From the analysis of the statistical behavior of a given performance metrics, we could also highlight whether there is a critical class of links for a given topology. Finally, since the G3-PLC specifications do not cover every single aspect, there are some PHY implementation issues that should be improved. For instance, the point-to-point adaptive tone mapping presented in Chapter 6 could be subjected to a network-wide optimization, where the tone mapping is adapted for more links simultaneously. It would also be worth noting the effect of those PHY improvements from the network layer point of view.

Chapter 8

Appendix

8.1 Karush Kuhn Tucker Conditions

A general optimization problem is written in standard form as follows,

$$\begin{aligned} \min_{\mathbf{x}\in\mathcal{D}} \quad & f_0(\mathbf{x}) \\ \text{s.t.} \quad & f_i(\mathbf{x}) \leq 0, \quad i = 1, \ldots, m \\ & h_i(\mathbf{x}) = 0, \quad i = 1, \ldots, p, \end{aligned} \tag{8.1}$$

where $\mathbf{x}$ is the optimization variable, f_0 is the objective or *cost* function, f_i are the inequality constraint functions, and g_i are the equality constraint functions. Moreover, the domain $\mathcal{C} = \left[\bigcap_{i=1}^{m} \operatorname{dom}(f_i)\right] \cap \left[\bigcap_{i=1}^{p} \operatorname{dom}(g_i)\right]$ is not empty.

The **Lagrangian** $L : \mathcal{D} \times \mathbb{R}^m \times \mathbb{R}^p \to \mathbb{R}$ associated to problem (8.1) is defined as

$$L(\mathbf{x}, \boldsymbol{\lambda}, \boldsymbol{\nu}) = f_0(\mathbf{x}) + \sum_{i=1}^{m} \lambda_i f_i(\mathbf{x}) + \sum_{i=1}^{p} \nu_i h_i(\mathbf{x}), \tag{8.2}$$

where λ_i is the multiplier associated to the i-th inequality, and ν_i is the multiplier associated to the i-th equality. The vectors $\boldsymbol{\lambda}$ and $\boldsymbol{\nu}$ are called *Lagrange multipliers* or *dual variables*. Hence, the Lagrangian is obtained from the objective function augmented with weighted sums of constraint functions.

The **Lagrange dual function** $g : \mathbb{R}^m \times \mathbb{R}^p \to R$ is defined as the minimum value of the Lagrangian over $\mathbf{x}$: for $\lambda \in \mathbb{R}^m$, $\nu \in \mathbb{R}^p$, i.e.,

$$g(\boldsymbol{\lambda}, \boldsymbol{\nu}) = \underset{\mathbf{x} \in \mathcal{D}}{inf} \quad L(\mathbf{x}, \boldsymbol{\lambda}, \boldsymbol{\nu}). \tag{8.3}$$

When the Lagrangian is unbounded below in x, the dual function takes on the value $-\infty$. It is noticeable that since the dual function is the pointwise infimum of a family of affine functions of $(\boldsymbol{\lambda}, \boldsymbol{\nu})$, it is concave, even when the problem (8.2) is not convex.

The **Lagrangian dual problem** is defined as

$$\begin{aligned} \max \quad & g(\boldsymbol{\lambda}, \boldsymbol{\nu}) \\ \text{s.t.} \quad & \lambda_i \geq 0, \ \ i = 1, \ldots, m. \end{aligned} \tag{8.4}$$

Problem (8.4) is said emphdual feasible if exists a pair $(\boldsymbol{\lambda}, \boldsymbol{\nu})$ with $\boldsymbol{\lambda} \geq 0$ and $g(\boldsymbol{\lambda}, \boldsymbol{\nu}) > -\infty$.

Now, suppose $\mathbf{x}^*$ to be the optimal solution to problem (8.1), with the pair $(\boldsymbol{\lambda}^*, \boldsymbol{\nu}^*)$ the optimal solution to the dual problem, and with d^* the corresponding value of g, namely $g(\boldsymbol{\lambda}^*, \boldsymbol{\nu}^*) = d^*$. We can then define the **duality gap** as $f_0(\mathbf{x}^*) - d^*$. It is said that the **strong duality** holds when the optimal duality gap is zero.

Assuming $f_0, \ldots, f_m, h_1, \ldots, h_p$ differentiable, $\mathbf{x}^*$ and $(\boldsymbol{\lambda}^*, \boldsymbol{\nu}^*)$ be any primal and dual optimal points with zero duality gap, the Karush Kuhn Tucker conditions can be expressed as:

$$\begin{aligned} f_i(\mathbf{x}^*) &\leq 0, \ \ i = 1, \ldots, m \\ h_i(\mathbf{x}^*) &= 0, \ \ i = 1, \ldots, p \\ \lambda_i^* &\geq 0, \ \ i = 1, \ldots, m \\ \lambda_i^* f_i(\mathbf{x}^*) &= 0, \ \ i = 1, \ldots, m \\ \nabla f_0(\mathbf{x}^*) + \sum_{i=1}^{m} \lambda_i^* \nabla f_i(\mathbf{x}^*) + \sum_{i=1}^{p} \nu_i^* \nabla f_i(\mathbf{x}^*) &= 0. \end{aligned} \tag{8.5}$$

In (8.5), the lines, from the first to the last, denote: the inequality constraints, the equality constraints, the non negativity condition of the Lagrange multipliers associated with the inequality constraints, the slackness conditions, and the condition that the gradient of the Lagrangian in the optimal point has to be null.

Therefore, we can summarize saying that for any optimization problem with differentiable objective and constraint functions for which strong duality obtains, any pair of primal and dual optimal points must satisfy the KKT conditions (8.5).

8.1.1 Optimal GTS Allocation for THR Maximization

Now, the optimization problem 6.1 can be written as follows,

$$\begin{aligned} \min_{\boldsymbol{\alpha}} \quad & -\sum_{u=1}^{N} \alpha^{(u)} THR^{(u)} \\ \text{s.t.} \quad & \sum_{u=1}^{N} \alpha^{(u)} - 1 = 0, \\ & \alpha^{(u)} - p^{(u)} \geq 0 \quad \forall u = 1, \ldots, N, \end{aligned} \tag{8.6}$$

where $\boldsymbol{\alpha} = \left[\alpha^{(1)}, \alpha^{(2)}, \ldots, \alpha^{(N)}\right] = \left[N_{TS}^{(1)}, N_{TS}^{(2)}, \ldots, N_{TS}^{(N)}\right] / N_{TS_{tot}}$ is the optimization variable. It is worth noting that the condition $0 \leq \alpha^{(u)} \leq 1$ is implicitly given by the second and third line of problem 8.6.

The Lagrangian associated to problem (8.6) is defined as

$$L\left(\boldsymbol{\alpha}, \boldsymbol{\lambda}, \boldsymbol{\nu}\right) = -\sum_{u=1}^{N} \alpha^{(u)} THR^{(u)} + \sum_{u=1}^{N} \lambda^{(u)} \left(p^{(u)} - \alpha^{(u)}\right) + \nu \left(\sum_{u=1}^{N} \alpha^{(u)} - 1\right), \tag{8.7}$$

and the KKT conditions are:

$$\begin{aligned} \nabla_\alpha L = -THR^{(u)} - \lambda^{(u)} + \nu = 0, \\ p^{(u)} - \alpha^{(u)} \leq 0, \\ \sum_{u=1}^{N} \alpha^{(u)} - 1 = 0, \\ \lambda^{(u)} \geq 0, \\ \lambda^{(u)} \left(p^{(u)} - \alpha^{(u)} \right) = 0. \end{aligned} \tag{8.8}$$

Since the problem 6.1 aims at THR maximization, we disregard the case $\alpha^{(u)} = 0$ because it correspond to $N_{TS}^{(u)} = 0$, i.e., the u-th node has no GTS allocated, hence it cannot transmit. Therefore, we consider the case $\alpha^{(u)} > 0$ that brings to

$$\lambda^{(u)} \left(p^{(u)} - \alpha^{(u)} \right) = 0 \quad \Leftrightarrow \quad \alpha^{(u)} = p^{(u)}, \tag{8.9}$$

$$-THR^{(u)} - \lambda^{(u)} + \nu = 0, \quad \lambda^{(u)} \geq 0 \quad \Leftrightarrow \quad \lambda^{(u)} = \nu - THR^{(u)} \geq 0$$

$$\Rightarrow \quad \nu \geq THR^{(u)}. \tag{8.10}$$

It is worth noting that Equation 8.9 takes into account the second and the last line of conditions 8.8, while Equation 8.10 takes into account the first and the fourth line of conditions 8.8. Exploiting the result obtained in Equation 8.9 and taking into account the third line of 8.8, we derive

$$\sum_{u=1}^{N} \alpha^{(u)} = 1, \quad \alpha^{(u)} = p^{(u)} \quad \Leftrightarrow \quad \sum_{u=1}^{N} p^{(u)} = 1. \tag{8.11}$$

Therefore, if we assume $p^{(u)} = 1/N$, the optimal solution to problem 8.6 is given by

$$\alpha^{(u)} = p^{(u)} = \frac{1}{N}, \quad \alpha^{(u)} = \frac{N_{TS}^{(u)}}{N_{TS_{tot}}} \quad \Rightarrow \quad N_{TS}^{(u)} = \frac{N_{TS_{tot}}}{N}. \tag{8.12}$$

Bibliography

[1] European Commission, *Energy 2020 – A Strategy for Competitive, Sustainable and Secure Energy*, 2010.

[2] L. Lampe, A. Tonello, and D. Shaver, "Power Line Communications for Automation Networks and Smart Grid," *IEEE Commun. Mag.*, vol. 49, pp. 26–27, Dec. 2011.

[3] A. Zaballos, A. Vallejo, and J. Selga, "Heterogeneous Communication Architecture for the Smart Grid," *IEEE Network*, vol. 25, pp. 30–37, Sept. 2011.

[4] IEEE Standards Association, "IEEE Recommended Practice for Information Technology - Telecommunications and Information Exchange Between Systems - Local and Metropolitan Area Networks - Specific Requirements Part 15.2: Coexistence of Wireless Personal Area Networks With Other Wireless Devices Operating in Unlicensed Frequency Bands," *IEEE Std 802.15.2-2003*, pp. 1–115, 2003.

[5] IEEE 802.19 Wireless Coexistence Working Group, *Operations Manual*, July 2011.

[6] IEEE Standards Association, "IEEE Standard for Broadband over Power Line Networks: Medium Access Control and Physical Layer Specifications," *IEEE Std 1901-2010*, pp. 1–1586, 2010.

[7] V. Oksman and S. Galli, "G.hn: The New ITU-T Home Networking Standard," *IEEE Commun. Mag.*, vol. 47, pp. 138–145, Oct. 2009.

[8] Telecommunication Standardization Sector of ITU, *Series G: Transmission Systems and Media, Digital Systems and Networks*. ITU-T, 2010.

[9] D. Varoutas, D. Katsianis, and M. Fokas, "Omega Project Deliverable D1.5: OMEGA Final Business Cases," tech. rep., ICT-213311 OMEGA, 2009.

[10] ISO/IEC 2382-1, *Information technology – Vocabulary – Part 1: Fundamental terms*, 3.0 ed., Nov. 1993.

[11] G. Coulouris, J. Dollimore, T. Kindberg, and G. Blair, *Distributed Systems: Concepts and Design*. Addison-Wesley, 5th ed., 2012.

[12] UPnP Forum, *UPnP Device Architecture 1.0*, 2008.

[13] OSGi Alliance, *About the OSGi Service Platform*, 2007.

[14] The Community Resource for Jini Technology, *Jini Architectural Overview*. Sun Microsystems, 1999.

[15] Digital Living Network Alliance, *DLNA for HD Video Streaming in Home Networking Environments*.

[16] IEEE Standards Association, "IEEE Standard for Information technology–Telecommunications and information exchange between systems–Local and metropolitan area networks–Specific requirements Part 3: Carrier Sense Multiple Access with Collision Detection (CSMA/CD) Access Method and Physical Layer Specifications," *IEEE Std 802.3-2008 (Revision of IEEE Std 802.3-2005)*, pp. 1–2977, 2008.

[17] Spirent Communications, *Deploying Enhanced media Service with MoCA*. An Implication paper prepared for the Society of Cable Telecommunications Engineers.

[18] H. C. Ferreira, L. Lampe, J. Newbury, and T. G. Swart, *Power Line Communications: Theory and Applications for Narrowband and Broadband Communications over Power Lines*. NY: Wiley & Sons, 2010.

[19] HomePNA, *No New Wires Hitting a Winning Triple-Play Home Networking Solution*, 2006.

[20] WiMedia Alliance, *Multiband OFDM Physical Layer Specification*, 2009.

[21] ZigBee Alliance, *ZigBee Specification*, Jan. 2008.

[22] IEEE Standards Association, "IEEE Standard for Information technology–Telecommunications and information exchange between systems Local and metropolitan area networks–Specific requirements Part 11: Wireless LAN Medium Access Control (MAC) and Physical Layer (PHY) Specifications," *IEEE Std 802.11-2012 (Revision of IEEE Std 802.11-2007)*, pp. 1–2793, 2012.

[23] The WirelessHD Consortium, *WirelessHD Specification Version 1.1 Overview*, 2010.

[24] C. Gomez and J. Paradells, "Wireless Home Automation Networks: A Survey of Architectures and Technologies," *IEEE Commun. Mag.*, vol. 48, pp. 92–101, June 2010.

[25] Bluetooth Special Interest Group, *Specification of the Bluetooth System*, 2004.

[26] HomePlug Powerline Alliance, *HomePlug AV White Paper*, 2005.

[27] HomePlug Powerline Alliance, *HomePlug Green PHY 1.1 Whitepaper*, Oct. 2012.

[28] ERDF, *PLC G3 Physical Layer Specification*.

[29] PRIME Alliance Technical Working Group, *Draft Specification for PoweRline Intelligent Metering Evolution*, R1.3.6.

[30] ITU-T G.9903, *Narrowband orthogonal frequency division multiplexing power line communication transceivers for G3-PLC networks*, Oct. 2012.

[31] ITU-T G.9904, *Narrowband orthogonal frequency division multiplexing power line communication transceivers for PRIME networks*, Oct. 2012.

[32] O. Logvinov, *Netricity PLC and the IEEE P1901.2 Standard*. HomePlug Powerline Alliance.

[33] ITU-T G.9902, *Narrowband orthogonal frequency division multiplexing power line communication transceivers for ITU-T G.hnem networks*, Oct. 2012.

[34] T. Winter, P. Thubert, A. Brandt, J. Hui, R. Kelsey, P. Levis, K. Pister, R. Struik, J. P. Vasseur, and R. Alexander, *RPL: IPv6 Routing Protocol for Low power and Lossy Networks*. Internet Engineering Task Force (IETF), 2012.

[35] S. Galli, A. Scaglione, and Z. Wang, "For the Grid and Through the Grid: The Role of Power Line Communications in the Smart Grid," *Proc. IEEE*, vol. 99, pp. 998–1027, June 2011.

[36] ADD Semiconductor, *ADD1010 Brief Datasheet*, 2010.

[37] DOMOLOGIC Home Automation GmbH, *Konnex PL132 – Power-Line-Communication using the CENELEC-C-Band*, 2003.

[38] G. Telkamp, "A low cost powerline node for domestic application," in *Proc. of Int. Symp. on Power Line Commun. and Its App. (ISPLC)*, (Essen, Germany), pp. 32–36, April 1997.

[39] Maxim Integrated Products, *MAX2990 Integrated Power-line Digital Transceiver Programming Manual*, 2010.

[40] ERDF, *PLC G3 MAC Layer Specification*.

[41] V. Oksman and J. Zhang, "G.HNEM: the New ITU-T Standard on Narrowband PLC Technology," *IEEE Commun. Mag.*, vol. 49, pp. 36–44, Dec. 2011.

[42] IEEE, *IEEE Std 802.15.4-2006, Part 15.4: Wireless Medium Access Control (MAC) and Physical Layer (PHY) Specifications for Low-Rate Wireless Personal Area Networks (WPANs)*, 2006.

[43] A. Varga and R. Hornig, "An Overview of the OMNeT++ Simulation Environment," in *Proc. of the First International Conference on Simulation Tools and Techniques for Communications, Networks and Systems & Workshops (SIMUTools 2008)*, 2008.

[44] G. S. Fishman, *Principles of Discrete Event Simulation*. New York, NY, USA: John Wiley & Sons, Inc., 1978.

[45] The VINT Project, *The ns Manual*, Nov. 2011.

[46] T. R. Henderson, S. Roy, S. Floyd, and G. F. Riley, "ns-3 project goals," in *Proc. from the 2006 workshop on ns-2: the IP network simulator (WNS2 2006)*, WNS2 '06, ACM, 2006.

[47] R. Barr, Z. J. Haas, and R. van Renesse, "JiST: an efficient approach to simulation using virtual machines: Research Articles," *Softw. Pract. Exper.*, vol. 35, pp. 539–576, May 2005.

[48] E. Weingartner, H. vom Lehn, and K. Wehrle, "A Performance Comparison of Recent Network Simulators," in *Communications, 2009. ICC '09. IEEE International Conference on*, pp. 1–5, 2009.

[49] *INET Framework for OMNeT++ Manual*, 2012.

[50] ITU-T G.9901, *Narrowband orthogonal frequency division multiplexing power line communication transceivers – Power spectral density specification*, Nov. 2012.

[51] G. Bianchi, "IEEE 802.11–Saturation Throughput Analysis," *IEEE Commun. Letters*, vol. 2, pp. 318–320, Dec. 1998.

[52] S. Boyd and L. Vandenberghe, "Convex Optimization," *Cambridge University Press*, 2004.

[53] National Institute of Standards and Technology, *NIST Framework and Roadmap for Smart Grid Interoperability Standards, Release 1.0.* Office of the National Coordinator for Smart Grid Interoperability, U.S. Department of Commerce, Jan. 2010.

[54] R. H. Khan and J. Y. Khan, "A comprehensive review of the application characteristics and traffic requirements of a smart grid communications network," *Computer Networks*, vol. 57, no. 3, pp. 825 – 845, 2013.

[55] J. Proakis, *Digital Communications.* McGraw-Hill series in electrical and computer engineering, McGraw-Hill Higher Education, 2001.

[56] A. Tonello and F. Versolatto, "Bottom-Up Statistical PLC Channel Modeling – Part II: Inferring the Statistics," *Power Delivery, IEEE Transactions on*, vol. 25, no. 4, pp. 2356–2363, 2010.

[57] A. Tonello, F. Versolatto, B. Bejar, and S. Zazo, "A Fitting Algorithm for Random Modeling the PLC Channel," *Power Delivery, IEEE Transactions on*, vol. 27, no. 3, pp. 1477–1484, 2012.

[58] L. D. Bert, P. Caldera, D. Schwingshackl, and A. M. Tonello, "On Noise Modeling for Power Line Communications," in *Proc. of IEEE Int. Symp. on Power Line Commun. and its App. (ISPLC)*, (Udine, Italy), Apr. 2011.

[59] W. Wang, Y. Xu, and M. Khanna, "Survey Paper: A survey on the communication architectures in smart grid," *Comput. Netw.*, vol. 55, pp. 3604–3629, Oct. 2011.

[60] F. Gomez-Cuba, R. Asorey-Cacheda, and F. Gonzalez-Castano, "Smart grid last-mile communications model and its application to the study of leased broadband wired-access," *Smart Grid, IEEE Transactions on*, vol. 4, no. 1, pp. 5–12, 2013.

[61] IEEE Standards Association, "IEEE Guide for Smart Grid Interoperability of Energy Technology and Information Technology Operation with the Electric Power System (EPS), End-Use Applications, and Loads," *IEEE Std 2030-2011*, pp. 1–126, 2011.

[62] M. Bauer, W. Plappert, C. Wang, and K. Dostert, "Packet-oriented communication protocols for Smart Grid Services over low-speed PLC," in *Proc. of IEEE Int. Symp. on Power Line Commun. and its App. (ISPLC)*, (Dresden, Germany), 2009.

[63] Opera Consortium, "Deliverable D4: Theoretical postulation of PLC channel model," tech. rep., 2005.

[64] H. Hrasnica, A. Haidine, and R. Lehnert, *Broadband Powerline Communications: Network Design*. Wiley, 2004.

[65] Z. Wang, A. Scaglione, and R. J. Thomas, "Generating Statistically Correct Random Topologies for Testing Smart Grid Communication and Control Networks," *IEEE Trans. On Smart Grid*, vol. 1, June 2010.

[66] M. Sigle, W. Liu, and K. Dostert, "On the impedance of the low-voltage distribution grid at frequencies up to 500 kHz," in *Proc. of Int. Symp. on Power Line Commun. and Its App. (ISPLC)*, (Bejing, China), pp. 30–34, March 2012.

[67] T. Zheng, X. Yang, B. Zhang, and et al., "Statistical analysis and modeling of noise on 10-kv medium-voltage power lines," *IEEE Transactions on Power Delivery*, vol. 22, pp. 1433–1439, July 2007.

[68] K. Razazian, A. Kamalizad, M. Umari, Q. Qu, V. Loginov, and M. Navid, "G3-plc field trials in u.s. distribution grid: Initial results and requirements," in *Proc. of Int. Symp. on Power Line Commun. and Its App. (ISPLC)*, pp. 153–158, April 2011.

[69] N. Papandreou and T. Antonakopoulos, "Bit and Power Allocation in Constrained Multi-carrier Systems: The Single-User Case," *EURASIP J. on Advances in Signal Processing*, vol. 2008, no. Article ID 643081, 2008.

[70] N. Kushalnagar, G. Montenegro, and C. Schumacher, *IPv6 over Low-Power Wireless Personal Area Networks (6LoWPANs): Overview, Assumptions, Problem Statement, and Goals*. Internet Engineering Task Force (IETF), 2007.

[71] D. Niyato, L. Xiao, and P. Wang, "Machine-to-machine communications for home energy management system in smart grid," *Communications Magazine, IEEE*, vol. 49, no. 4, pp. 53–59, 2011.